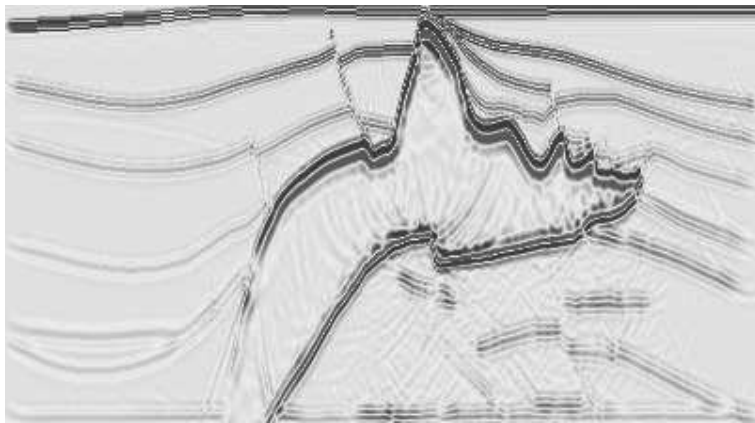

GEOPH-326
Introduction to Seismic Imaging
(Refraction and Reflection Seismology)



Mauricio D. Sacchi
Department of Physics
University of Alberta

Last Revision January 2019

Contents

1	Elasticity	3
1.1	Introduction	3
1.2	Continuum	3
1.3	The Stress Tensor	4
1.3.1	Balance of forces	6
1.3.2	Equilibrium equations	8
1.3.3	Balance of moments	11
1.3.4	Invariants	12
1.4	Einstein summation convention	13
1.5	Strain	14
1.5.1	What is ϵ_{ik} ?. A simple interpretation	16
1.6	Constitutive Law of Linear Elasticity	17
2	Waves in elastic media	21
2.1	Equation of motion for elastic disturbances	21
2.2	Propagation of volumetric perturbations	23
2.3	Propagation of shape perturbations	24
2.4	Equation of motion in vector form	25
2.5	Derivation of the 1D wave (Review)	26
2.5.1	Visualizing waves in t and x	28

2.5.2	Why do we adopt harmonic solutions ?	32
2.6	Plane Waves	33
2.7	Spherical Waves	40
2.8	Energy of waves	40
2.8.1	Geometrical spreading	40
2.8.2	Attenuation	43
3	Rays	47
3.1	Introduction	47
3.2	Snell's Law	48
3.2.1	$T - X$ refraction profiles	52
3.2.2	$T - X$ refraction curves for a dipping layer	55
3.2.3	Fitting straight lines to first arrivals.	57
3.3	Reflections	59
3.3.1	$T - X$ curves for a primary reflection	61
3.3.2	Relative position of the reflection and the head wave in the $T - X$ plane	65
3.4	Reflections in horizontally stratified media	66
3.4.1	Root-mean-square (RMS) velocity	68
3.5	Seismic reflection data in offset and midpoint coordinates	70
3.5.1	Multiples	72
3.6	Normal Moveout (NMO) correction	73
4	Reflection seismology: Normal Moveout Correction, Velocity Analysis and Stacking	79
4.1	Stacking charts	79
4.2	Velocity analysis	81
4.2.1	Velocity Scans	83
4.2.2	Constant velocity stacks	87

4.2.3	The seismic section	87
4.3	Stacking and its the frequency response	91
5	Modeling Normal Incidence Seismograms	95
5.1	Normal incidence	95
5.1.1	Impulse response	96
5.1.2	Example	100
6	Deconvolution	103
6.1	Deconvolution in the frequency domain	103
6.2	Example	105
7	The tomographic problem and introduction to linear inverse theory	107
7.1	Inverse Theory	107
7.2	Tomography	108

Preface

Applied geophysics is the study of the subsurface or more precisely that shallow part of the crust which supplies us with mineral resources and where human activity takes place. The traditional goal of applied geophysics is to prospect for minerals. Nowadays, however, applied geophysics has also become important in assessing environmental damage and in the design of remediation strategies for contaminated areas. Applied geophysical methods are also an integral part of geotechnical studies in civil and mining engineering for risk assessment and hazard control.

The study of the subsurface is in the most part, *indirect*. In other words, the properties of the subsurface are often inferred from surface measurements. Applied geophysicists use essentially two methods for obtaining these properties. The first of these, the seismic method uses variations in the travel time of propagating waves to infer elastic properties of the subsurface. Human-made explosive or vibratory disturbances are used to emit seismic waves into the interior of the earth. Geological interfaces reflect these waves, they propagate upwards and are finally recorded by an array of receivers (geophones). The data (seismograms) are used to infer the structure of the earth via computationally intensive signal processing and inversion techniques. The second class of methods are entirely different in principle. They are often called *potential methods* because they depend on the distortion of a scalar or vector potential field caused by some perturbation of a suitable physical property in the subsurface¹.

In GEOPH-326 we will study physical and mathematical aspects of wave propagation and their application to seismic imaging.

¹GEOPH-325 and GEOPH-424 consider gravitational, magnetic and electrical potentials (non-seismic techniques)

Chapter 1

Elasticity

1.1 Introduction

The theory of elasticity provides the fundamental relationship between stress and strain in an elastic medium. To study the elastic behaviour of a solid, we will use the idealized concept of a *continuum*. In a continuum, the matter is considered continuously distributed in space. In other words, we will analyze problems at a scale where the atomic structure of the matter is not considered.

Seismology often deals with very small deformations (infinitesimal strain theory); this assumption simplifies the mathematical treatment of many seismological problems. In the vicinity of a seismic source, or when we analyze deformations over a long period, infinitesimal strain theory is no longer valid, a more complicated treatment is required.

The seismic method uses the propagation of seismic waves through the earth. The propagation of seismic waves depends on the elastic properties of the rocks in the subsurface. When forces are applied to an elastic body, the distance between the points of the body varies. This variation is proportional to the applied force. The external forces are opposed by internal forces that resist the change in size and shape. As a result, the body tends to its original size and shape. This property of resisting changes in size and shape and returning to the original form when external forces are removed is called elasticity. *A perfectly elastic body under deformation recovers the original size and shape completely when external forces are suppressed.*

If the deformation induced by external forces are small, we can consider that the material behaves like an elastic body. The latter is an assumption valid for many rocks.

1.2 Continuum

Elasticity is a special part of continuum mechanics. Continuum mechanics is based on the application of Newton's laws to the so called continuum. In a continuum we assume the existence (anywhere) of three densities:

1. The density of mass $\frac{dM}{dV}$
2. The density of linear momentum $\frac{d(m\mathbf{v})}{dV}$
3. The density of energy $\frac{dE}{dV}$

A more intuitive definition:

A *continuum* is a piece of matter that can be subdivided an arbitrary number of times and still remains a piece of the same type of matter

1.3 The Stress Tensor

When an external force is applied to a continuum, that force influences every point in the body. Two type of forces can act on a continuum:

1. Body forces
2. Surface forces

Body forces are proportional to the volume and density of the material. An example is the acceleration due to gravity, $\mathbf{F} = m\mathbf{g}$, where the mass m depends on the volume and density. Surface forces depend on the surface they act on. For example, hydrostatic pressure and atmospheric pressure are surface forces.

When external forces act on a continuum, internal forces must act (react) within the continuum. Imagine a plane that cuts the idealized body (rock) in Figure 1.1. The normal to the plane is denoted by \mathbf{n} . We define the stress that acts on a point P on the surface element with normal \mathbf{n} as follows

$$\mathbf{T}(\mathbf{n}) = \lim_{\Delta A \rightarrow 0} \frac{\Delta \mathbf{F}}{\Delta A} = T_1 \mathbf{e}_1 + T_2 \mathbf{e}_2 + T_3 \mathbf{e}_3 \quad (1.1)$$

Since our plane in Figure 1.1 is arbitrary, we can also use planes with normal directions \mathbf{e}_1 , \mathbf{e}_2 , and \mathbf{e}_3 . In this case, we define the stress components acting on a plane with normal \mathbf{e}_1 as

$$\begin{aligned} \sigma_{11} &= \lim_{\Delta A_1 \rightarrow 0} \frac{\Delta F_1}{\Delta A_1} \\ \sigma_{12} &= \lim_{\Delta A_1 \rightarrow 0} \frac{\Delta F_2}{\Delta A_1} \\ \sigma_{13} &= \lim_{\Delta A_1 \rightarrow 0} \frac{\Delta F_3}{\Delta A_1}. \end{aligned} \quad (1.2)$$

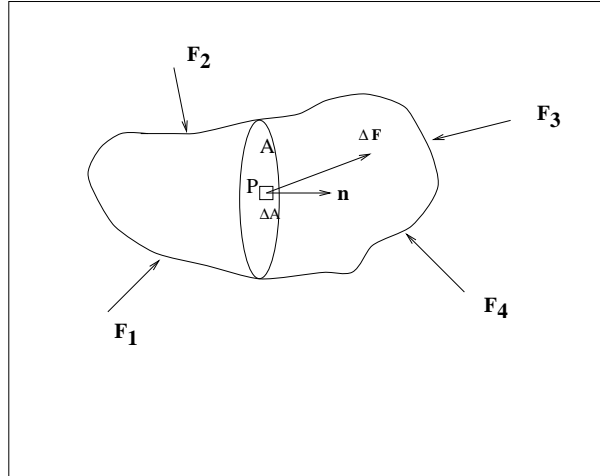


Figure 1.1: \mathbf{F}_1 , \mathbf{F}_2 , \mathbf{F}_3 , \mathbf{F}_4 are external forces acting on a continuum. The body has been cut by a plane A , ΔA is an elementary surface with normal \mathbf{n} , $\Delta \mathbf{F}$ is the internal force acting at location P . It is important to stress that we have a distribution of internal forces. To simplify the diagram, however, we only draw the force acting at the point denoted P .

Similarly, we can define the stress components acting on a plane with normal \mathbf{e}_2

$$\begin{aligned}
 \sigma_{21} &= \lim_{\Delta A_2 \rightarrow 0} \frac{\Delta F_1}{\Delta A_2} \\
 \sigma_{22} &= \lim_{\Delta A_2 \rightarrow 0} \frac{\Delta F_2}{\Delta A_2} \\
 \sigma_{23} &= \lim_{\Delta A_2 \rightarrow 0} \frac{\Delta F_3}{\Delta A_2}.
 \end{aligned} \tag{1.3}$$

Finally, the stress components acting on a plane with normal \mathbf{e}_3 are given by

$$\begin{aligned}
 \sigma_{31} &= \lim_{\Delta A_3 \rightarrow 0} \frac{\Delta F_1}{\Delta A_3} \\
 \sigma_{32} &= \lim_{\Delta A_3 \rightarrow 0} \frac{\Delta F_2}{\Delta A_3} \\
 \sigma_{33} &= \lim_{\Delta A_3 \rightarrow 0} \frac{\Delta F_3}{\Delta A_3}.
 \end{aligned} \tag{1.4}$$

The components σ_{ij} , $i, j = 1 : 3$ constitute the Stress Tensor. It is important to note that the Stress Vector $\mathbf{T}(\mathbf{n})$ can be written in terms of the components σ_{ij} .

We can visualize the stress components via the small elementary tetrahedron portrayed in Figure 1.2. We can imagine that the tetrahedron has been extracted from the body in Figure 1.1. By examining the elementary tetrahedron, we can quickly identify the stress components

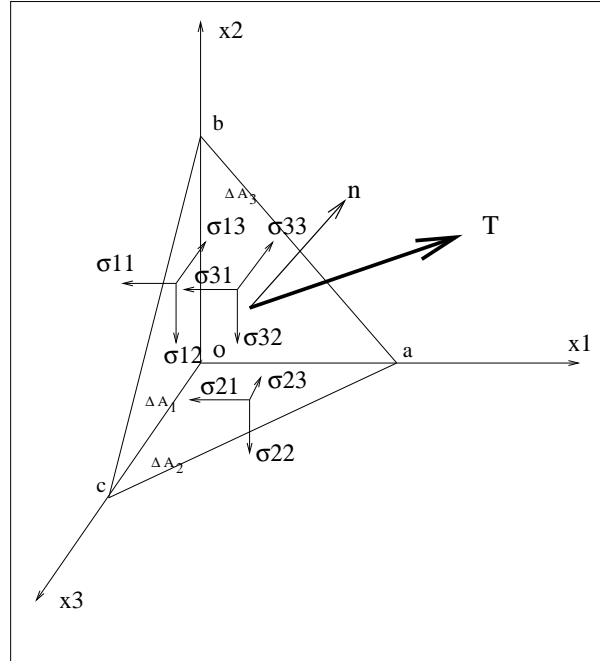


Figure 1.2: Elementary tetrahedron. Components of the stress tensor σ_{ij} acting on the faces of the tetrahedron with normal unitary vectors \mathbf{e}_1 , \mathbf{e}_2 and \mathbf{e}_3 . The stress vector acting on face with normal \mathbf{n} is denoted \mathbf{T} .

- $\sigma_{11}, \sigma_{12}, \sigma_{13}$ act on the surface ΔA_1 (boc) with normal $-\mathbf{e}_1$
- $\sigma_{21}, \sigma_{22}, \sigma_{23}$ act on the surface ΔA_2 (aoc) with normal $-\mathbf{e}_2$
- $\sigma_{31}, \sigma_{32}, \sigma_{33}$ act on the surface ΔA_3 (aob) with normal $-\mathbf{e}_3$
- The stress vector $\mathbf{T}(\mathbf{n})$ acts on the surface ΔA (abc) with normal \mathbf{n}

1.3.1 Balance of forces

If the body is in equilibrium, the sum of forces and the sum of moments acting on the body must be zero. First, we will write down the balance of forces for our small tetrahedron. Remember that the stresses are forces per area. The balance of forces will require to multiply the stress by its associated elementary area. We will adopt a positive sign convention for stress components acting on faces with a positive normal.

As an example we will write down the balance of forces in the direction x_1 , you can also derive the balance for the remaining two components using the following procedure

$$\sum F_{x_1} = \underbrace{T_1 \Delta A}_1 - \underbrace{\sigma_{11} \Delta A_1}_2 - \underbrace{\sigma_{21} \Delta A_2}_3 - \underbrace{\sigma_{31} \Delta A_3}_4 \quad (1.5)$$

1. Stress in the x_1 direction \times Area of face abc
2. Stress in the x_1 direction \times Area of face boc
3. Stress in the x_1 direction \times Area of face aoc
4. Stress in the x_1 direction \times Area of face aob .

The surfaces ΔA_1 , ΔA_2 and ΔA_3 are expressed as a function of ΔA (abc) using the following expressions

$$\begin{aligned}\Delta A_1 &= \Delta A \times \cos(\theta_1) \\ \Delta A_2 &= \Delta A \times \cos(\theta_2) \\ \Delta A_3 &= \Delta A \times \cos(\theta_3)\end{aligned}\tag{1.6}$$

where the surfaces are projected via the direction cosines

$$\mathbf{n} = n_1\mathbf{e}_1 + n_2\mathbf{e}_2 + n_3\mathbf{e}_3 = \cos(\theta_1)\mathbf{e}_1 + \cos(\theta_2)\mathbf{e}_2 + \cos(\theta_3)\mathbf{e}_3.\tag{1.7}$$

After combining equations (1.5) and (1.7) we obtain

$$\sum F_{x_1} = T_1\Delta A_1 - \sigma_{11}\Delta A\cos(\theta_1) - \sigma_{21}\Delta A\cos(\theta_2) - \sigma_{31}\Delta A\cos(\theta_3)\tag{1.8}$$

We can cancel ΔA to obtain the following expression

$$T_1 = \sigma_{11}\cos(\theta_1) + \sigma_{21}\cos(\theta_2) + \sigma_{31}\cos(\theta_3)\tag{1.9}$$

or

$$T_1 = \sigma_{11}n_1 + \sigma_{21}n_2 + \sigma_{31}n_3\tag{1.10}$$

A balance of forces in the x_2 and x_3 directions leads to the following two expressions

$$T_2 = \sigma_{12}n_1 + \sigma_{22}n_2 + \sigma_{32}n_3\tag{1.11}$$

$$T_3 = \sigma_{13}n_1 + \sigma_{23}n_2 + \sigma_{33}n_3.\tag{1.12}$$

The last three equations in a compact form become

$$T_i = \sum_{j=1}^3 \sigma_{ji}n_j = \underbrace{\sigma_{ji}n_j}_{\text{Summation convention for repeated subscripts}}\tag{1.13}$$

Example

We consider a simple case where we evaluate the stress vector acting on the plane with normal $\mathbf{n} = (1, 0, 0)$. In this simple example $n_1 = 1$, $n_2 = n_3 = 0$. Using equation 1.13 we have

$$\begin{aligned} T_1 &= \sigma_{11} \times 1 + \sigma_{12} \times 0 + \sigma_{13} \times 0 \\ T_2 &= \sigma_{21} \times 1 + \sigma_{22} \times 0 + \sigma_{23} \times 0 \\ T_3 &= \sigma_{31} \times 1 + \sigma_{32} \times 0 + \sigma_{33} \times 0 \end{aligned} \tag{1.14}$$

The stress vector becomes

$$\mathbf{T}(\mathbf{n}) = T_1\mathbf{e}_1 + T_2\mathbf{e}_2 + T_3\mathbf{e}_3 = \sigma_{11}\mathbf{e}_1 + \sigma_{21}\mathbf{e}_2 + \sigma_{31}\mathbf{e}_3$$

Finally, it is important to mention that the stress components can be arranged in 3×3 matrix (the stress tensor)

$$\begin{pmatrix} \sigma_{11} & \sigma_{12} & \sigma_{13} \\ \sigma_{21} & \sigma_{22} & \sigma_{23} \\ \sigma_{31} & \sigma_{32} & \sigma_{33} \end{pmatrix}.$$

The geophysical units for stress are *bars* (10^6 dyn/cm^2), where the atmospheric pressure at sea level is $\approx 1 \text{ bar}$.

1.3.2 Equilibrium equations

We will abandon our simple tetrahedron and introduce an elementary cube of a continuum. The latter will facilitate our analysis. In Figure 1.3 we portray a cubic element bounded by faces that are parallel to the coordinate planes. To avoid notational clutter, only stresses acting on the faces A_1 and A_1' are shown. Similar stress components operate on the other faces. In Figure 1.3 we have the following components:

- Acting on the face A_1 : σ_{11} , σ_{12} , σ_{13}
- Acting on the face A_1' : σ_{11}' , σ_{12}' , σ_{13}'

Since the distance between the two faces is small, we can expand the stress components in the face A_1' using a first order expansion

$$\begin{aligned}\sigma_{11}' &= \sigma_{11} + \frac{\partial\sigma_{11}}{\partial x_1} \Delta x_1 \\ \sigma_{12}' &= \sigma_{12} + \frac{\partial\sigma_{12}}{\partial x_2} \Delta x_1 \\ \sigma_{13}' &= \sigma_{13} + \frac{\partial\sigma_{13}}{\partial x_1} \Delta x_1\end{aligned}\tag{1.15}$$

A similar analysis is carried out on the other four faces of the cube. If we consider the faces with normals \mathbf{e}_2 and $-\mathbf{e}_2$ we obtain

$$\begin{aligned}\sigma_{21}' &= \sigma_{21} + \frac{\partial\sigma_{21}}{\partial x_2} \Delta x_2 \\ \sigma_{22}' &= \sigma_{22} + \frac{\partial\sigma_{22}}{\partial x_2} \Delta x_2 \\ \sigma_{23}' &= \sigma_{23} + \frac{\partial\sigma_{23}}{\partial x_2} \Delta x_2\end{aligned}\tag{1.16}$$

Finally, we can write a similar expression for the faces with normals $-\mathbf{e}_2$ and $-\mathbf{e}_3$

$$\begin{aligned}\sigma_{31}' &= \sigma_{31} + \frac{\partial\sigma_{31}}{\partial x_3} \Delta x_3 \\ \sigma_{32}' &= \sigma_{32} + \frac{\partial\sigma_{32}}{\partial x_3} \Delta x_3 \\ \sigma_{33}' &= \sigma_{33} + \frac{\partial\sigma_{33}}{\partial x_3} \Delta x_3\end{aligned}\tag{1.17}$$

First, we will balance forces acting in the x_1 direction:

$$\begin{aligned}\sum F_{x_1} &= \underbrace{\left(\sigma_{11} + \frac{\partial\sigma_{11}}{\partial x_1} \Delta x_1 - \sigma_{11}\right)\Delta x_2 \Delta x_3}_1 \\ &+ \underbrace{\left(\sigma_{21} + \frac{\partial\sigma_{21}}{\partial x_2} \Delta x_2 - \sigma_{21}\right)\Delta x_1 \Delta x_3}_2 \\ &+ \underbrace{\left(\sigma_{31} + \frac{\partial\sigma_{31}}{\partial x_3} \Delta x_3 - \sigma_{31}\right)\Delta x_1 \Delta x_2}_3 \\ &= 0\end{aligned}\tag{1.18}$$

In the last equation each contribution has the following meaning:

1. Net stress acting in the x_1 direction on the faces with normals \mathbf{e}_1 and $-\mathbf{e}_1 \times \text{Area} (\Delta x_2 \Delta x_3)$

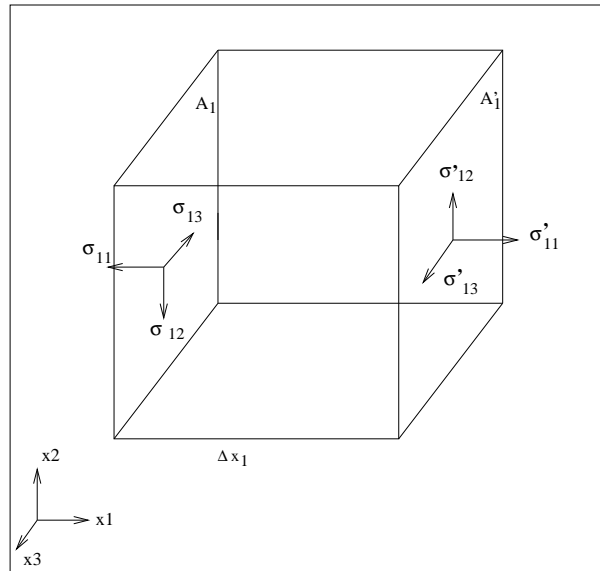


Figure 1.3: A cubic element extracted from a continuum. Only stress components in the faces denoted A_1 and A_1' are portrayed.

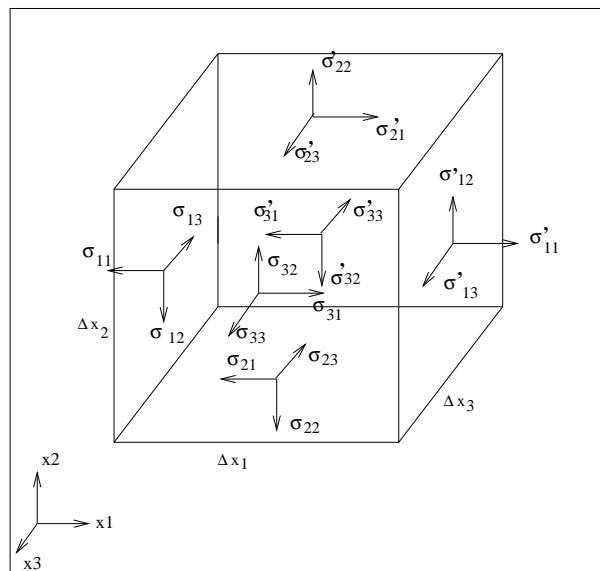


Figure 1.4: A cubic element in a continuum. All stress components acting on the cube are portrayed.

2. Net stress acting in the x_1 direction on the faces with normals \mathbf{e}_2 and $-\mathbf{e}_2 \times \text{Area} (\Delta x_1 \Delta x_3)$
3. Net stress acting in the x_1 direction on the faces with normals \mathbf{e}_3 and $-\mathbf{e}_3 \times \text{Area} (\Delta x_1 \Delta x_2)$

After a few manipulations we end up with the following expression

$$\frac{\partial \sigma_{11}}{\partial x_1} + \frac{\partial \sigma_{21}}{\partial x_2} + \frac{\partial \sigma_{31}}{\partial x_3} = 0. \quad (1.19)$$

A similar analysis for the remaining directions ($\sum F_{x_2} = 0, \sum F_{x_3} = 0$) leads to the following results

$$\frac{\partial \sigma_{12}}{\partial x_1} + \frac{\partial \sigma_{22}}{\partial x_2} + \frac{\partial \sigma_{32}}{\partial x_3} = 0 \quad (1.20)$$

$$\frac{\partial \sigma_{13}}{\partial x_1} + \frac{\partial \sigma_{23}}{\partial x_2} + \frac{\partial \sigma_{33}}{\partial x_3} = 0 \quad (1.21)$$

These are equilibrium equations that state that the spatial gradients are in balance. We can write equations (1.19), (1.20), and (1.21) in compact form,

$$\sum_{i=1}^3 \frac{\partial \sigma_{ij}}{\partial x_i} = 0. \quad j = 1, 2, 3. \quad (1.22)$$

Similarly, one could also use the summation convention for repeated subscripts (Einstein notation)

$$\frac{\partial \sigma_{ij}}{\partial x_i} = 0. \quad j = 1, 2, 3 \quad (1.23)$$

1.3.3 Balance of moments

The second condition of equilibrium is that the sum of moments acting on the body must be zero. The rotational moment in the direction \mathbf{e}_3 is given by

$$\sum M_{x_3} = \underbrace{(\sigma_{12} + \frac{\partial \sigma_{12}}{\partial x_1} \Delta x_1 + \sigma_{12}) \Delta x_2 \Delta x_3 \frac{\Delta x_1}{2}}_1$$

$$- \underbrace{(\sigma_{21} + \frac{\partial \sigma_{21}}{\partial x_2} \Delta x_2 + \sigma_{21}) \Delta x_1 \Delta x_3 \frac{\Delta x_2}{2}}_2 \quad (1.24)$$

$$= \underbrace{\hspace{10em}}_0 \quad (1.25)$$

1. Net moment in the \mathbf{e}_3 direction produced by the stress components acting on the faces with normals \mathbf{e}_1 and $-\mathbf{e}_1$.
2. Net moment in the \mathbf{e}_3 direction produced by the stress components acting on the faces with normals \mathbf{e}_2 and $-\mathbf{e}_2$.

Equation (1.25) leads to

$$2\sigma_{12} + \frac{\partial\sigma_{12}}{\partial x_1}\Delta x_1 - 2\sigma_{21} - \frac{\sigma_{21}}{\partial x_2}\Delta x_2 = 0. \quad (1.26)$$

After taking limits ($\Delta x_1, \Delta x_2 \rightarrow 0$) we end up with the following expression

$$\sigma_{12} = \sigma_{21}. \quad (1.27)$$

We can also evaluate moments in the direction x_2 and x_1 and obtain the following

$$\sigma_{13} = \sigma_{31}, \quad (1.28)$$

$$\sigma_{23} = \sigma_{32}. \quad (1.29)$$

In a more general form, we write

$$\sigma_{ij} = \sigma_{ji}.$$

We have proved that the stress tensor is symmetric. Now instead of nine independent component we have six,

$$\begin{pmatrix} \sigma_{11} & \sigma_{12} & \sigma_{13} \\ \sigma_{12} & \sigma_{22} & \sigma_{23} \\ \sigma_{13} & \sigma_{23} & \sigma_{33} \end{pmatrix}. \quad (1.30)$$

The diagonal terms of the stress tensor are the *Normal Stresses*. The off-diagonal terms are the *Shear Stresses*.

1.3.4 Invariants

The stress tensor is symmetric, and therefore it can be diagonalized. In other words, we can always find a new system of coordinates where the tensor is a diagonal matrix (the off-diagonal terms vanish). In order to diagonalize the stress tensor we must solve an eigenvalue problem:

$$\begin{vmatrix} \sigma_{11} - \lambda & \sigma_{12} & \sigma_{13} \\ \sigma_{12} & \sigma_{22} - \lambda & \sigma_{23} \\ \sigma_{13} & \sigma_{23} & \sigma_{33} - \lambda \end{vmatrix} = 0.$$

The above determinant leads to the following expression

$$\lambda^3 - I_1\lambda^2 + I_2\lambda - I_3 = 0. \quad (1.31)$$

The quantities I_1 , I_2 and I_3 are called *invariants*

$$I_1 = \sigma_{11} + \sigma_{22} + \sigma_{33} \quad (1.32)$$

$$I_2 = \sigma_{11}\sigma_{22} + \sigma_{22}\sigma_{33} + \sigma_{11}\sigma_{33} - \sigma_{12}^2 - \sigma_{13}^2 - \sigma_{23}^2 \quad (1.33)$$

$$I_3 = |\sigma| \quad (1.34)$$

$I_3 = |\sigma|$ is the determinant of the matrix in equation (1.30). The invariants are independent of the coordinate system. The hydrostatic stress is defined as the average of the normal stresses,

$$P = \frac{\sigma_{11} + \sigma_{22} + \sigma_{33}}{3} \quad (1.35)$$

P is an invariant because $P = I_1/3$ and I_1 is invariant.

1.4 Einstein summation convention

The following simple example shows the summation convention for repeated subscripts often called Einstein notation. Consider the dot product between two vectors

$$\mathbf{x} \cdot \mathbf{y} = x_1y_1 + x_2y_2 + x_3y_3$$

or,

$$\mathbf{x} \cdot \mathbf{y} = \sum_{i=1}^3 x_i y_i$$

but because the summation always goes from 1 to 3, we can save some ink by writing

$$\mathbf{x} \cdot \mathbf{y} = x_i y_i$$

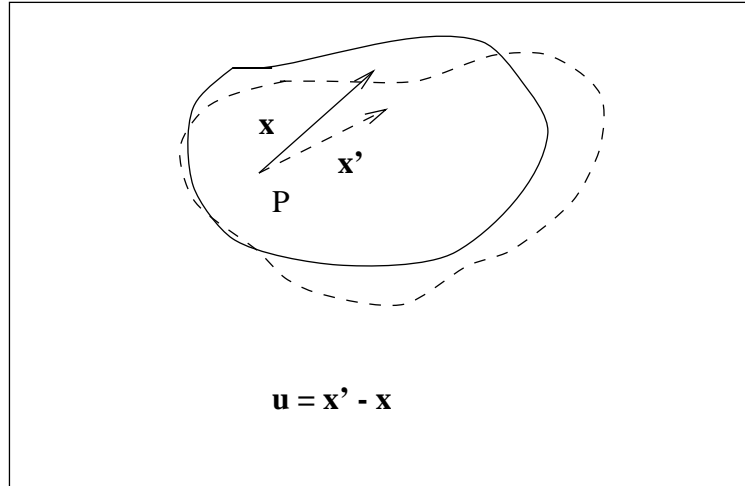


Figure 1.5: Change of the position of a point after deformation.

and understanding that the repeated indexes imply summing from index $i = 1$ to index $i = 3$.

Another example, consider a Cartesian vector

$$\mathbf{v} = v_1 \mathbf{e}_1 + v_2 \mathbf{e}_2 + v_3 \mathbf{e}_3 = \sum_{i=1}^3 v_i \mathbf{e}_i = v_i \mathbf{e}_i .$$

1.5 Strain

When forces are applied upon a body, the body experiments a deformation, and the distance between the material points will change. Let us consider Figure 1.5 where a point of the elastic body represented by its position \mathbf{x} . The position of the point after deformation is \mathbf{x}' . The displacement vector after the deformation is given by

$$\mathbf{u} = \mathbf{x}' - \mathbf{x} . \quad (1.36)$$

The distance between two infinitely close points before deformation is given by

$$dl = (dx_1^2 + dx_2^2 + dx_3^2)^{1/2} \quad (1.37)$$

Similarly, the distance between infinitely close points after deformation is given by the following expression

$$dl' = (dx_1'^2 + dx_2'^2 + dx_3'^2)^{1/2} . \quad (1.38)$$

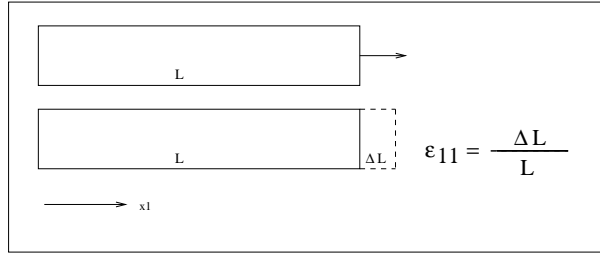


Figure 1.6: Linear deformation of an body.

According to equation (1.36), we can express dl' as follows

$$dl' = [(dx_1 + du_1)^2 + (dx_2 + du_2)^2 + (dx_3 + du_3)^2]^{1/2}. \quad (1.39)$$

Now consider the following differential increments

$$\begin{aligned} du_1 &= \frac{\partial u_1}{\partial x_1} dx_1 + \frac{\partial u_1}{\partial x_2} dx_2 + \frac{\partial u_1}{\partial x_3} dx_3 \\ du_2 &= \frac{\partial u_2}{\partial x_1} dx_1 + \frac{\partial u_2}{\partial x_2} dx_2 + \frac{\partial u_2}{\partial x_3} dx_3 \end{aligned} \quad (1.40)$$

$$du_3 = \frac{\partial u_3}{\partial x_1} dx_1 + \frac{\partial u_3}{\partial x_2} dx_2 + \frac{\partial u_3}{\partial x_3} dx_3. \quad (1.41)$$

If we substitute the increments du_1, du_2, du_3 into equation 1.39

$$dl'^2 = dl^2 + 2\epsilon_{ik} dx_i dx_k \quad (1.42)$$

where the summation is considered to be on repeated subscripts (Einstein notation). The element ϵ_{ik} is defined as

$$\epsilon_{ik} = \frac{1}{2} \left(\frac{\partial u_i}{\partial x_k} + \frac{\partial u_k}{\partial x_i} + \frac{\partial u_i}{\partial x_k} \frac{\partial u_k}{\partial x_i} \right). \quad (1.43)$$

The scale ϵ_{ik} represent the i, k components of the *Strain Tensor*. For small deformations, the variation in distances between the material points is small compared with the distance itself. Therefore, the product of derivatives $\frac{\partial u_i}{\partial x_k} \frac{\partial u_k}{\partial x_i}$ is ignored. After eliminating the product of derivates, the strain tensor becomes

$$\epsilon_{ik} = \frac{1}{2} \left(\frac{\partial u_i}{\partial x_k} + \frac{\partial u_k}{\partial x_i} \right). \quad (1.44)$$

It is clear from the definition of the strain component ϵ_{ik} that the strain tensor is symmetric $\epsilon_{ik} = \epsilon_{ki}$. Obe can interpret the strain tensors as the rate of change of the displacements u_1, u_2, u_3

with respect to spatial coordinates x_1, x_2, x_3 . The strain tensor is also expressed via a 3×3 symmetric matrix

$$\begin{pmatrix} \epsilon_{11} & \epsilon_{12} & \epsilon_{13} \\ \epsilon_{12} & \epsilon_{22} & \epsilon_{23} \\ \epsilon_{13} & \epsilon_{23} & \epsilon_{33} \end{pmatrix}. \quad (1.45)$$

1.5.1 What is ϵ_{ik} ?. A simple interpretation

We first consider the variation in length in the direction x_1 . Let us assume the variation in length of a rod where $dx_2 = dx_3 = 0$. In this case equation (1.42) leads to

$$dx_1'^2 = dx_1^2(1 + 2\epsilon_{11}). \quad (1.46)$$

The latter can be rewritten as

$$\frac{dx_1'^2 - dx_1^2}{dx_1^2} = 2\epsilon_{11}. \quad (1.47)$$

Given that we are assuming small increments, one can write down the following approximation

$$dx_1'^2 - dx_1^2 \approx (dx_1' - dx_1) 2dx_1.$$

After a little of algebra, we can write

$$\delta_1 = \frac{dx_1' - dx_1}{dx_1} = \epsilon_{11}. \quad (1.48)$$

In other words, ϵ_{11} corresponds to a small dilatation in the direction x_1 (Figure 1.6). We can perform a similar analysis for ϵ_{22} and ϵ_{33} and conclude that the diagonal elements of the strain tensor represent linear dilatation in the directions x_2 and x_3 , respectively.

Now we consider a cube that suffers a deformation (dilatation only) due to external forces. The dilatation in each component is given by

$$\begin{aligned} \delta_1 &= \frac{dx_1' - dx_1}{dx_1} = \epsilon_{11} \\ \delta_2 &= \frac{dx_2' - dx_2}{dx_2} = \epsilon_{22} \end{aligned} \quad (1.49)$$

$$\delta_3 = \frac{dx_3' - dx_3}{dx_3} = \epsilon_{33} \quad (1.50)$$

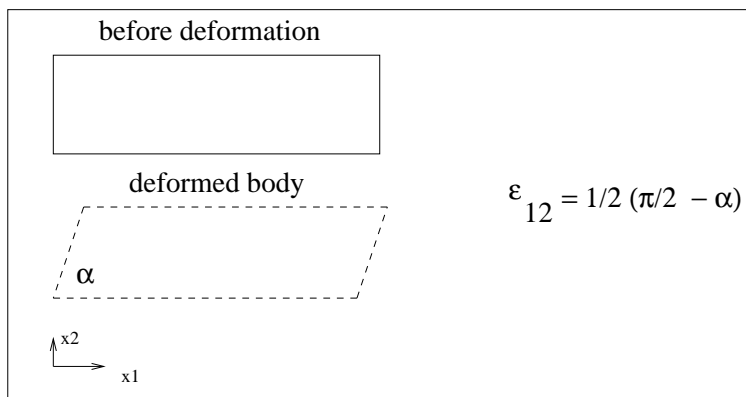


Figure 1.7: Shear strain involving angular changes (change of shape).

The volume of the cube after and before deformation is given by $dv = dx_1 dx_2 dx_3$ and $dv' = dx_1' dx_2' dx_3'$, respectively. Using the equations in (1.50) yield the following

$$\theta = \frac{dv' - dv}{dv} = \epsilon_{11} + \epsilon_{22} + \epsilon_{33}, \quad (1.51)$$

where θ is the volumetric strain. Note that this is the volumetric strain approximation to second order (I have neglected terms like $\epsilon_{11} \times \epsilon_{22}$). In short, assuming a small deformation the volumetric strain is equal to the divergence of \mathbf{u} ¹

$$\Theta = \epsilon_{11} + \epsilon_{22} + \epsilon_{33} = \frac{\partial u_1}{\partial x_1} + \frac{\partial u_2}{\partial x_2} + \frac{\partial u_3}{\partial x_3} = \text{div}(\mathbf{u}). \quad (1.52)$$

If we analyze the transformation of the scalar product after deformation, we will prove that the non-diagonal terms of the strain tensor characterize the change in angle between two vectors. Figure 1.7 shows the effect of pure shear deformation.

1.6 Constitutive Law of Linear Elasticity

So far we have been able to obtain equilibrium equations. On the one hand, we have three differential equations (see equation 1.23), on the other, we have nine unknowns (6 stress components and 3 displacements u_1, u_2, u_3). To proceed, we need a relationship between the elements of the stress tensor and displacement.

For small magnitude short duration stresses, almost all material in the earth show proportionality between stress and strain. This property is demonstrated empirically by applying forces to rocks and measuring deformations. The general constitutive law of linear elasticity also called *Hooke's Law* is given by

¹ $\text{div}(\mathbf{u}) = \nabla \cdot \mathbf{u}$

$$\sigma_{ij} = C_{ijkl}\epsilon_{kl}. \quad (1.53)$$

The constant of proportionality is a fourth-order tensor C_{ijkl} called stiffness tensor or elasticity tensor. The tensor C_{ijkl} constitutes a fourth-order tensor with $81 = 3 \times 3 \times 3 \times 3$ terms. Owing to the symmetries of the stress and strain tensor, the elastic tensor C_{ijkl} , must satisfy the following expressions

$$C_{ijkl} = C_{jikl} = C_{ijlk} \quad (1.54)$$

The last expressions reduce the components of the elastic tensor C_{ijkl} from 81 to 36. A second relation follows by considering the strain energy function ($\sigma_{ij} \times \epsilon_{ij}$), leaving 21 elastic moduli to define a material with *general anisotropy*. In other words, material properties depend on the orientation of the material. Fortunately, the elastic properties for many of Earth's materials are independent of the direction or orientation of the sample. It is possible to show that for the *isotropic case*, one only needs two independent elastic moduli, called the *Lamé constants*². The Lamé constants are called λ and μ

$$c_{ijkl} = \lambda\delta_{ij}\delta_{kl} + \mu(\delta_{ik}\delta_{jl} + \delta_{il}\delta_{jk}). \quad (1.55)$$

Replacing equation 1.55 into equation 1.53 leads to the constitutive law of linear elasticity for an isotropic elastic material

$$\begin{aligned} \sigma_{ij} &= \lambda\epsilon_{kk}\delta_{ij} + 2\mu\epsilon_{ij} \\ &= \lambda\theta\delta_{ij} + 2\mu\epsilon_{ij}, \end{aligned} \quad (1.56)$$

where $\theta = \epsilon_{kk}$ is the volumetric strain or cubic dilatation. The equations for normal stresses are given by

$$\begin{aligned} \sigma_{11} &= \lambda\theta + 2\mu\epsilon_{11} \\ \sigma_{22} &= \lambda\theta + 2\mu\epsilon_{22} \\ \sigma_{33} &= \lambda\theta + 2\mu\epsilon_{33} \end{aligned}$$

Similarly, the equations for shear stresses are

$$\begin{aligned} \sigma_{12} &= 2\mu\epsilon_{12} \\ \sigma_{13} &= 2\mu\epsilon_{13} \\ \sigma_{32} &= 2\mu\epsilon_{32} \end{aligned}$$

The constant μ is also called the rigidity factor. The parameter μ is a measure of resistance to shear stress. For a fluid $\mu = 0$ (no resistance to shear stresses). Other elastic moduli can be written as a function of λ and μ . Some of them have physical significance. These include

²Gabriel Lamé (1795 - 1870) was a French mathematician who contributed to the theory of partial differential equations and elasticity.

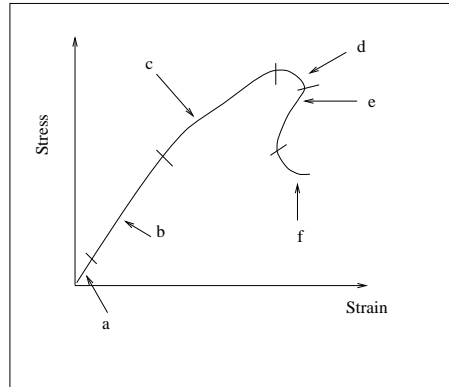


Figure 1.8: Stress-strain curve for a typical uniaxial compression test. a: closure of cracks. b: Linear elastic regime c and d: dilatation of the sample due to lateral expansion of the rock and micro-cracking. e: macroscopic shear failure. f: The stress is determined by the residual friction of the shear zone.

- Young's modulus $E = \mu \frac{3\lambda + 2\mu}{\lambda + \mu}$
- Bulk modulus³ $k = \lambda + \frac{2\mu}{3}$
- Poisson's ratio $\nu = \frac{\lambda}{2(\lambda + \mu)}$

³also called incompressibility

Chapter 2

Waves in elastic media

2.1 Equation of motion for elastic disturbances

In section 1.3.2 we derived the stress conditions for an elementary cube in equilibrium

$$\begin{aligned}\frac{\partial\sigma_{11}}{\partial x_1} + \frac{\partial\sigma_{21}}{\partial x_2} + \frac{\partial\sigma_{31}}{\partial x_3} &= 0 \\ \frac{\partial\sigma_{12}}{\partial x_1} + \frac{\partial\sigma_{22}}{\partial x_2} + \frac{\partial\sigma_{32}}{\partial x_3} &= 0 \\ \frac{\partial\sigma_{13}}{\partial x_1} + \frac{\partial\sigma_{23}}{\partial x_2} + \frac{\partial\sigma_{33}}{\partial x_3} &= 0.\end{aligned}\tag{2.1}$$

In our analysis, we did not consider body forces and an inertial term. The elementary cube was at rest. The above equations have units of force per volume. The integral over the volume of the body V yields the total force. For the first component, we can write

$$\int_V \left[\frac{\partial\sigma_{11}}{\partial x_1} + \frac{\partial\sigma_{21}}{\partial x_2} + \frac{\partial\sigma_{31}}{\partial x_3} \right] dv = 0.\tag{2.2}$$

To develop the equation of motion, we must balance forces using Newton's law. The net force due to stresses is equal to the inertial term (*mass* \times *acceleration*). For the first component, we have

$$\underbrace{\int_V \frac{\partial\sigma_{11}}{\partial x_1} + \frac{\partial\sigma_{21}}{\partial x_2} + \frac{\partial\sigma_{31}}{\partial x_3} dv}_1 = \underbrace{\int_V \rho \frac{\partial^2 u_1}{\partial t^2} dv}_2.\tag{2.3}$$

1. Net force due to the stress components
 2. Inertial term, $\text{mass} \times \text{acceleration}$, ρ is the density. In fact, $\rho \frac{\partial^2 u_1}{\partial t^2}$ is the inertial force term per volume in the x_1 direction.
-

We can write the last equation as follows

$$\int_V \left[\frac{\partial \sigma_{11}}{\partial x_1} + \frac{\partial \sigma_{21}}{\partial x_2} + \frac{\partial \sigma_{31}}{\partial x_3} - \rho \frac{\partial^2 u_1}{\partial t^2} \right] dv = 0, \quad (2.4)$$

and given that the volume V cannot be zero, the last equation is satisfied if

$$\frac{\partial \sigma_{11}}{\partial x_1} + \frac{\partial \sigma_{21}}{\partial x_2} + \frac{\partial \sigma_{31}}{\partial x_3} - \rho \frac{\partial^2 u_1}{\partial t^2} = 0. \quad (2.5)$$

One can write similar expressions for forces in x_1 and x_2 and arrive at the following general expression

$$\rho \frac{\partial^2 u_i}{\partial t^2} = \frac{\partial \sigma_{ij}}{\partial x_j} \quad i = 1, 2, 3. \quad (2.6)$$

These three partial differential equations constitute the *equations of motion for a continuum*. These are essential equations in seismology; they relate forces in the medium to measurable displacements (u_1, u_2, u_3). Displacements can be measured by placing tri-axial seismometers on the surface of the earth.

We have already defined the relationship that exists between the stress tensor and displacements (Hooke's law, see equation 1.56)

$$\begin{aligned} \sigma_{ij} &= \lambda \theta \delta_{ij} + 2\mu \epsilon_{ij} \\ \epsilon_{ij} &= \frac{1}{2} \left(\frac{\partial u_i}{\partial x_j} + \frac{\partial u_j}{\partial x_i} \right). \end{aligned} \quad (2.7)$$

If we assume that the constants μ and λ do not depend on x_i , $i = 1, 2, 3$ (homogeneity assumption), we end up with the following expression

$$\rho \frac{\partial^2 u_i}{\partial t^2} = (\lambda + \mu) \frac{\partial \theta}{\partial x_i} + \mu \nabla^2 u_i, \quad i = 1, 2, 3 \quad (2.8)$$

where the scalar Laplacian is given by

$$\nabla^2 u_i = \frac{\partial^2 u_i}{\partial x_1^2} + \frac{\partial^2 u_i}{\partial x_2^2} + \frac{\partial^2 u_i}{\partial x_3^2}. \quad (2.9)$$

The variable θ is the dilatation given by

$$\theta = \epsilon_{ii} = \frac{\partial u_i}{\partial x_i}. \quad (2.10)$$

This equation describes the propagation of a perturbation in an elastic material. In the next section, we will try to decouple volumetric deformations from deformations that only involve changes in shape.

2.2 Propagation of volumetric perturbations

The three equations that define propagation of the displacement field $\mathbf{u} = \mathbf{u}(x_1, x_2, x_3, t)$ in an elastic material are given by

$$\rho \frac{\partial^2 u_1}{\partial t^2} = (\lambda + \mu) \frac{\partial \theta}{\partial x_1} + \mu \nabla^2 u_1 \quad (2.11)$$

$$\rho \frac{\partial^2 u_2}{\partial t^2} = (\lambda + \mu) \frac{\partial \theta}{\partial x_2} + \mu \nabla^2 u_2 \quad (2.12)$$

$$\rho \frac{\partial^2 u_3}{\partial t^2} = (\lambda + \mu) \frac{\partial \theta}{\partial x_3} + \mu \nabla^2 u_3. \quad (2.13)$$

These three partial differential equations can be simplified. Our first simplification is to derive the associated equation for the variable θ . For this purpose, we differentiate the first equation of motion with respect to x_1 , the second with respect to x_2 and the third with respect to x_3 , and then we add them up. The resulting equation is a wave equation for the variable θ

$$\rho \frac{\partial^2 \theta}{\partial t^2} = (\lambda + 2\mu) \nabla^2 \theta \quad (2.14)$$

or

$$\frac{\partial^2 \theta}{\partial t^2} = v_p^2 \nabla^2 \theta \quad (2.15)$$

where

$$v_p^2 = \frac{\lambda + 2\mu}{\rho}. \quad (2.16)$$

At this point the following comments are in order. The so-called scalar wave equation (2.15) simplifies the three partial differential equations describing the propagation of $\mathbf{u} = (u_1, u_2, u_3)$. Secondly, the constant v_p has units of speed [Distance/Time]. At this point, it might not appear clear that the constant v_p is the speed of propagation of the displacement field $\mathbf{u} = \mathbf{u}(t, x_1, x_2, x_3)$. One can reduce the scalar wave equation to one-dimensional propagation by considering $\theta = \theta(t, x_1)$

$$\frac{\partial^2 \theta}{\partial t^2} = v_p^2 \frac{\partial^2 \theta}{\partial x_1^2} \quad (2.17)$$

and, easily show that the solution is giving by an expression of the form

$$\theta(x_1, t) = f(x_1 - v_p t). \quad (2.18)$$

with $f()$ a function to be determined via initial conditions.

The expression in equation 2.18 is known as *d'Alembert's solution*. It states that there is a perturbation that travels through the medium with velocity v_p . In this case, the perturbation is the volumetric perturbation θ . The latter corresponds to a P wave ($P \equiv Primary$). The speed, v_p , of the volumetric perturbation or the speed of the P wave is a function of the density ρ and the elastic parameters λ and μ . We can have an infinite number of solutions, for example, the following solutions satisfy the one-dimensional wave equation for the variable θ

$$\begin{aligned} & A e^{ik(x_1 - v_p t)} \\ & A (x_1 - v_p t)^5 \\ & A \sin(a(x_1 - v_p t) + \pi/2). \end{aligned}$$

The solution to a specific problem is found by considering among all the possible answers the one that satisfies initial conditions.

2.3 Propagation of shape perturbations

We can combine our equations of motion differently than in the previous section to obtain wave equations for the following variables

$$\psi_1 = \frac{\partial u_3}{\partial x_2} - \frac{\partial u_2}{\partial x_3} \quad (2.19)$$

$$\psi_2 = \frac{\partial u_1}{\partial x_3} - \frac{\partial u_3}{\partial x_1} \quad (2.20)$$

$$\psi_3 = \frac{\partial u_2}{\partial x_1} - \frac{\partial u_1}{\partial x_2} \quad (2.21)$$

The above variables define simple rotations about the three axes, and they correspond to changes in shape. Moreover, the shape of an elementary volume changes but not its volume when the ϕ_i wave travels in the medium.

After differentiating pairs of equations of motion and subtracting them (believe me this is easy!!) you can arrive to the following expressions for ψ_1 , ψ_2 , ψ_3 :

$$\frac{\partial^2 \psi_1}{\partial t^2} = v_s^2 \nabla^2 \psi_1 \quad (2.22)$$

$$\frac{\partial^2 \psi_2}{\partial t^2} = v_s^2 \nabla^2 \psi_2 \quad (2.23)$$

$$\frac{\partial^2 \psi_3}{\partial t^2} = v_s^2 \nabla^2 \psi_3 \quad (2.24)$$

where

$$v_s^2 = \frac{\mu}{\rho}. \quad (2.25)$$

We have three scalars wave equations that correspond to waves ψ_i travelling with velocity v_s . These are called S waves ($S \equiv \text{Secondary}$). Notice that $v_p > v_s$ because $\lambda > 0$.

The P waves are also known as dilatational, compressional, or irrotational waves. The S waves are also known as shear, transverse, or rotational waves.

Why P and S ? After an earthquake, the first wave that reaches a seismological station is a P wave (P Primary) and S is usually the second event recorded (S Secondary).

2.4 Equation of motion in vector form

The equations of motion for the displacement components u_i , $i = 1, 2, 3$ in equations 2.11, 2.12 and 2.13 can be expressed in vector form

$$\rho \frac{\partial^2 \mathbf{u}}{\partial t^2} = (\lambda + \mu) \nabla \theta + \mu \nabla^2 \mathbf{u} \quad (2.26)$$

where $\mathbf{u} = u_i \mathbf{e}_i$. I would like to remind the following expressions valid in Cartesian coordinates¹

Gradient of θ :

$$\nabla \theta = \frac{\partial \theta}{\partial x_i} \mathbf{e}_i$$

Divergence of \mathbf{u} :

$$\theta = \nabla \cdot \mathbf{u} = \frac{\partial u_i}{\partial x_i}$$

Vector Laplacian of \mathbf{u} :

$$\nabla^2 \mathbf{u} = \nabla(\nabla \cdot \mathbf{u}) - \nabla \times (\nabla \times \mathbf{u})$$

which in Cartesian coordinates is given by

$$\nabla^2 \mathbf{u} = \frac{\partial^2 u_1}{\partial x_1^2} \mathbf{e}_1 + \frac{\partial^2 u_2}{\partial x_2^2} \mathbf{e}_2 + \frac{\partial^2 u_3}{\partial x_3^2} \mathbf{e}_3$$

The definitions above permit to replace $\nabla^2 \mathbf{u}$ in equation 2.26 and by considering $\nabla \theta = \nabla(\nabla \cdot \mathbf{u})$,

$$\rho \frac{\partial^2 \mathbf{u}}{\partial t^2} = (\lambda + 2\mu) \nabla(\nabla \cdot \mathbf{u}) - \mu \nabla \times (\nabla \times \mathbf{u}). \quad (2.27)$$

Now I would like to remind you of two theorems

¹Remember that I am using Einstein notation.

Th1: If \mathbf{a} is a vector field then $\nabla \cdot (\nabla \times \mathbf{a}) = 0$ (*The divergence of the curl is zero*)

Th2: If α is scalar field $\nabla \times (\nabla \alpha) = 0$ (*The curl of the gradient is zero*)

We now apply the divergence operator to both sides of equation 2.27 and **Th1** to obtain

$$\rho \frac{\partial^2 \theta}{\partial t^2} = (\lambda + 2\mu) \nabla^2 \theta \quad (2.28)$$

the above equation was already derived via a different route in section 2.2. Equation 2.28 corresponds to the scalar wave equation for θ . The wave, as we have discussed propagates with P-wave velocity $v_p = \sqrt{(\lambda + 2\mu)/\rho}$. We can also apply the curl operator to both sides of equation 2.27 and making use of **Th2** we obtain

$$\rho \frac{\partial^2 \boldsymbol{\psi}}{\partial t^2} = \mu \nabla^2 \boldsymbol{\psi} \quad (2.29)$$

where $\boldsymbol{\psi} = \psi_1 \mathbf{e}_1 + \psi_2 \mathbf{e}_2 + \psi_3 \mathbf{e}_3$ and $\boldsymbol{\psi} = \nabla \times \mathbf{u}$. Notice that equation 2.29 is the vector form of equations 2.22, 2.23 and 2.24 that were derived via a different route. $\boldsymbol{\psi} = \psi_1 \mathbf{e}_1 + \psi_2 \mathbf{e}_2 + \psi_3 \mathbf{e}_3$. In this section I have derived P and S-wave equations using vector calculus and arrived to the results already given by sections 2.2 and 2.3.

2.5 Derivation of the 1D wave (Review)

You probably have seen this section in a first-year introductory course to physics. We could have obtained the wave equation for a one-dimensional rod using a straightforward method.

We first consider an elastic infinitely long rod extending along x_1 . Consider a *source* that produces a disturbance in the rod. The disturbance will induce stresses within the rod which are unbalanced. In other words, the equations for static equilibrium are no longer valid, and the balance of forces requires the inclusion of an inertial term. In Figure 2.1 we illustrate the stress differences induced by the presence of the disturbance. The net force is given by

$$\sum F_{x_1} = m \frac{\partial^2 u_1}{\partial t^2} = (\sigma_{11} - \sigma_{11}') \Delta A_1, \quad (2.30)$$

where we can write

$$\sigma_{11}' = \sigma_{11} + \frac{\partial \sigma_{11}}{\partial x_1} \Delta x_1 \quad (2.31)$$

In other words, I have linearized the stress using a first order Taylor approximation (see section 1.3.2). The equation of motion for our simple problem is given by

$$\sum F_{x_1} = m \frac{\partial^2 u_1}{\partial t^2} = \rho \Delta A_1 \Delta x_1 \frac{\partial^2 u_1}{\partial t^2} = \frac{\partial \sigma_{11}}{\partial x_1} \Delta x_1 \Delta A_1. \quad (2.32)$$

Last equation can be written as follows

$$\rho \frac{\partial^2 u_1}{\partial t^2} = \frac{\partial \sigma_{11}}{\partial x_1}. \quad (2.33)$$

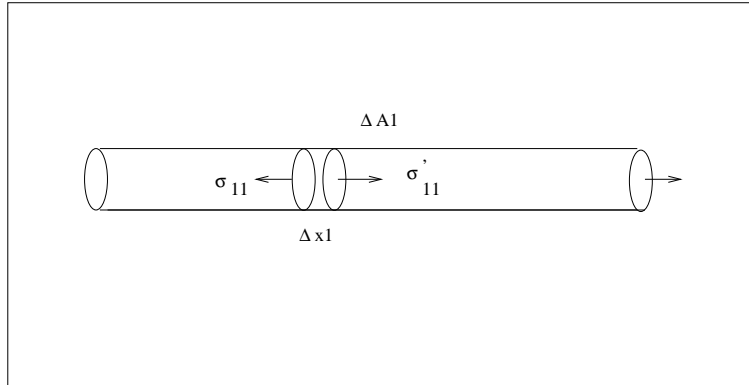


Figure 2.1: 1D wave equation. The rod is under an unbalanced stress field (see text for details).

The constitutive law (Hooke's law) for this particular problem is given by

$$\sigma_{11} = E\epsilon_{11} = E\frac{\partial U_1}{\partial x_1} \quad (2.34)$$

where E is Young's modulus. After replacing the last equation in equation (2.33) we obtain the one-dimensional wave equation

$$\frac{\partial^2 u_1}{\partial t^2} = c^2 \frac{\partial^2 u_1}{\partial x_1^2}. \quad (2.35)$$

The direction of propagation of the perturbation is x_1 , and the speed of propagation is given by c

$$c = \sqrt{\frac{E}{\rho}} \quad (2.36)$$

The general solution for the 1D wave equation is

$$u_1(x_1, t) = f(x_1 - ct) + g(x_1 + ct), \quad (2.37)$$

where f and g are arbitrary function to determine from initial conditions.

Remarks

- f propagates in the direction $+x_1$
- g propagates in the direction $-x_1$

The arguments $x_1 + ct$ and $x_1 - ct$ are called the phase of the wave. The functionals f and g are called wavefronts. One can propose the so-called *Harmonic Solutions*. These are solutions of

the following form

$$u_1(x_1, t) = Ae^{ia(x_1-ct)} + Be^{ib(x_1+ct)} \quad (2.38)$$

The latter is called a *Monochromatic Wave*. Before describing 3D waves, we will study the meaning of the different variables that are involved in the harmonic solution. For simplicity, I will only consider a wave travelling in the direction $+x_1$

$$u_1(x_1, t) = Ae^{i\omega(t-x_1/c)} \quad (2.39)$$

Equations 2.38 and 2.39 are equivalent one takes $\omega = -a/c$. The above expression can be written as

$$\begin{aligned} u_1(x_1, t) &= Ae^{i\omega(t-x_1/c)} \\ &= Ae^{i(\omega t - \omega x_1/c)} \\ &= Ae^{i(\omega t - kx_1)} \\ &= Ae^{i(2\pi ft - kx_1)} \\ &= Ae^{i2\pi(ft - kx_1/2\pi)} \\ &= Ae^{i2\pi(ft - x_1/\lambda)} \\ &= Ae^{i2\pi(t/T - x_1/\lambda)} \end{aligned}$$

where

- Angular frequency ω [radians/seconds]
- Frequency $f = \frac{\omega}{2\pi}$ [Hertz \equiv 1/second]
- Period $T = \frac{1}{f}$ [seconds]
- Wavenumber $k = \frac{\omega}{c}$ [radians/meter]
- Wavelength $\lambda = \frac{2\pi}{k}$ [meters]

We will come back to harmonic solutions and analyze them in the context of Fourier analysis.

2.5.1 Visualizing waves in t and x

It is clear that the solution to the wave equation is a function of t (time) and \mathbf{x}^2 . We will consider the experiment illustrated in Figure 2.2. A source indicated with the symbol “*” excites a perturbation that travels to the right in a homogeneous rod. We have been able to attach small receivers³ evenly distributed along the rod. The receivers measure the variable u_1 versus time. We know that the perturbation traveling to the right has the following form

² $\mathbf{x} = (x_1, x_2, x_3)$

³Transducers, or geophones as they are often called in seismic exploration.

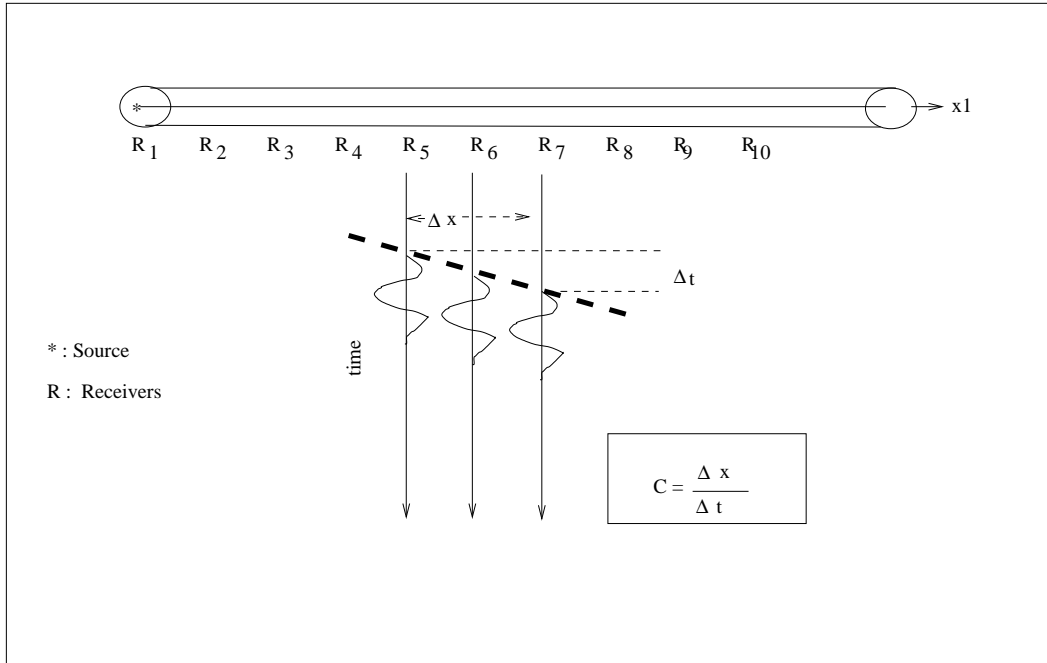


Figure 2.2: 1D wave equation. A source indicated by “*” excites a P wave traveling to the right. The receivers ”R” record a waveform at different positions. If the rod is homogeneous, the velocity of propagation (c) can be extracted from the $t - x$ diagram.

$$u_1(x_1, t) = f(x_1 - ct)$$

and that the latter is a solution to the 1D wave equation. In our toy experiment, the variable x_1 is not continuously sampled. Receivers measure the wavefield at discrete positions $x_1 = r_i$ (position of the receiver i). Our observations at the position r_i is given by

$$u_1(r_i, t) = f(r_i - ct), \quad i = 1, \dots, NR.$$

NR indicates the number of receivers. To calculate the speed of the rod, we will display the time data in a $t - x$ diagram. In Figure 2.2, we portrayed the seismograms corresponding to the receivers R_5 , R_6 , and R_7 . The travel-time difference Δt is measured from the diagram and used to estimate the velocity of propagation c .

In Figure 2.3, we have the $t - x$ diagram for the experiment (this is a computer simulation, not an actual test). In this case the velocity of the rod is $c = 0.5 \text{ km/s}$. In Figure 2.3a, we show the data plotted in *Seismic Style*⁴ where we display seismograms (seismic traces) versus position (x_1). Figure 2.3b presents seismograms displayed as spatial traces versus time (this is uncommon). In both cases, one can estimate the speed of the wave from the diagrams. Figure 2.4 shows the same experiment but for a different velocity. Can you measure c from the data?.

⁴Wiggle plot

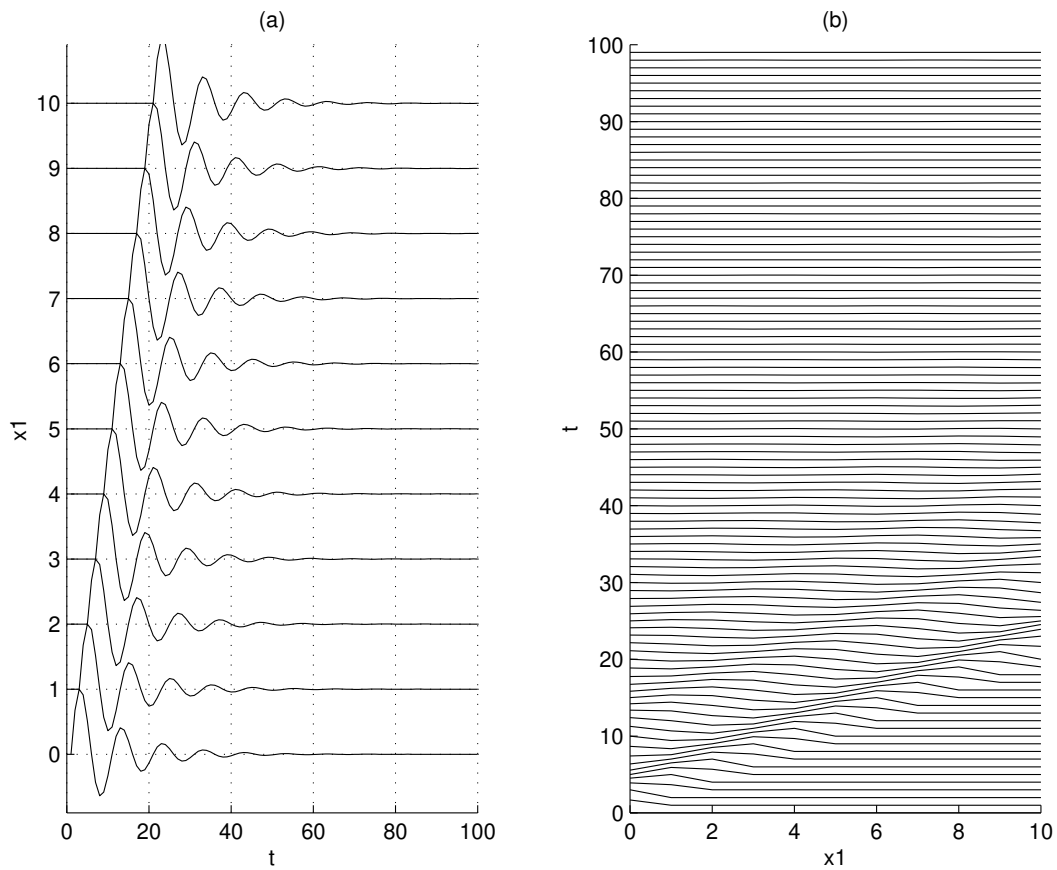


Figure 2.3: 1D wave equation. (a) A diagram of $u(x_1, t)$ in seismic style, time series (seismograms or seismic traces) versus space. (b) The same information is plotted as spatial traces versus time. The time is given in *sec* and the distance in *km/sec*, $c = 0.5 \text{ km/sec}$. Can you determine c from the diagram?

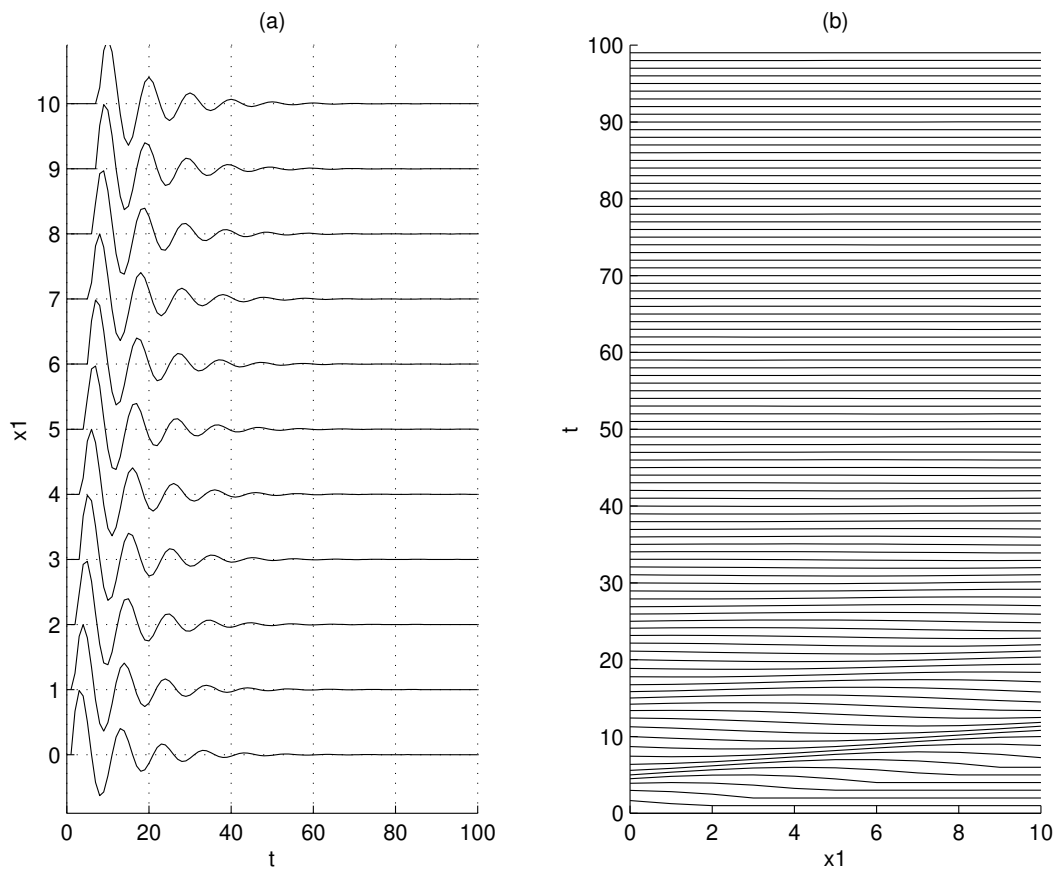


Figure 2.4: 1D wave equation. Can you determine c from the diagram? The units are *sec* and *km*.

2.5.2 Why do we adopt harmonic solutions ?

In section 2.3, we discussed the solution of the 1D wave equation. We also wrote down a particular solution to the wave an equation called the harmonic solution

$$u_1(x_1, t) = Ae^{i\omega(t-x_1/c)}$$

In this section, we will try to highlight the importance of the harmonic solution in wavefield analysis and in seismology.

The following equation is also a solution of the wave equation

$$u_1(x_1, t) = \sum_n A_n e^{i\omega_n(t-x_1/c)}. \quad (2.40)$$

we have already mentioned that the "solution" is the one that satisfies initial conditions of the type $u(x_1 = 0, t) = s(t)$

If we write the general solution as

$$u_1(x_1, t) = f(t - x_1/c) \quad (2.41)$$

it is easy to see that

$$u_1(0, t) = f(t) = s(t) \text{ (initial condition)}. \quad (2.42)$$

$$u_1(x_1, t) = s(t - x_1/c) \quad (2.43)$$

According to Fourier analysis, any function defined in an interval $[t_0, t_0 + T]$ can be represented as a superposition of harmonics

$$s(t) = \sum_{n=-\infty}^{\infty} \alpha_n e^{in\omega_0 t}. \quad (2.44)$$

The latter is also called a *Fourier Series*. The variable ω_0 (the fundamental frequency) is given by

$$\omega_0 = \frac{2\pi}{T} \quad (2.45)$$

The coefficients α_n are computed via the following expression:

$$\alpha_n = \frac{1}{T} \int_{t_0}^{t_0+T} s(t) e^{-in\omega_0 t} dt. \quad (2.46)$$

we can call $w_n = \omega_0 \times n$ and the Fourier representation $s(t)$ becomes,

$$s(t) = \sum_{n=-\infty}^{\infty} \alpha_n e^{i\omega_n t}. \quad (2.47)$$

Then, the solution of the 1D wave equation becomes

$$u_1(x_1, t) = s(t - x_1/c) = \sum_{n=-\infty}^{\infty} \alpha_n e^{i\omega_n(t-x_1/c)}. \quad (2.48)$$

We have been able to write the solution of the wave equation with initial condition $u_1(0, t) = s(t)$ as a superposition of complex exponentials. Now, we can analyze our wave equation problems with a single harmonic component of the form $e^{i\omega t - x_1/c}$, the generalization to more complicated problems is straightforward via the Fourier decomposition.

In Figure 2.5, we show a function $s(t)$. In Figure 2.6 we show the Fourier analysis and reconstruction of $s(t)$. In Figure 2.6a, we have the real part of each Fourier component.

$$\text{Real}[\alpha_n e^{i\omega_n t}], \quad (2.49)$$

the diagram shows the above function versus time and n . Figure 2.6b, displays the imaginary part of each Fourier component as a function of t and n ,

$$\text{Imag}[\alpha_n e^{i\omega_n t}]. \quad (2.50)$$

Figures 2.7c and d are the Fourier synthesis of the real and imaginary parts

$$\sum_n \text{Real}[\alpha_n e^{i\omega_n t}], \quad (2.51)$$

$$\sum_n \text{Imag}[\alpha_n e^{i\omega_n t}]. \quad (2.52)$$

The sum of the real components recovers the original function $s(t)$ (Figure 2.6c). Given that the original function $s(t)$ is real, the sum of the imaginary components is zero as it should be!

2.6 Plane Waves

We return to the 3D equation of motion for the propagation of volumetric and shear perturbations

$$\frac{\partial^2 \theta}{\partial t^2} = v_p^2 \nabla^2 \theta \quad (2.53)$$

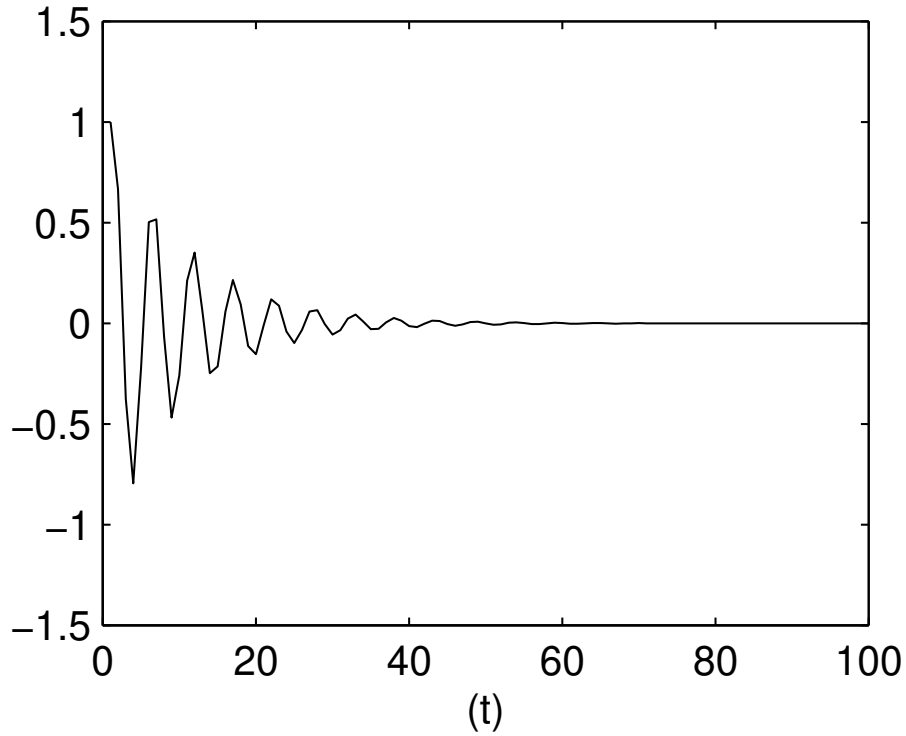


Figure 2.5: A synthetic waveform, $s(t)$.

$$\frac{\partial^2 \psi_i}{\partial t^2} = v_s^2 \nabla^2 \psi_i, \quad i = 1, 2, 3. \quad (2.54)$$

I will solve the wave equation for the variable $\theta = \nabla \mathbf{u}$, but keep in mind that the same procedure can be used to solve for ψ_i or any other variable. I will use a method called *separation of variables* to reduce a complicated second order partial differential equation into ordinary differential equations. First, we will assume that the solution has the following form

$$\theta(x_1, x_2, x_3, t) = X_1(x_1) X_2(x_2) X_3(x_3) T(t). \quad (2.55)$$

If we replace the separable expression of θ in the wave equation, we will find the following expression

$$\begin{aligned} X_1'' + k_1^2 X_1 &= 0 \\ X_2'' + k_2^2 X_2 &= 0 \\ X_3'' + k_3^2 X_3 &= 0 \\ T'' + \omega^2 T &= 0 \end{aligned} \quad (2.56)$$

$$(2.57)$$

where the following dispersion relation must be satisfied

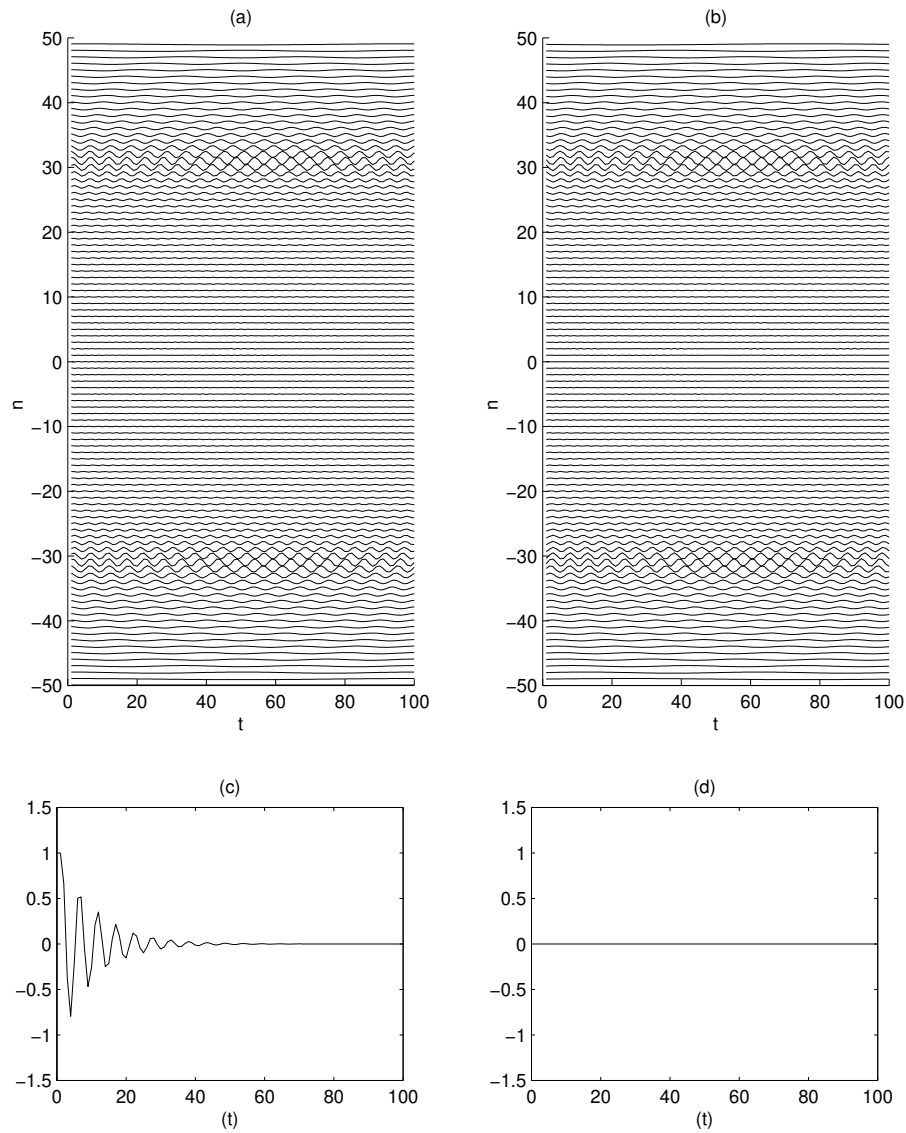


Figure 2.6: Fourier decomposition of the synthetic waveform. (a) Real part. (b) Imaginary part. (c) Reconstruction of the real part. (d) Reconstruction of the imaginary part

$$\frac{\omega^2}{v_p^2} = k_1^2 + k_2^2 + k_3^2. \quad (2.58)$$

We can now solve for X_1 , X_2 , X_3 and T

$$\begin{aligned} X_1 &= A_1 e^{\pm i k_1 x_1} \\ X_2 &= A_2 e^{\pm i k_2 x_1} \\ X_3 &= A_3 e^{\pm i k_3 x_1} \\ T &= A_t e^{\pm i \omega t}. \end{aligned} \quad (2.59)$$

It is evident that I have assumed harmonic solutions. The final answer is given by

$$\theta(x_1, x_2, x_3, t) = A e^{i(\omega t \pm k_1 x_1 \pm k_2 x_2 \pm k_3 x_3)}. \quad (2.60)$$

Last equation is the 3D harmonic solution of the wave equation. The solution again assumes a d'Alembert form. This solution corresponds to a set of *plane waves*, free to propagate in any direction. The direction of propagation of the wave is given by the wave vector \mathbf{k}

$$\mathbf{k}_p = |\mathbf{k}| \hat{k} = \frac{\omega}{v_p} \hat{k}. \quad (2.61)$$

Let us assume that the plane wave propagates with a wavenumber vector \mathbf{k}_p which is completely contained in the plane $x_1 x_3$. In this case, $k_2 = 0$ and $\partial/\partial x_2 = 0$. Now, the dispersion equation is given by

$$\frac{\omega^2}{v_p^2} = k_1^2 + k_3^2. \quad (2.62)$$

The wavenumber vector is perpendicular to the plane wave. In Figure 2.7, I display the wavenumber vector. I also define the angle i . We can see from the figure that

$$k_1 = \frac{\omega}{v_p} \sin i = \omega p \quad (2.63)$$

and

$$k_3 = \frac{\omega}{v_p} \cos i = \omega \eta. \quad (2.64)$$

The variable p is called the *ray parameter* or *horizontal slowness* and η is called the *vertical slowness* or *vertical ray parameter*. Figures 2.8 and 2.9 show a plane wave of the form $f(t - px_1 - \eta x_2)$. We have already discussed that a superposition of harmonic waves can be used to construct any arbitrary wave.

Can you determine from the diagrams in Figure 2.8 and 2.9 and the parameters p and ν ?

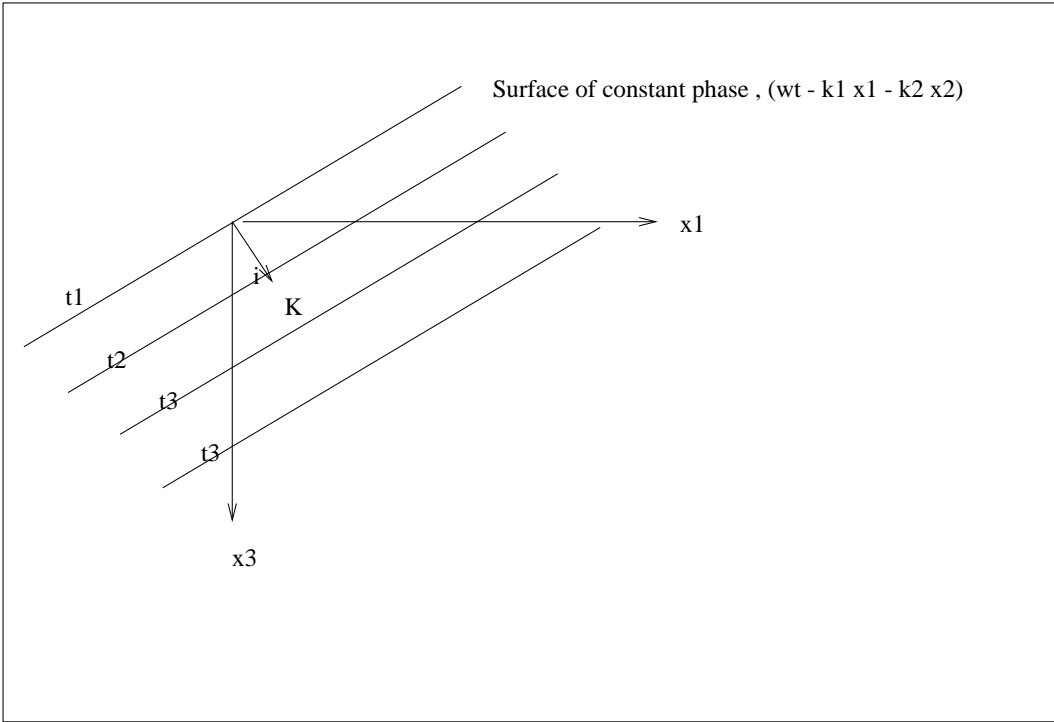


Figure 2.7: Plane wave in the plane x_1x_3 .

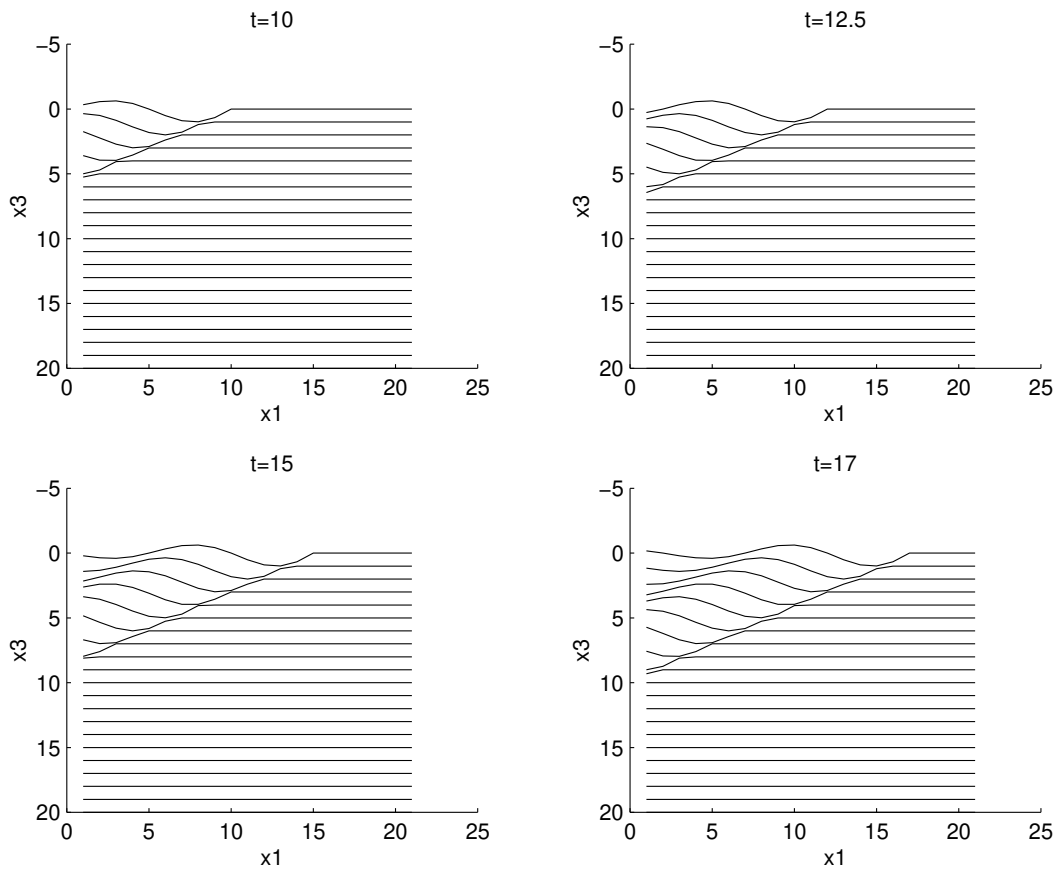


Figure 2.8: Plane wave. $i = 30\pi/180$, $c = 0.5$ km/s. Units in km and sec

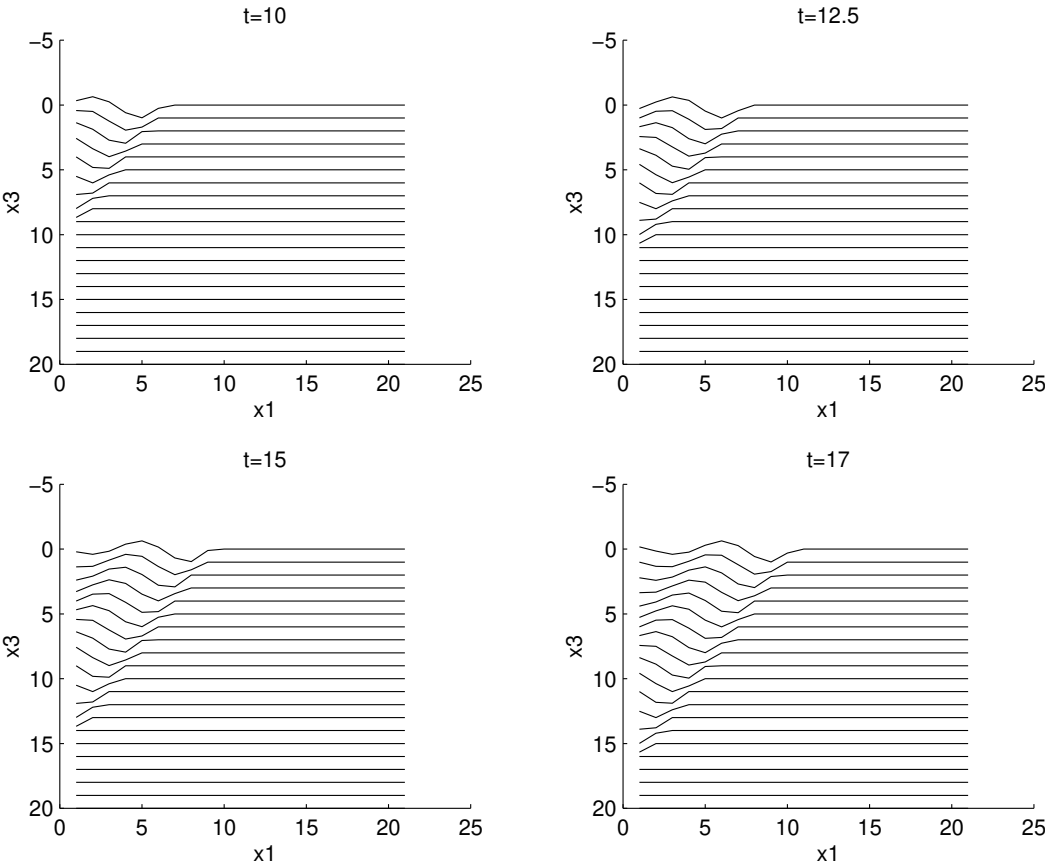


Figure 2.9: Plane wave. $i = 60\pi/180$, $c = 0.5 \text{ km/s}$. Units in km and sec

2.7 Spherical Waves

We will consider waves that depend only on r and t , where r is the distance $r = \sqrt{x_1^2 + x_2^2 + x_3^2}$. In this case the wave equation in spherical coordinates is given by

$$\frac{1}{v_p^2} \frac{\partial^2 \theta}{\partial t^2} = \frac{1}{r^2} \frac{\partial}{\partial r} \left(r^2 \frac{\partial \theta}{\partial r} \right). \quad (2.65)$$

The solution for the volumetric perturbation becomes

$$\theta(r, t) = \frac{1}{r} f(r - v_p t) + \frac{1}{r} f(r + v_p t). \quad (2.66)$$

The first term corresponds to a wave expanding outward from a central point ($r = 0$) that corresponds to the source location. The second term represents a collapsing wave (implosion). We will consider waves generated at a point P and traveling outward from P , $u = 1/r f(r - v_p t)$ (Figure 2.10).

As r increases outward from the source a portion of the spherical waveform near any particular point can be approximated by a plane wave. Plane waves are mathematically simple, and therefore, we will generally use the plane wave approximation.

2.8 Energy of waves

2.8.1 Geometrical spreading

We are interested in an expression for the energy of a point perturbed by the motion of a wave. If we consider a spherical wave where the radial displacement $u(r, t)$ is given by

$$u(r, t) = \frac{1}{r} A \cos(\omega t - kr), \quad (2.67)$$

at a fixed point r , u is given by

$$u(t) = A \cos(\omega t + \phi), \quad (2.68)$$

where A and ϕ are constants. The kinetic energy per unit of volume is given by

$$L = \frac{1}{2} \rho \left(\frac{\partial u}{\partial t} \right)^2 = \frac{1}{2} \rho \omega^2 A^2 \sin^2(\omega t + \phi) \quad (2.69)$$

The total energy is the kinetic plus the potential energy P ,

$$E = L + P. \quad (2.70)$$

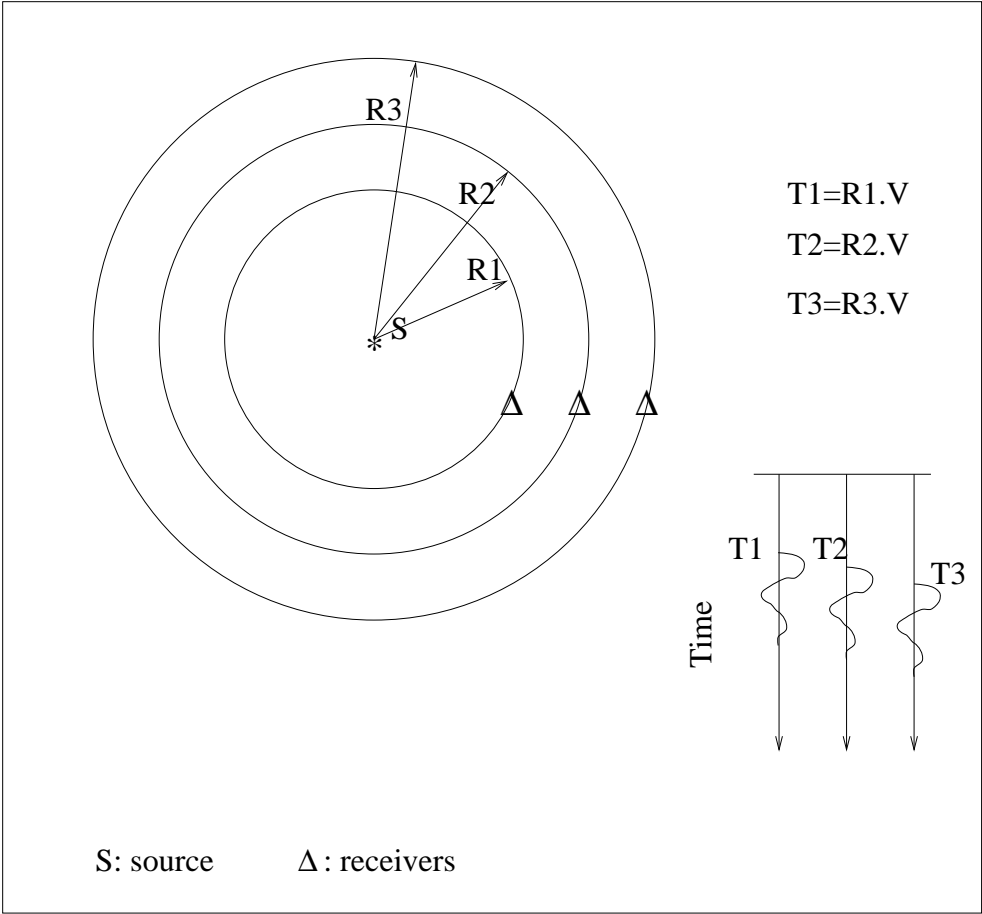


Figure 2.10: A spherical wave reaching an array of receivers.

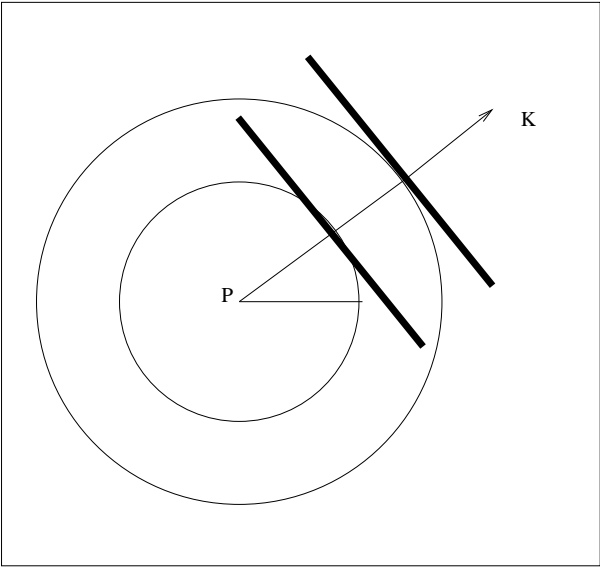


Figure 2.11: Spherical waves and the plane wave approximation.

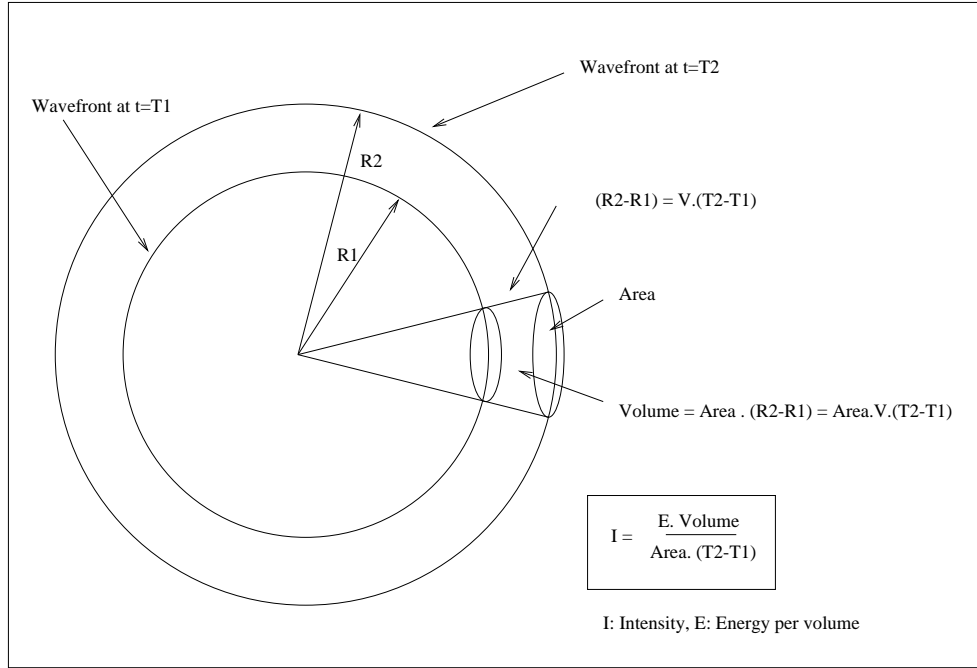


Figure 2.12: Intensity of a spherical wave.

As the medium oscillates, the energy is converted back and forth from kinetic into potential energy. When the kinetic energy is maximum the potential is minimum and vice-versa. The total energy can be computed at the point where the kinetic energy is maximum and therefore, the potential reaches its minimum value ($P = P_{min} = 0$),

$$E = L_{max} + P_{min} = \frac{1}{2} \rho \omega^2 A^2. \quad (2.71)$$

The intensity of the spherical wave is the rate of flow of energy per area in 1 sec (Figure (2.12))

$$I = \frac{E \times Volume}{Area \times \delta t} = \frac{E \times v_p \times \delta t \times Area}{Area \times \delta t} \quad (2.72)$$

For simplicity, I have considered a spherical wave of type P . If we consider that the total energy per time is conserved, we can write

$$\frac{I_2}{I_1} = \left(\frac{r_1}{r_2}\right)^2 \quad (2.73)$$

The intensity decreases inversely to the square root of the distance from the source. This phenomenon is called geometrical spreading or spherical divergence. In a constant velocity medium, a spherical wave expanding outward from a central source can be written as follows

$$u(r, t) = \frac{1}{r} f(r - v_p . t). \quad (2.74)$$

Geometrical spreading can be compensated using a *gain function*. Seismic data must be gained at initial processing stages to compensate for the amplitude decay caused by geometrical spreading. This task involves multiplying seismograms by a gain function that $g(t)$

$$g(t) \times u(r, t) = g(t) \times \frac{1}{r} f(r - v_p t). \quad (2.75)$$

The spreading term can be corrected by

$$g(t) = r = v_p \times t \propto t \quad (2.76)$$

In a constant velocity medium, a gain function of the type $g(t) \propto t$ will correct the amplitude decay introduced by the term $1/r$. In a medium, with variable velocity, this type of correction is difficult to apply. Practical flows for seismic data processing often adopt an empirical gain function $g(t)$ to compensate the amplitude decay introduced by geometrical spreading and attenuation.

In Figures (2.13) and (2.14) we can visualize the combined effect of geometrical spreading and attenuation of a field record (shot gather). Seismic reflections (hyperbolic events) become weaker with time. To visualize deep reflections (reflections that arrive at late times), we multiple each seismogram by the gain function. In our example (Figure (2.14)), I applied the following gain function

$$g(t) = t^2 \times e^{0.5t}. \quad (2.77)$$

2.8.2 Attenuation

Absorption or attenuation is another mechanism which causes the energy of a wave to decay. In an ideal elastic medium, the amplitude of waves is controlled by geometrical spreading and the reflection and transmission of energy at boundaries or interfaces. In a more realistic scenario, the rocks do not behave like perfect elastic bodies. Waves travelling in the *real earth* attenuate due to various types of energy-loss mechanisms. The conversion of kinetic energy into potential energy in a real rock is not an entirely reversible process. This phenomenon is named internal friction. The simplest description of attenuation can be developed by considering a mass-spring system where we introduce attenuation by adding a damping force (friction) into the problem. The equation of motion for the system is given by

$$\frac{d^2 x}{dt^2} + \gamma \frac{dx}{dt} + kx = 0. \quad (2.78)$$

where m is the mass, k is the constant of the spring and γ the coefficient of friction. The following expression is the solution to the spring-mass system with attenuation

$$x(t) = A_0 e^{-\epsilon \omega_0 t} \sin(\omega_0 t \sqrt{1 - \epsilon^2}) \quad (2.79)$$

where $\epsilon = \gamma/(m\omega_0)$. If $\epsilon = 0$ there is no attenuation and we will say that we are in the perfectly elastic case (no energy losses due to friction). Friction introduces the exponential decay into the solution. The exponential decay is usually expressed in terms of the quality factor Q ,

$$\epsilon = \frac{1}{2Q}. \quad (2.80)$$

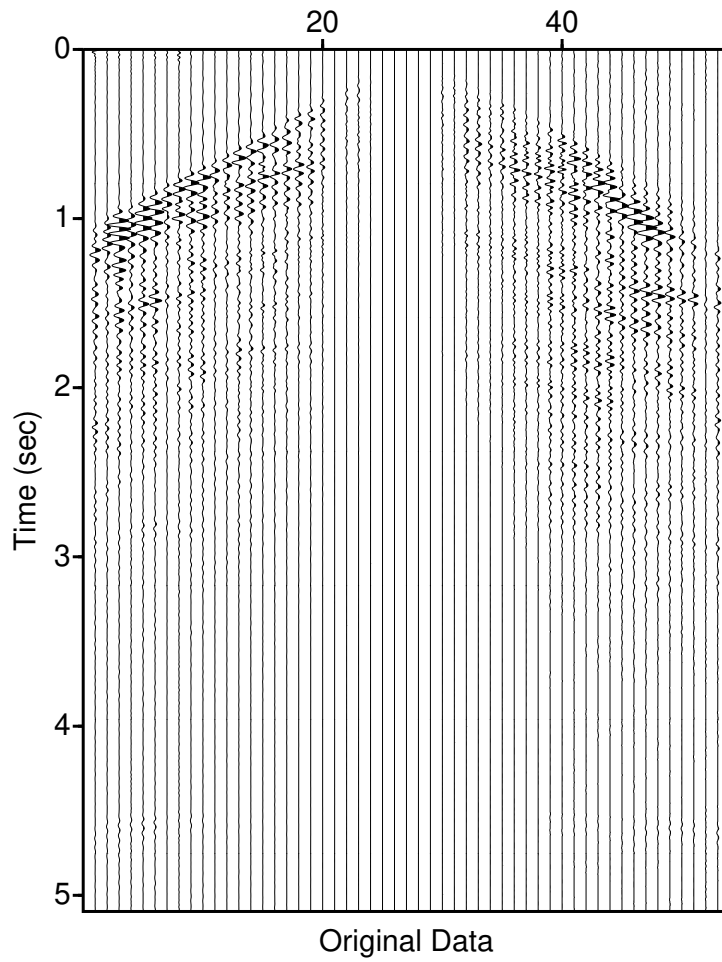


Figure 2.13: Field seismic record before gain correction. The combine effect of geometrical spreading and attenuation inhibits the proper visualization of seismic events.

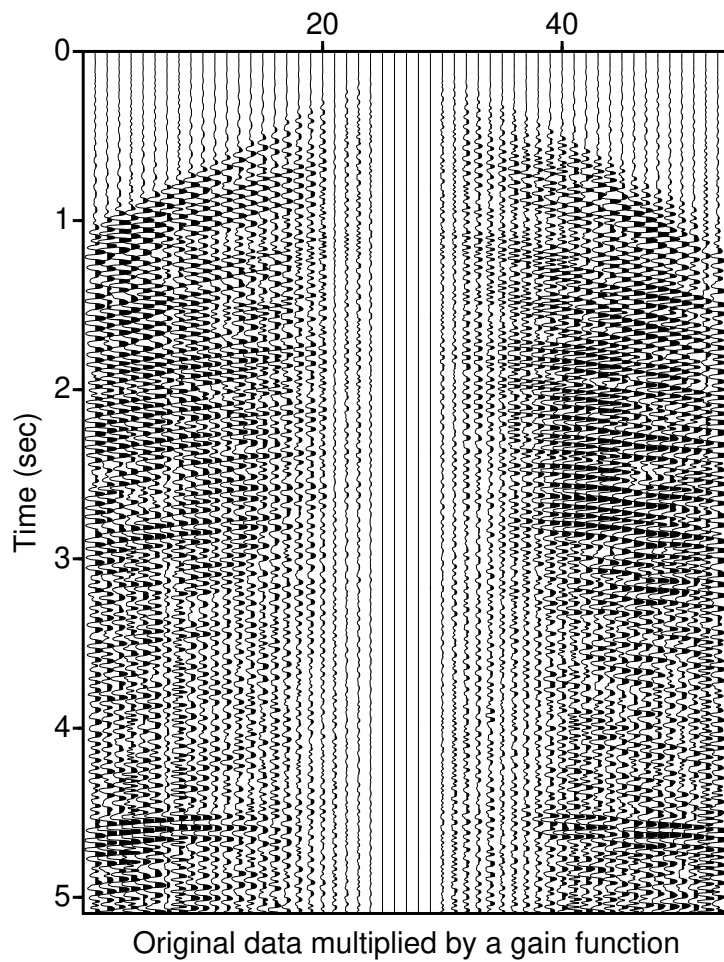


Figure 2.14: A gain function of the form $g(t) = t^2 \times e^{0.5t}$ was applied to correct for the temporal amplitude decay.

The quality factor is defined in terms of the fractional loss of energy per cycle of oscillation,

$$\frac{1}{Q} = -\frac{\Delta E}{2\pi E}. \quad (2.81)$$

Chapter 3

Rays

3.1 Introduction

In preceding chapters, we have analyzed the solution of the wave equation. We have shown that the solution of the wave equation leads to the concept of wavefronts. A wavefront is the set of points that at a given time undergo the same motion. *Rays* are defined as the normal to the wavefronts, in other words, rays describe the direction of propagation of the perturbation.

For a plane wave, the rays are a family of parallel straight lines. In the spherical wave case, rays are straight lines radiating from the centre of the spherical wave (the position of the source) (Figure (3.1)). Rays provide an intuitive scenario to understand wave propagation. We will abandon partial differential equations, and we will concentrate on describing time-space curves which arise from ray theory. For this purpose we will use two fundamental principles which you might have already seen in optics: Huygens' and Fermat's principles.

The geometry of a wavefront is governed by Huygens' principle which states that every point in a wavefront can be considered a small secondary wavelet which travels outward in every

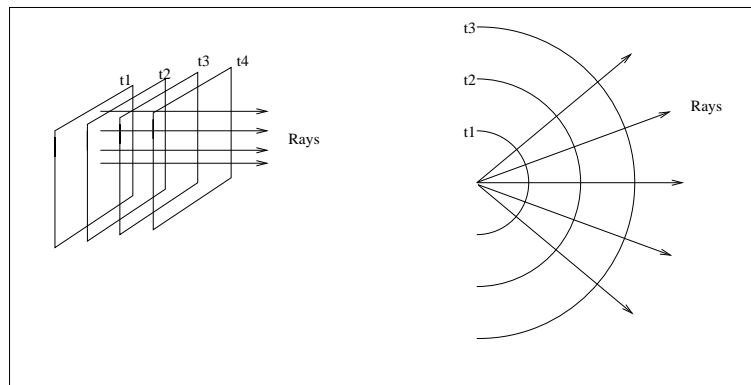


Figure 3.1: Plane waves and spherical waves.

direction with the velocity of propagation of the medium at that point. If we know the wavefront at a given instant, we can use this principle to draw the wavefront at a position in a future time.

Huygens' principle governs the geometry of wavefronts. Fermat's principle governs the geometry of ray-paths. This principle states that the ray will follow a *minimum time path*.

3.2 Snell's Law

It is possible to use Fermat's principle to derive Snell's law. Consider a ray leaving a point P (Figure (3.2)) in a medium with velocity v_1 . Which path will the ray take to reach the point Q ? Assume the velocity of the second medium is v_2 .

In Figure (3.2), I plotted three alternative paths, which one is the right path? According to Fermat's principle, the seismic ray will travel along a minimum time path. To solve the problem, one needs to obtain an expression of T (traveltime) as a function of a suitable variable. In this case, I will write the problem as a function of the distance x (Figure (3.3)). The traveltime for the wave to travel from P to Q is given by

$$T(x) = \frac{\overline{PO}}{v_1} + \frac{\overline{OQ}}{v_2} \quad (3.1)$$

where

$$\overline{PO} = \sqrt{(x - x_P)^2 + y_P^2} \quad (3.2)$$

$$\overline{OQ} = \sqrt{(x_Q - x)^2 + y_Q^2}. \quad (3.3)$$

The minimum is found by equating to zero the derivative of $T(x)$ with respect to the variable x :

$$\frac{dT}{dx} = 0 \quad (3.4)$$

$$\frac{dT}{dx} = \frac{2(x - x_P)}{v_1 \overline{PO}} - \frac{2(x_Q - x)}{v_2 \overline{OQ}} = 0 \quad (3.5)$$

from the above equation, we can recognize the following

$$\sin(i) = \frac{(x - x_P)}{\overline{PO}} \quad (3.6)$$

$$\sin(j) = \frac{(x_Q - x)}{\overline{OQ}} \quad (3.7)$$

Replacing $\sin(i)$ and $\sin(j)$ into equation (3.5)

$$\frac{dT}{dx} = \frac{2}{v_1} \sin(i) - \frac{2}{v_2} \sin(j) = 0, \quad (3.8)$$

the latter is called Snell's law, which I will re-write as follows:

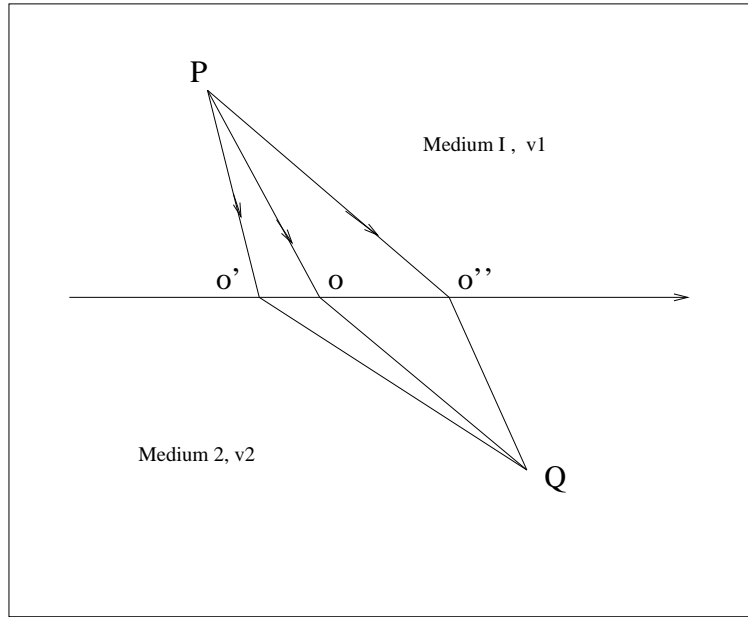


Figure 3.2: Ray paths connecting two points. Which is the correct path for a wave traveling from P to Q ?

$$\frac{\sin(i)}{v_1} = \frac{\sin(j)}{v_2}. \tag{3.9}$$

In Figure 3.4, I plotted different ray trajectories for a model like the one given in Figure 3.2. In the numerical example, I have adopted velocities $v_1 = 2000m/s$ and $v_2 = 3000m/s$. The traveltime curve ($T(x)$) shows a minimum at $x = 1000m$. The point $x = 1000m$ corresponds to the minimum time path or, in other words, the trajectory required by the ray to travel from P to Q . I also plotted the curves $\sin(i)/v_1$ and $\sin(j)/v_2$ versus x . Snell's law is satisfied when the two curves intercept.

We have analyzed what is called a transmitted wave. It is important to note that when a seismic wave reaches a boundary between different materials, we have also reflected waves. We can use Fermat's principle principle to compute the minimum travel-time condition for a reflected wave. Part of the incident energy is transmitted, and a portion is reflected (Figure 3.6). Snell's law governs the geometry of the ray paths. For the transmitted wave, we have

$$\frac{\sin(i)}{v_1} = \frac{\sin(j)}{v_1} \tag{3.10}$$

and for the reflected wave,

$$\frac{\sin(i)}{v_1} = \frac{\sin(i')}{v_1} \Rightarrow i = i' \tag{3.11}$$

If the velocity of the second half space is greater than the velocity of the upper half space ($v_2 > v_1$) the angles satisfy the following condition

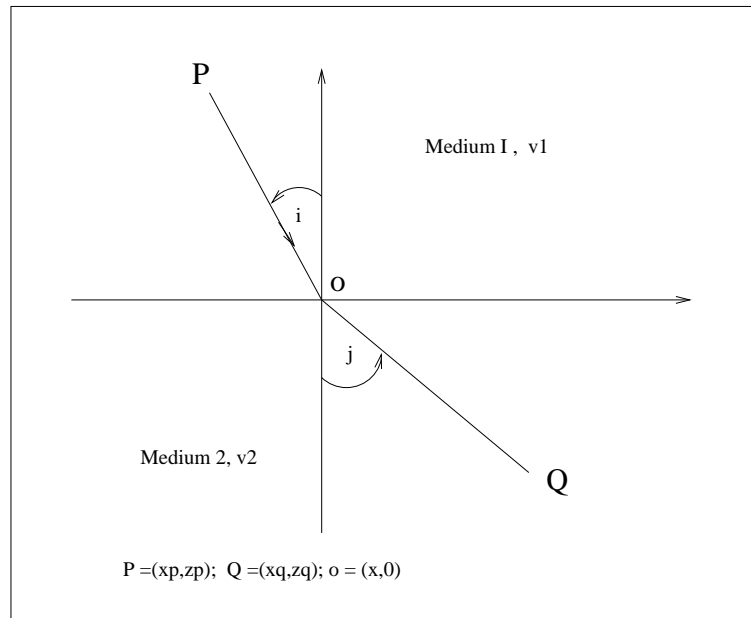


Figure 3.3: Ray path connecting P and Q , x is the variable of our problem.

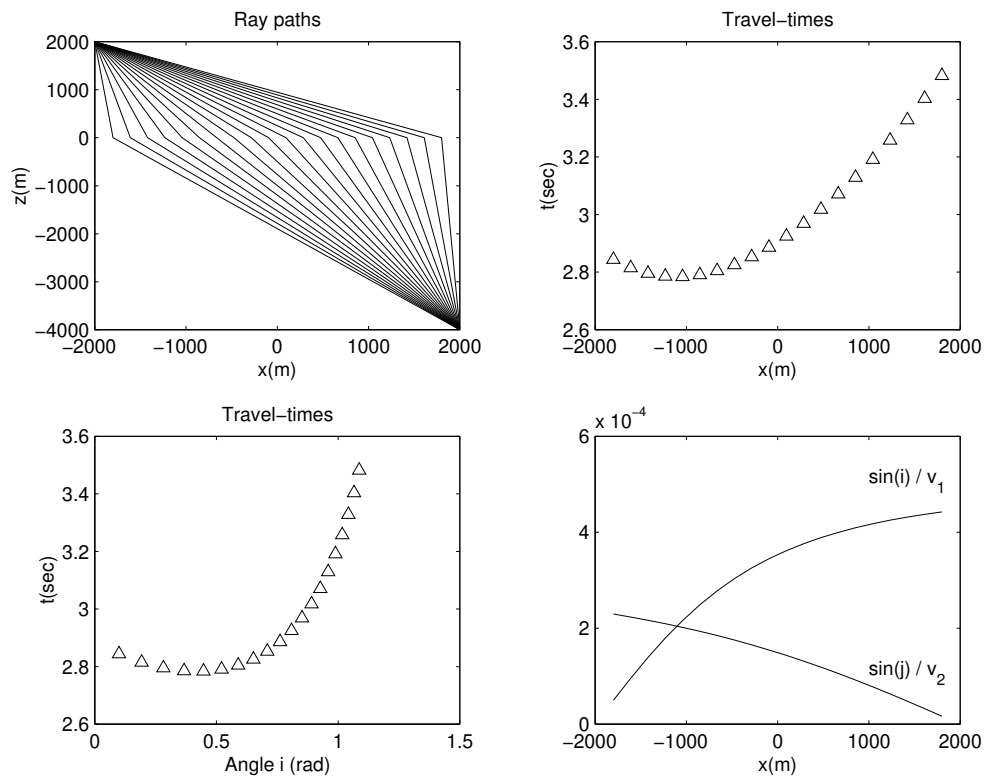


Figure 3.4: Different rays can connect P and Q . A seismic perturbation will travel via a minimum time path. In this example the velocity of the upper medium is $v_1 = 2000\text{m/s}$, the lower medium velocity is $v_2 = 3000\text{m/s}$.

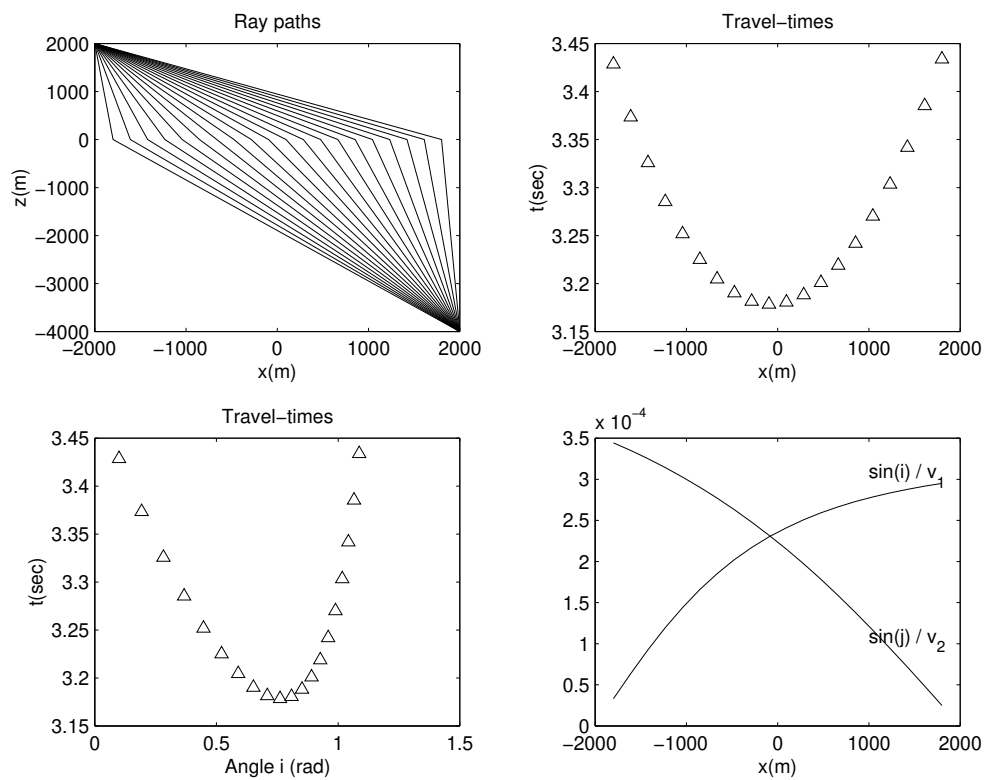


Figure 3.5: Different rays can connect P and Q . A seismic perturbation will travel via a minimum time path. In this example, the velocity of the upper medium is $v_1 = 3000\text{m/s}$, the lower medium has a velocity $v_2 = 2000\text{m/s}$.

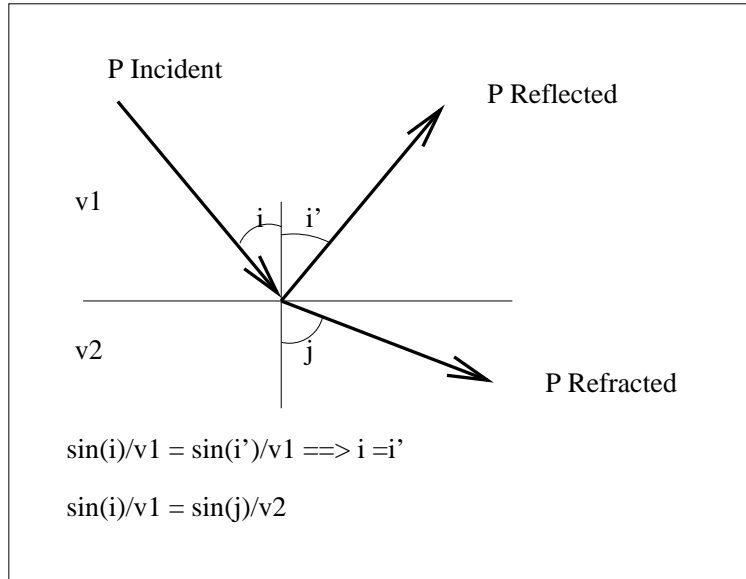


Figure 3.6: A P wave incident on an interface between contrasting materials.

$$\text{if } v_2 > v_1 \implies j > i. \quad (3.12)$$

One could adopt i as the variable of our problem and write

$$j = \text{asin}\left(\frac{v_2}{v_1} \sin(i)\right) \quad (3.13)$$

It is clear that at some point $i = i_c$ (critical angle) the following condition is satisfied

$$90^\circ = \text{asin}\left(\frac{v_2}{v_1} \sin(i_c)\right), \quad (3.14)$$

which I write as follows

$$\sin(i_c) = \frac{v_1}{v_2}. \quad (3.15)$$

The critical angle i_c defines a wave that travels horizontally parallel to the interface. This wave is a *Head Wave* or a refraction. The head wave transmits energy back into the upper medium as it travels along the interface (Figure 3.7).

3.2.1 $T - X$ refraction profiles

In a refraction experiment, we attempt to estimate the velocity and depth of layers which are assumed to be of constant velocity and sub-horizontal. We will start to analyze the most straightforward scenario that includes one geological layer over a half-space.

A source placed in position A emits energy and receivers distributed on the surface of the earth will record waves (Figure 3.7). We will compute the traveltime for a perturbation originated at the point A that arrives at a point D . The distance receiver-source is x .

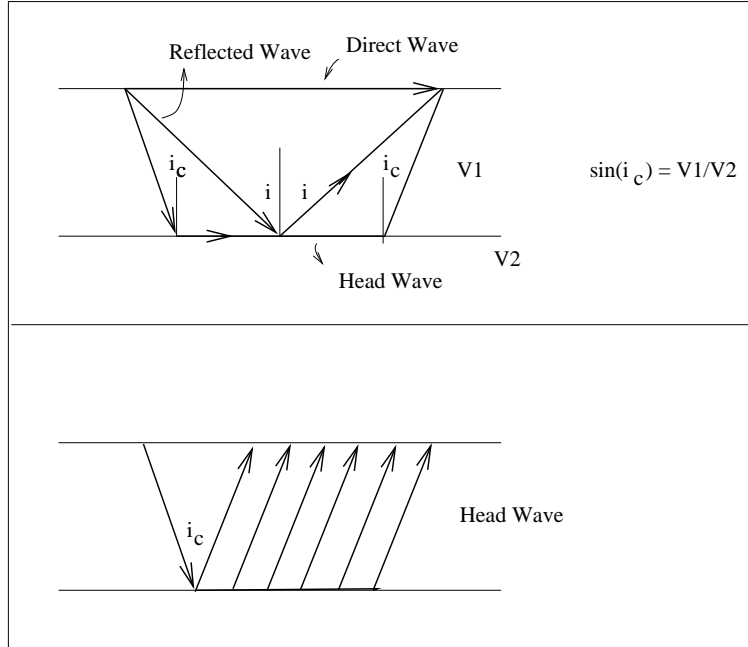


Figure 3.7: Rays in a one layer structure over a half space.

First, we will analyze the **direct wave**. The total traveltime for a direct wave travelling from point A to point D is given by

$$T_d(x) = x/v_1. \tag{3.16}$$

This equation defines a straight line in the $T - x$ plane. The slope of the line defines the slowness $1/v_1$.

Now, we will concentrate on the **head wave**. At critical angle $i = i_c$ the travel time for the head wave is given by the time to travel from A to D via the path $ABCD$

$$T_{Head}(x) = \frac{AB}{v_1} + \frac{BC}{v_2} + \frac{CD}{v_1}. \tag{3.17}$$

It is clear from the diagram that $AB = CD$, then

$$T_{Head} = 2\frac{AB}{v_1} + \frac{BC}{v_2} \tag{3.18}$$

$$T_{Head}(x) = \frac{2z}{v_1 \cos(i_c)} + \frac{x - 2z \tan(i_c)}{v_2}. \tag{3.19}$$

Using the critical angle condition $\sin(i_c) = v_1/v_2$ we can write

$$\begin{aligned} T_{Head}(x) &= \frac{x}{v_2} + \frac{2z \cos(i_c)}{v_1} \\ &= \frac{x}{v_2} + T_1 \end{aligned} \tag{3.20}$$

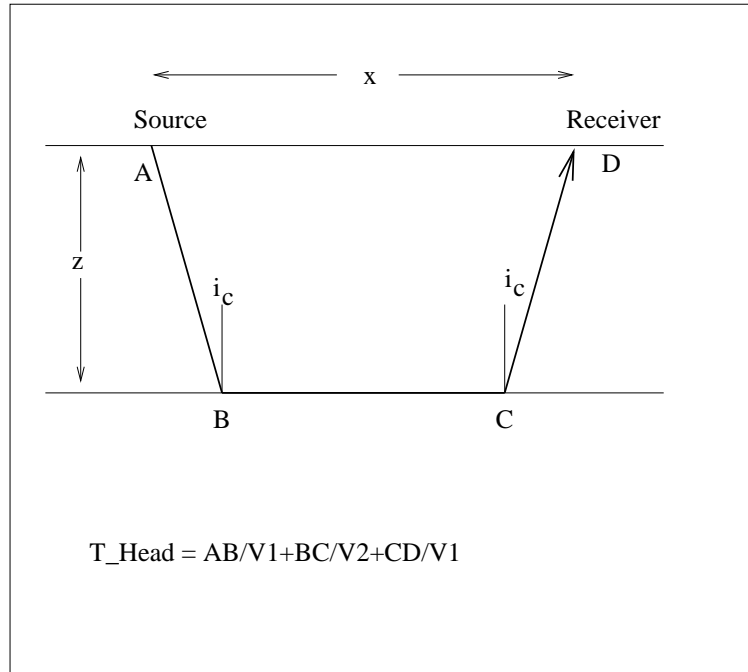


Figure 3.8: Geometry of a refraction profile.

where

$$T_1 = \frac{2z \cos(i_c)}{v_1}. \quad (3.21)$$

The head wave defines a straight line in $T - x$ (Figure 3.9). We can compute the velocity of the layer v_1 , the velocity of the half-space v_2 and z by the following procedure:

1. From $T(x)$ measure the slope of the the direct wave and head wave to determine v_1 and v_2 , respectively.
2. Compute i_c using the expression $\sin(i_c) = v_1/v_2$.
3. Measure t_1 from the figure and compute $z = (v_1 t_1)/(2 \cos(i_c))$

The procedure outlined above has permitted us to estimate the subsurface parameters v_1, v_2, z from traveltimes measures on the surface of the earth. The procedure also describes the solution of the simplest inverse problem that one can find in seismology. The critical distance x_c in Figure 3.9 defines the distance where the head wave is first recorded on the surface of the earth

$$x_c = 2z \tan(i_c). \quad (3.22)$$

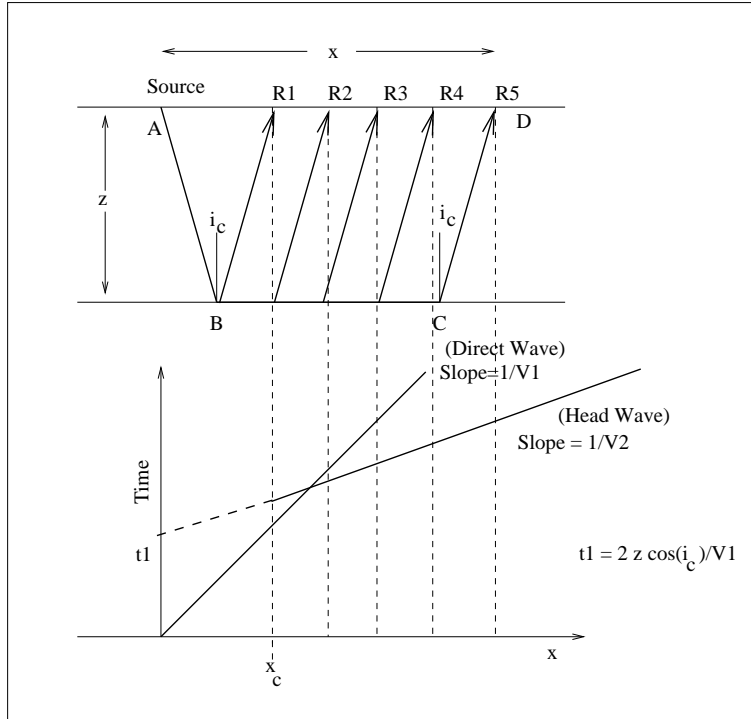


Figure 3.9: Traveltime curve for a refraction profile.

3.2.2 $T - X$ refraction curves for a dipping layer

We will examine the case when a single dipping reflector is excited by a seismic perturbation at a critical angle. The problem is defined in Figures 3.10 a and b. We have two possible profiles, the first one corresponds to a source located in the shallower part of the dipping bed, the second corresponds to the case when the source is in the deeper part of the dipping bed. We will see that the combination of these two experiments will allow us to estimate the unknowns of the problems. These experiments are also called the *Profile* and the *Reverse Profile*.

In the preceding section, we solved the refraction problem for a non-dipping interface. We use a single profile and derived v_1 , v_2 and z . In the dipping layer case, we need to estimate another variable ϕ (the dip of the layer). The total traveltime for the Experiment I (Figure 3.10a) is given by

$$T_I = \frac{AB}{v_1} + \frac{BC}{v_2} + \frac{CD}{v_1}. \tag{3.23}$$

We also know that

$$AB = \frac{z}{\cos(i_c)}, \tag{3.24}$$

$$CD = \frac{Z}{\cos(i_c)} \tag{3.25}$$

and

$$BC = x \cos(\phi) - Z \tan(i_c) - z \tan(i_c). \tag{3.26}$$

The traveltime as a function of variables and unknowns is given by

$$T_I = z \left[\frac{1}{v_1 \cos(i_c)} - \frac{\tan(i_c)}{v_2} \right] + Z \left[\frac{1}{v_1 \cos(i_c)} - \frac{\tan(i_c)}{v_2} \right] + \frac{x \cos(\phi)}{v_1}. \quad (3.27)$$

The last equation simplifies by introducing the following equations

$$\frac{1}{v_2} = \frac{\sin(i_c)}{v_1} \quad \text{Critical angle condition.} \quad (3.28)$$

and

$$Z = z + x \sin(\phi). \quad (3.29)$$

After substituting the last two equation into equation (3.27), we obtain

$$\begin{aligned} T_I &= \frac{2z}{v_1} \cos(i_c) + \frac{x}{v_1} [\sin(\phi) \cos(i_c) + \cos(\phi) \sin(i_c)] \\ &= \frac{2z}{v_1} \cos(i_c) + \frac{x}{v_1} \sin(i_c + \phi). \end{aligned} \quad (3.30)$$

The last expression corresponds to a straight line with a slope given by

$$\text{slope}_I = \frac{\sin(i_c + \phi)}{v_1} \quad (3.31)$$

and intercept time ($T(x = 0)$) given by

$$\text{Intercept}_I = \frac{2z}{v_1} \cos(i_c). \quad (3.32)$$

The direct ray can be used to estimate v_1 . We can obtain a similar expression for the Experiment II (source in D and receiver in A). In this case, we have

$$T_{II} = \frac{2Z}{v_1} \cos(i_c) + \frac{x}{v_1} \sin(i_c - \phi). \quad (3.33)$$

which also defines a straight line in $T - X$. Now the slope of the line is given by

$$\text{slope}_{II} = \frac{\sin(i_c - \phi)}{v_1} \quad (3.34)$$

and it intercept

$$\text{Intercept}_{II} = \frac{2Z}{v_1} \cos(i_c). \quad (3.35)$$

In Figure 3.11, I show the $T - X$ curve for the Experiments I and II.

The procedure to compute our unknowns can be summarized as follows:

1. From the direct wave traveltime compute v_1 . You can use both profiles and average the results or use the profile with higher SNR.

2. The $slope_I$ and $slope_{II}$ are measured. At this point, we have two equations with two unknowns i_c and ϕ . You can easily solve the $2 \times$ system of equations to determine i_c and ϕ .
3. Once we have obtained v_1 and i_c use the critical angle condition ($\sin(i_c) = v_1/v_2$) to compute v_2 .
4. Use the intercept times to compute z and Z .

3.2.3 Fitting straight lines to first arrivals.

In a real experiment, we will pick first arrivals and construct a table that looks like the following

event: Direct wave

r	x(m)	t(ms)
1	15	10
2	30	30
3	40	42

event: Refracted wave

r	x(m)	t(ms)
1	100	51
2	120	63
3	150	74
4	185	85

We seldom have traveltimes laying on perfectly straight lines when analyzing field refraction data. In this case, we need a technique to fit lines to noisy observations. As an example, let's consider the estimation of the best line that matches the traveltimes picks for the head wave. Traveltimes picks for the refracted wave are given by $x_i, t_i, i = 1, N_p$ where N_p is the number of picks. The analytical expression of the line is

$$t(x) = ax + b. \quad (3.36)$$

We can use the *least squares method*¹ to find the unknowns a and b that yield the line approximating the observed traveltimes picks. The least squares method finds a solution for a and b based on the following model. First, we assume that the traveltimes picks contain errors

$$t_i = ax_i + b + e_i \quad i = 1 \dots N_p. \quad (3.37)$$

We seek a slope a and intercept b that minimize the sum of squared errors (*SSE*)

$$SSE = \sum_{i=1}^{N_p} (e_i)^2 = \sum_{i=1}^{N_p} (t_i - ax_i - b)^2. \quad (3.38)$$

¹The least squares method is the standard approach in regression analysis to solve overdetermined systems of equations, i.e. a system of equations that contains more equations than unknowns.

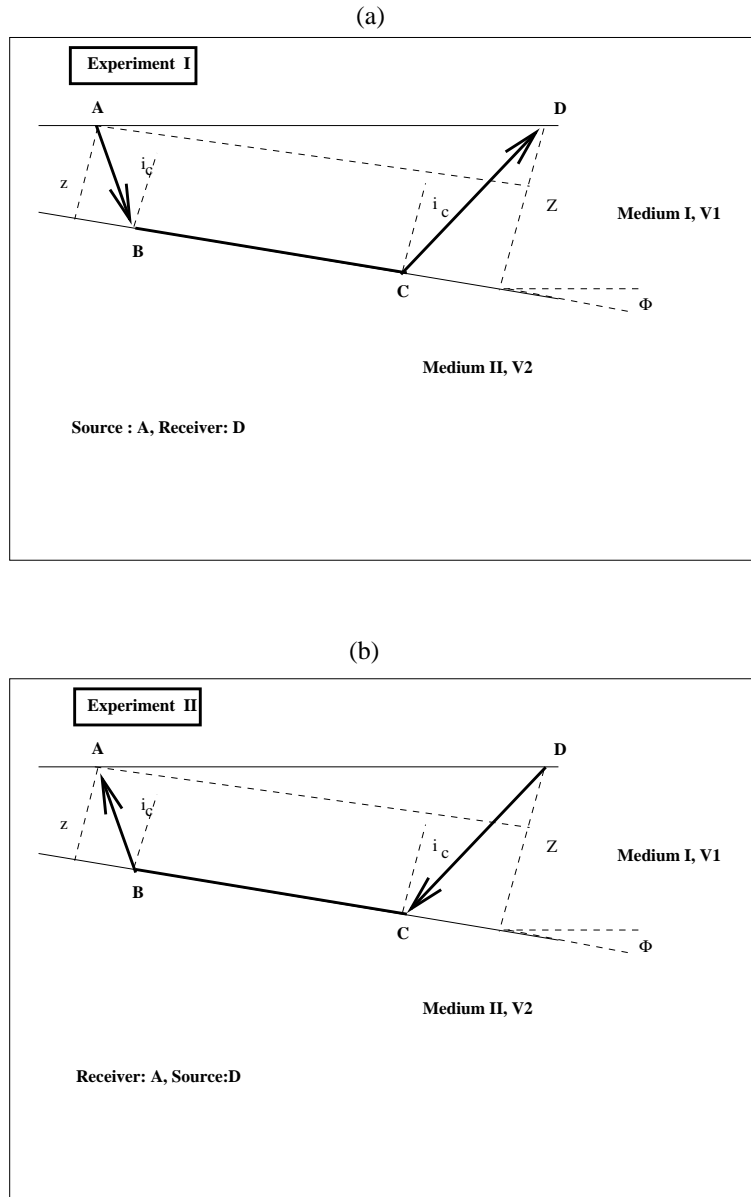


Figure 3.10: Refraction experiment. Now we have an extra unknown ϕ , we will run two experiments (a) and (b) to determine z , v_1 , v_2 and ϕ .

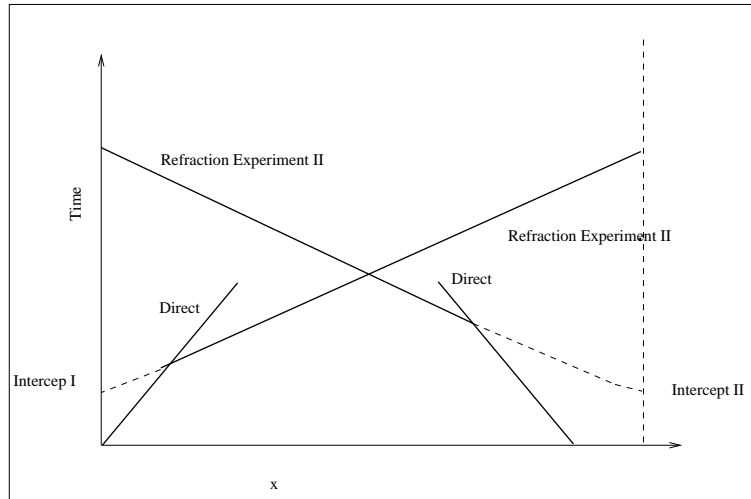


Figure 3.11: Refraction experiment. Travel-time curves

Where \sqrt{SSE} is also the Euclidean norm of the errors². The least-squares solution is found by taking the derivatives of SSE with respect to a and b and by then equating them to zero. The latter leads to a 2×2 system of equations from where one can compute a and b . Once we have a and b , you can estimate the analytical line that best fit the observations in the least-squares sense.

Sometimes, the least squares regression is not good enough to fit the line to observed traveltime picks. The problem is significant when outliers³ contaminate observations. In this case, we need a *robust estimation method*⁴. For instance, one can minimize the *absolute sum of errors* that is often also called the l_1 norm of the error (pronounced "the *ell - one* norm").

$$l_1 = \sum_i |t_i - ax_i - b|. \quad (3.39)$$

The minimization of l_1 leads to the unknowns of our problem a and b . In Figure 3.12, I use least-squares to fit the direct, and the refracted traveltime picks to a set of noisy observations. In Figure 3.13, we analyze the effect of one outlier in the least-squares fitting. The robust fitting technique via the l_1 norm yields a solution that is immuned to outliers.

3.3 Reflections

In this section, we will study the time-distance curves for seismic reflections. Reflection seismology is the subfield of seismology that investigates the interior of the earth using reflected waves. In general, exploration seismology for oil and gas relies upon the study of reflected waves collected by seismic surveys. These waves are processed via digital signal processing methods and then used to

² l_2 or Euclidean norm of x_i is $l_2 = \sqrt{\sum_i x_i^2}$

³Gross or erratic errors.

⁴A robust estimator of a parameter is an estimator that is resistant to outliers. In other words, if your data contain large and often isolated errors not following a nice normal distribution, then parameters such as a and b are not properly estimated by minimizing SSE . In this case, one must adopt a robust parameter estimation technique.

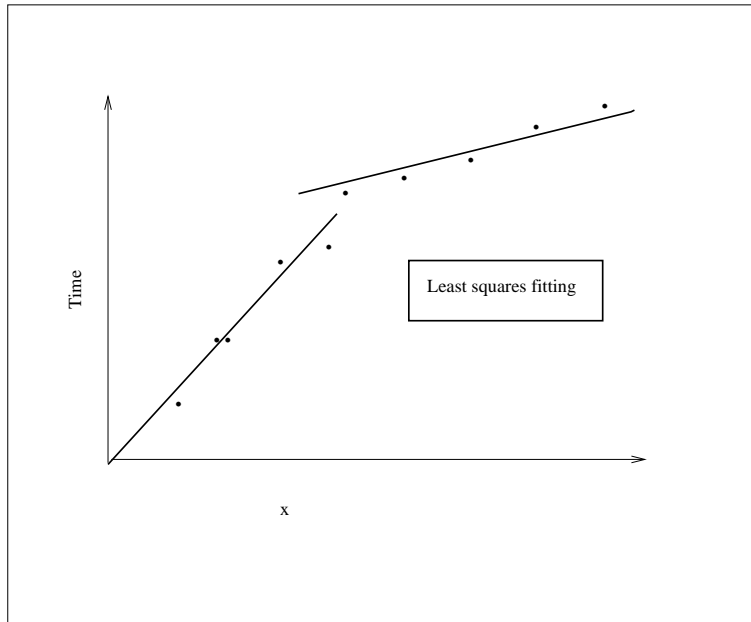


Figure 3.12: Least-squares curve fitting.

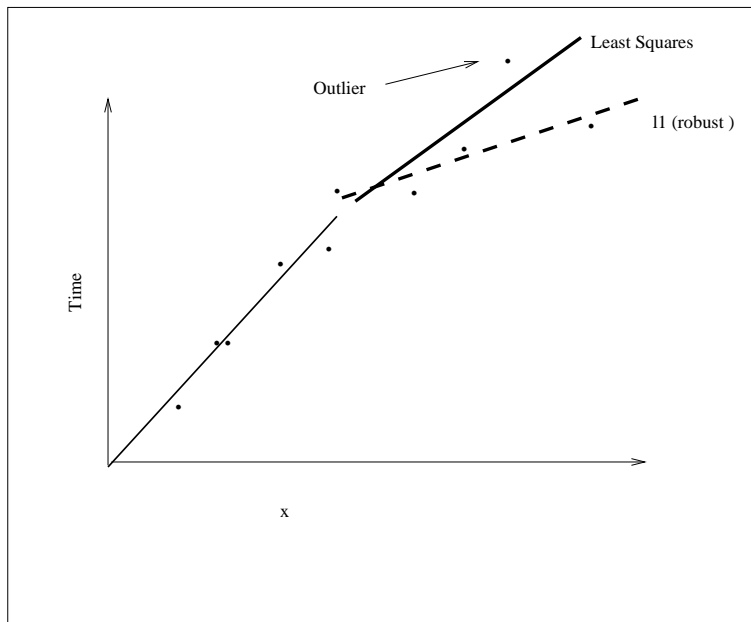


Figure 3.13: Least-squares curve fitting in the presence of outliers.

estimate images of the interior of the earth. The process of imaging entails using the wave equation to map wavefields measured on the surface of the earth into a picture of subsurface geological structures (sediments, folds, faults, unconformities, salts domes, etc.).

3.3.1 $T - X$ curves for a primary reflection

Horizontal Interface

We will compute the traveltime for a primary reflection. A primary reflection is a wave that reflects only one time in the subsurface. In the first case, we will assume a horizontal layer over a half space.

We will assume that a P wave impinges at an angle of incidence i on the interface, the reflection will emerge at an angle $i' = i$ (Snell's law). In Figure 3.14 we portray the geometry of the experiment. The total traveltime is given by

$$T = \frac{AD}{v_1} + \frac{DE}{v_1} = \frac{CE}{v_1}, \quad (3.40)$$

where

$$CE^2 = (2z_s)^2 + x^2. \quad (3.41)$$

The time as a function of the source receiver distance x becomes

$$T(x) = \sqrt{\left(\frac{2z_s}{v_1}\right)^2 + \left(\frac{x}{v_1}\right)^2}. \quad (3.42)$$

We now define the two-way zero offset traveltime

$$T(x=0) = T_0 = \frac{2z_s}{v_1}, \quad (3.43)$$

after substituting equation (3.43) into equation (3.42) we obtain the following final expression

$$T(x)^2 = T_0^2 + \frac{x^2}{v_1^2}. \quad (3.44)$$

The last equation can be rearranged in the following form

$$\frac{-x^2}{T_0^2 v_1^2} + \frac{T(x)^2}{T_0^2} = 1 \quad (3.45)$$

which is the equation of a hyperbola⁵ in $T - X$.

Dipping Interface

The traveltime for the dipping interface case can be derived with the aid of Figure 3.16

$$T = \frac{AD + DE}{v_1} = \frac{CE}{v_1}. \quad (3.46)$$

⁵Hyperbola: $\frac{u^2}{a^2} - \frac{v^2}{b^2} = 1$

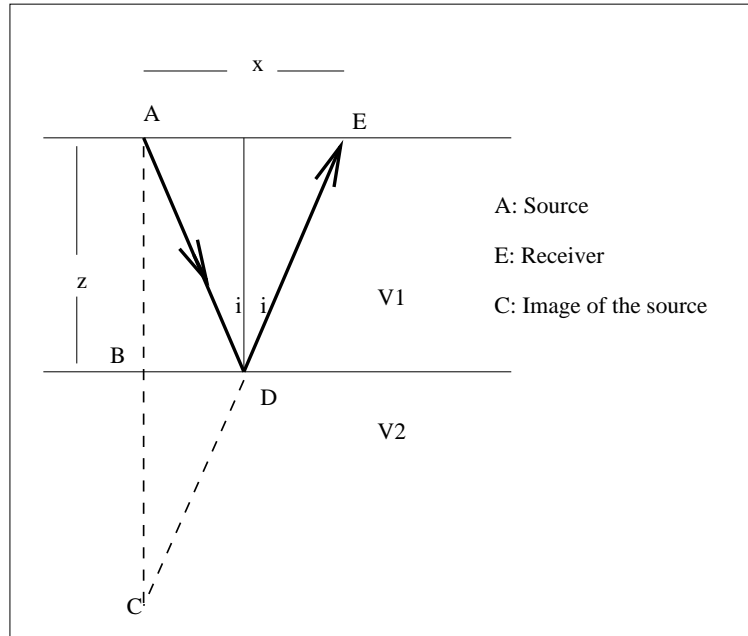


Figure 3.14: A primary reflection. The horizontal layer case.

We can use the cosine theorem to write

$$CE^2 = (2z_s)^2 + x^2 - 4z_s x \cos(\gamma), \quad (3.47)$$

where

$$\gamma = 90^\circ + \phi \Rightarrow \cos(90^\circ + \phi) = -\sin(\phi). \quad (3.48)$$

The travelttime becomes

$$T(x)^2 = \frac{(2z_s)^2 + x^2 + 4x z_s \sin(\phi)}{v_1^2} \quad (3.49)$$

if $T(x=0) = T_0 = 2z_s/v_1$,

$$T(x)^2 = T_0^2 + \frac{x^2}{v_1^2} + \frac{4x z_s \sin(\phi)}{v_1^2}. \quad (3.50)$$

We can rewrite the latter as

$$\frac{T(x)^2}{T_0^2} - \frac{(x + v_1 T_0 \sin(\phi))^2}{v_1^2 T_0^2} = \cos(\phi) \quad (3.51)$$

which is also a hyperbola in $T - X$. In the above equation, we have been able to write $T(x)$ as a function of x the source-receiver distance for a fixed source that is a distance z from the interface. A collection of seismograms sharing the same source (x_s is constant and x is variable) is called a **Common Source Gathers (CSG)** or a **Common Shot Gather**.

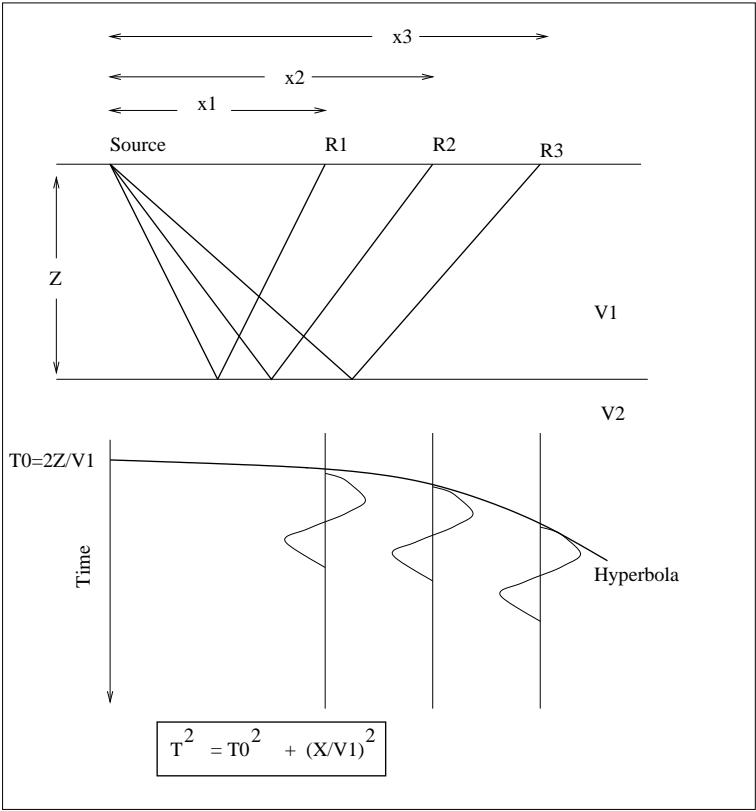


Figure 3.15: Common Shot Gather(CSG).

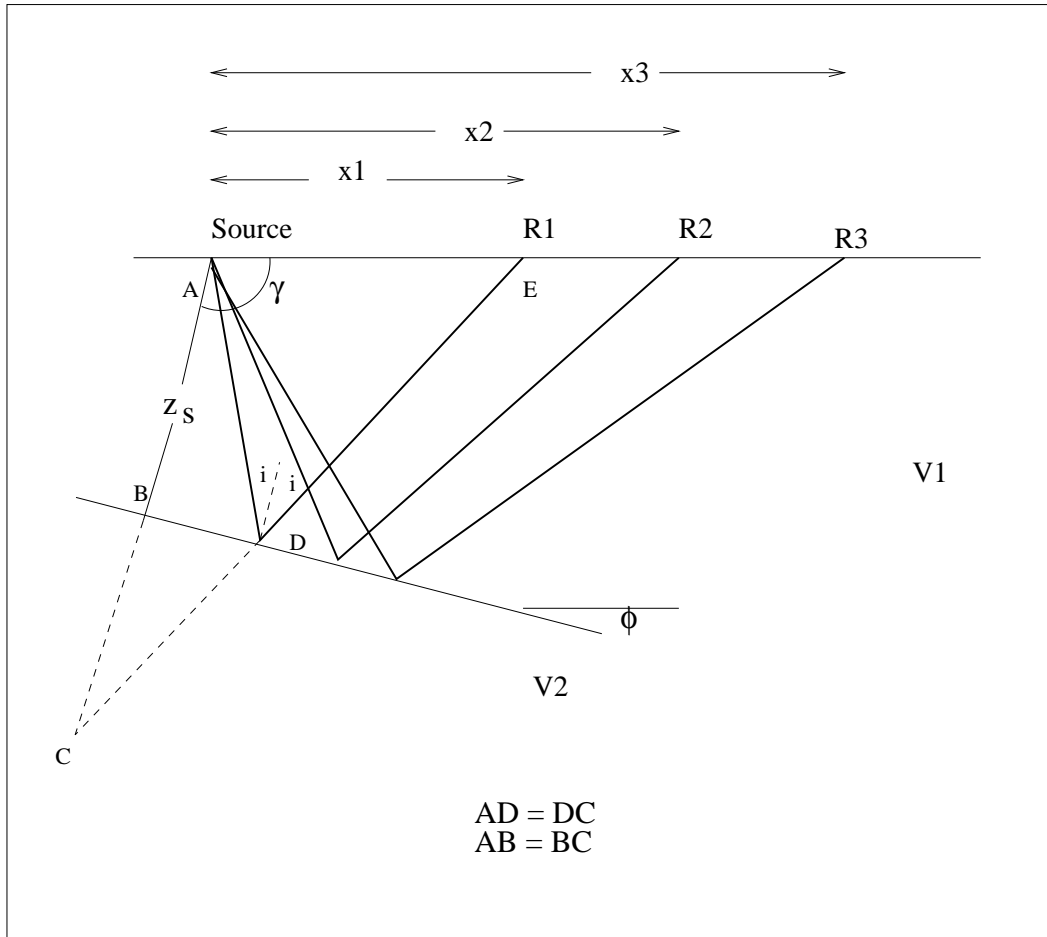


Figure 3.16: A primary reflection. The dipping interface case.

3.3.2 Relative position of the reflection and the head wave in the $T - X$ plane

In Figure (3.17) we portray the $T - X$ diagram for a single horizontal layer over a half space. We can visualize the travel-time for the following waves

$$\text{Direct wave: } T_d = \frac{x}{v_1}$$

$$\text{Head wave: } T_h = \frac{2z \cos(i_c)}{v_1} + \frac{x}{v_2}$$

$$\text{Reflection: } T_r = \sqrt{T_0^2 + \frac{x^2}{v_1^2}}, \quad T_0 = \frac{2z}{v_1}$$

The geological model that I used to obtain Figure (3.17) is summarized as follows:

$$v_1 = 2000\text{m/s}$$

$$v_2 = 3500\text{m/s}$$

$$z = 200\text{m}$$

First, we study the asymptotic behaviour of the reflection. In other words, we compute

$$\lim_{x \rightarrow \infty} \frac{dT_r}{dx}. \quad (3.52)$$

We can start by taking derivatives of T_r

$$\frac{dT_r}{dx} = \frac{x}{v_1^2 \sqrt{T_0^2/x^2 + 1/v_1^2}} \quad (3.53)$$

from where it is easy to show that

$$\lim_{x \rightarrow \infty} \frac{dT_r}{dx} = \frac{1}{v_1}. \quad (3.54)$$

In other words, the asymptotic line can be written as

$$T_a = ax + b = \frac{1}{v_1}x + b. \quad (3.55)$$

At ∞ we expect

$$\lim_{x \rightarrow \infty} (T_r - T_a) = 0 \quad (3.56)$$

last condition is satisfied if $b = 0$. Therefore, the asymptotic line $T_a = \frac{x}{v_1}$ coincides with the travel-time of the direct wave T_d . We can also compute the distance x' for which the time of the refraction and the reflection is equal

$$T_d = T_h$$

or

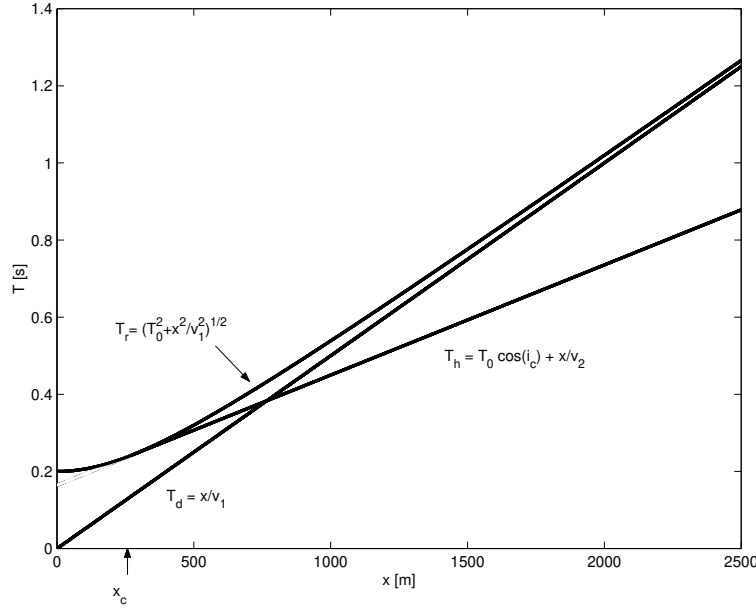


Figure 3.17: Travetime curves for the direct wave T_d , the reflected wave T_r and the head wave T_h in the $T - X$ plane.

$$\begin{aligned} \left(\frac{2z}{v_1} \cos(i_c) + \frac{x'}{v_2}\right)^2 &= T_0^2 + \frac{x'^2}{v_1^2} \\ &= \left(\frac{2z}{v_1}\right)^2 + \frac{x'^2}{v_1^2}. \end{aligned}$$

After a few manipulations, we arrive at the solution x'

$$x' = 2z \tan(i_c). \quad (3.57)$$

It is interesting to note that x' is equal to the critical distance x_c (see equation (3.22)). Where x_c represents the minimum distance at which the head wave reaches the surface. It is also interesting to compute the slope of the reflection at $x = x' = x_c$

$$\frac{dT_r}{dx} \Big|_{x=2z \tan(i_c)} = \frac{1}{v_2} \quad (3.58)$$

the latter shows that at $x = x_c$ the reflection and the head wave are tangent to each other. Figure (3.17) summarizes the relative position of the direct wave, reflection and reflection in a $T - X$ diagram.

3.4 Reflections in horizontally stratified media

In this section, we will analyze the time-offset response of a layered Earth model. We will assume that our geological model is composed of a stack of n horizontal layers (Figure 3.18).

First, we will compute the traveltime for a reflection generated at the $n - th$ layer. According to Snell's law

$$\begin{aligned} \frac{\sin(i_1)}{\sin(i_2)} &= \frac{v_1}{v_2} \\ \frac{\sin(i_2)}{\sin(i_3)} &= \frac{v_2}{v_3} \\ &\dots\dots\dots \\ \frac{\sin(i_{n-1})}{\sin(i_n)} &= \frac{v_{n-1}}{v_n} \end{aligned}$$

we now multiply all the left-hand-side terms and equate them to the multiplication of all the right-hand-side terms to obtain the following expressions

$$\frac{\sin(i_1)}{\sin(i_2)} \frac{\sin(i_2)}{\sin(i_3)} \dots \frac{\sin(i_{k-1})}{\sin(i_k)} = \frac{v_1}{v_2} \frac{v_2}{v_3} \dots \frac{v_{k-1}}{v_k}. \tag{3.59}$$

It is easy to show that for the $k - th$ layer the following condition is satisfied

$$\frac{\sin(i_1)}{\sin(i_k)} = \frac{v_1}{v_k}. \tag{3.60}$$

or

$$\frac{\sin(i_l)}{v_k} = \frac{\sin(i_1)}{v_1} = p \tag{3.61}$$

we have just proved that in a **horizontally stratified media** the horizontal ray parameter p is **constant**. In Figure (3.18) we are assuming that the emanating wave is of the same type of the incident wave ($P - P$ or $S - S$). The total offset x is given by

$$x = 2 \sum_{k=1}^n h_k \tan(i_k). \tag{3.62}$$

Similarly, we can compute the total time as the sum of the time the wave travels in each layer

$$T = 2 \sum_{k=1}^n \frac{h_k}{v_k \cos(i_k)}. \tag{3.63}$$

We can use the fact that the ray parameter is constant to simplify equations (3.62) and (3.63) and write

$$x = 2 \sum_{k=1}^n \frac{h_k v_k p}{\sqrt{1 - (v_k p)^2}}, \tag{3.64}$$

$$T = 2 \sum_{k=1}^n \frac{h_k}{v_k \sqrt{1 - (v_k p)^2}}. \tag{3.65}$$

The last two equations express the time of the reflection at the $n - th$ layer and the distance x in parametric form (p is the parameter). One can specify a value of p and use (3.64)-(3.65) to build a time-distance table for each reflector. To simplify the processing of seismic data, in the next section we will try to find a direct relationship between T and x ($T = f(x)$).

3.4.1 Root-mean-square (RMS) velocity

We will attempt to find a function that relates T and x via a simple expression. Clearly, it is not possible to find a closed form solution of the type $T = f(x)$ by simple algebraic manipulations of equations (3.64) and (3.65). Our approach entails finding an approximation to the function $T = f(x)$. Let us start with the Taylor expansion of the traveltime curve

$$T(x) = T(0) + T'(x)|_{x=0} x + T''(x)|_{x=0} \frac{x^2}{2} + \dots \quad (3.66)$$

where $T(0)$ is the time for $x = 0$. Therefore, $T(0)$ can be obtained as the sum of the vertical two-way travel-time in each layer

$$T(0) = 2 \sum_{k=1}^n \frac{h_k}{v_k}. \quad (3.67)$$

One can show that $T'(x)|_{x=0} = 0$. The traveltime should not change if we interchange the position of the source and the receiver. Therefore, the following condition should be satisfied

$$T(x) = T(-x)$$

The latter indicates that all the odd power terms in the Taylor expansion must vanish

$$T'(x)|_{x=0} = 0, \quad T'''(x)|_{x=0} = 0 \dots$$

If we also assume that the coefficient $T''''(x)|_{x=0}$ is small, the only coefficient that we need to compute is $T''(x)|_{x=0}$. Applying the chain rule

$$\frac{d^2 T}{dx^2} = \frac{d}{dx} \left(\frac{dT}{dx} \right) = \frac{d^2 T}{dp^2} \left(\frac{dp}{dx} \right)^2 + \frac{dT}{dp} \frac{d^2 p}{dx dp} \frac{dp}{dx}$$

and after evaluating all the terms in the last equation at $x = 0$ (they can be computed from equations 3.65 and 3.64) we obtain

$$T''(x)|_{x=0} = \frac{1}{2 \sum_{k=1}^n h_k v_k}. \quad (3.68)$$

Now, our traveltime expression becomes

$$T(x) = T(0) + \frac{1}{2 \sum_{k=1}^n h_k v_k} \frac{x^2}{2}. \quad (3.69)$$

Note that

$$T(0) = \sum_{k=1}^n \frac{2h_k}{v_k} = \sum_{k=1}^n t_k,$$

where $t_k = 2d_k/v_k$ is the two-way transit time for a way travelling vertically in each layer. The second term in the right-hand side of equation 3.69 can be written as a function of t_k

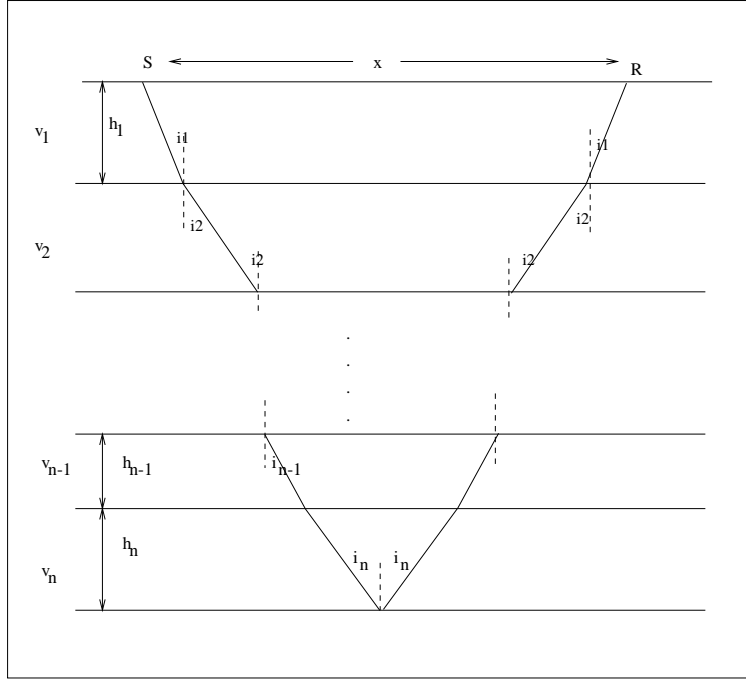


Figure 3.18: Reflections in horizontally stratified media.

$$T(x) = T(0) + \frac{1}{\sum_{k=1}^n t_k v_k^2} \frac{x^2}{2}. \quad (3.70)$$

To make the last equation look like the equation that corresponds to the single layer case (Hyperbola), we can apply the following trick

$$T(x)^2 = \left(T(0) + \frac{1}{\sum_{k=1}^n t_k v_k^2} \frac{x^2}{2} \right)^2. \quad (3.71)$$

after expanding the square and neglecting fourth-order term, we obtain

$$T(x)^2 = T(0)^2 + \frac{x^2}{v_{rms}^2} \quad (3.72)$$

$$v_{rms} = \sqrt{\frac{\sum_{k=1}^n t_k v_k^2}{\sum_{k=1}^n t_k}}. \quad (3.73)$$

The latter is called **Root Mean Squared Velocity** or **RMS velocity**. The seismic record is a superposition of events that display a hyperbolic moveout. The *RMS* velocity of each layer can be identified (measured) together with the associated $T(0)$ and used to find the actual interval velocities ⁶ Notice that the traveltime approximation for a group of horizontal layers corresponds to the expression of one layer with a velocity that is equivalent to the RMS velocity for the group of

⁶Dix C H, "Seismic Velocities from Surface Measurements," *Geophysics* 20, no. 1 (January 1955): 68-86.

layers. Having a simple hyperbola to describe the traveltime of all the reflections simplifies different processes that we apply to the seismic data to obtain an image of the subsurface.

3.5 Seismic reflection data in offset and midpoint coordinates

In section (3.2), we derived an expression for the travel-time for a Common Shot Gather (**CSG**) for a single dipping interface. The traveltime of a reflection is also parameterized by adopting a new system of coordinates. Figure (3.19) displays several acquisition variables that can be used to describe a seismic survey and to parameterize traveltime curves.

x_r Position of the receiver

x_s Position of the source

The source-receiver distance is called **offset**,

$$h = x_r - x_s \text{ Offset} \quad (3.74)$$

The point m in Figure (2.19) is called the **midpoint**, the coordinate of the midpoint is related to x_r and x_g by the following expression

$$x_m = \frac{x_r + x_s}{2} \text{ Midpoint} \quad (3.75)$$

The traveltime curve can be either defined as a function of (x_r, x_s) or as a function of (h, x_m) :

$T(h, x_m)$: Time in offset-midpoint coordinates

$T(x_r, x_s)$: Time in receiver-source coordinates

In a seismic experiment different source positions, x_s , are utilized. Each time a source generates energy that propagates down into the earth receivers at position x_r record reflected waves. Therefore, seismic data constitute a 3D volume⁷. The data is stored in a 3D acquisition volume can be represented as $D(x_r, x_s, t)$ or $D(h, x_m, t)$.

Our original expression for the traveltime for a dipping layer (equation (3.48)) as a function of the variable offset h becomes

$$T^2 = \frac{(2z_s)^2 + h^2 + 4hz_s \sin(\phi)}{v_1^2} \quad (3.76)$$

It is clear (Figure (3.19)) that z_s is a function of the source position. Let's try to remove the dependency of the experiment on z_s and try to write the traveltime as a function of Z the depth under the midpoint (x_m). After analyzing Figure (3.19), we can write

$$Z = z_s + \frac{h}{2} \sin(\phi). \quad (3.77)$$

⁷We are assuming a 2D seismic acquisition along a seismic line.

After substituting (3.77) into (3.76) we obtain

$$T^2 = \left(\frac{2Z}{v_1}\right)^2 + \left(\frac{h}{v_1/\cos(\phi)}\right)^2 \quad (3.78)$$

We have been able to write the traveltime as a function of h and Z but since Z is a function of the midpoint x_m , we can write

$$T(h, x_m)^2 = \left(\frac{2Z}{v_1}\right)^2 + \left(\frac{h}{v_1/\cos(\phi)}\right)^2, \quad (3.79)$$

or

$$T(h, x_m)^2 = T_0^2 + \left(\frac{h}{v_1/\cos(\phi)}\right)^2. \quad (3.80)$$

If our observations are acquired with an experiment where the midpoint position is kept constant ($x_m = \text{constant}$) we have a **Common Midpoint (CMP) Gather**. It is interesting to mention that for CMP gather the hyperbola is symmetric. Also, note that the velocity that controls the curvature of the hyperbola is now given by $v' = v_1/\cos(\phi)$ which can be considered the velocity associated to a reflection from a horizontal layer with velocity v' .

The data cube can be arranged in gathers according to the way one organizes the data

1. Common Midpoint (CMP) gather:

$$h = \text{variable}, \quad x_m = \text{constant}$$

2. Common Offset (COF) gather:

$$x_m = \text{variable}, \quad h = \text{constant}$$

3. Common Source (CS) gather:

$$x_r = \text{variable}, \quad x_s = \text{constant}$$

4. Common Receiver (CR) gather:

$$x_s = \text{variable}, \quad x_r = \text{constant}.$$

We will concentrate our attention on CMP gathers. These gathers are an essential part of seismic data processing because two processes called Velocity Analysis and Normal Moveout Correction require data organized into CMP gathers (*Stay tuned!*). We will use CMP gathers to estimate a **seismic section**. The latter is an image of the underlying geology in the $t - x_m$ space. A time-domain seismic section is also the image of the subsurface that is often used to interpret⁸ geological sediments and structures.

⁸If you are interested in the geological interpretation of seismic sections; I suggest "Introduction to Seismic Interpretation by Bruce S. Hart" published by AAPG.

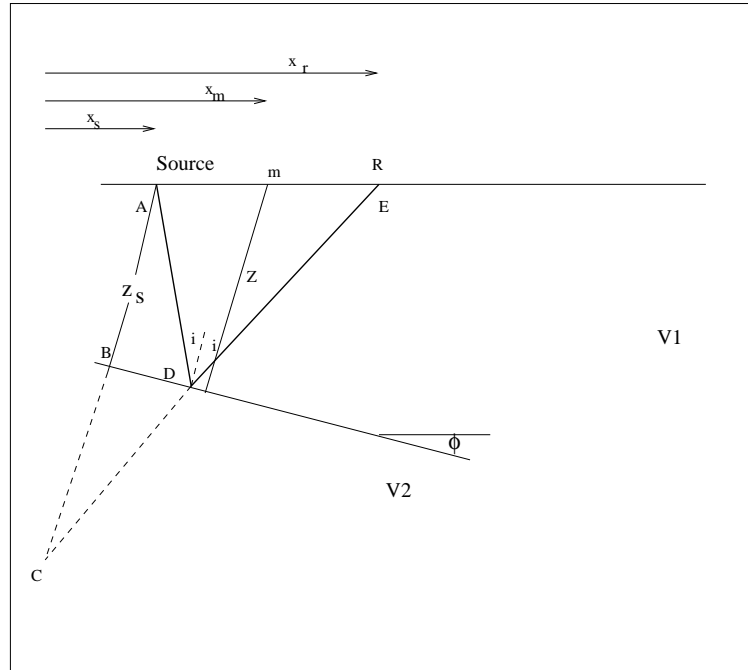


Figure 3.19: A primary reflection. The dipping interface case.

3.5.1 Multiples

Multiply reflected seismic waves, or "multiples" are seismic waves that have incurred more than one reflection in its travel path. Seismic events that are reflected once in the subsurface are called primary reflections or "primaries." Multiples are a real problem in seismic exploration. Seismic data are composed of signal and noise. The term noise does not only define random noise. Deterministic noise also contaminates seismic data. Multiples can be considered deterministic noise or, in other words, unwanted waveforms. For a seismologist, noise is everything that corrupts the analysis and interpretation of seismic data. A seismic interpreter uses primary reflection events to create a geological model of the subsurface. We may end up with a wrong seismic image, and consequently with an incorrect geological interpretation if multiple reflections are not eliminated.

The traveltime for the primary reflection in Figure (3.20) is given by

$$T_d^2 = T_0^2 + \left(\frac{h}{v_1}\right)^2, \quad T_0 = \frac{2z}{v_1} \quad (3.81)$$

For the first order multiple reflection, we have

$$T_m^2 = (2T_0)^2 + \left(\frac{h}{v_1}\right)^2 \quad (3.82)$$

Multiple reflections define a hyperbola parametrized with the velocity v_1 . The intercept time for the first order multiple is $2T_0$. We can have higher order multiples. They will show up at intercept times $3T_0, 4T_0, \dots$. We can recognize multiples by its periodic behaviour at small offsets $h \approx 0$. In the dipping layer case, we have

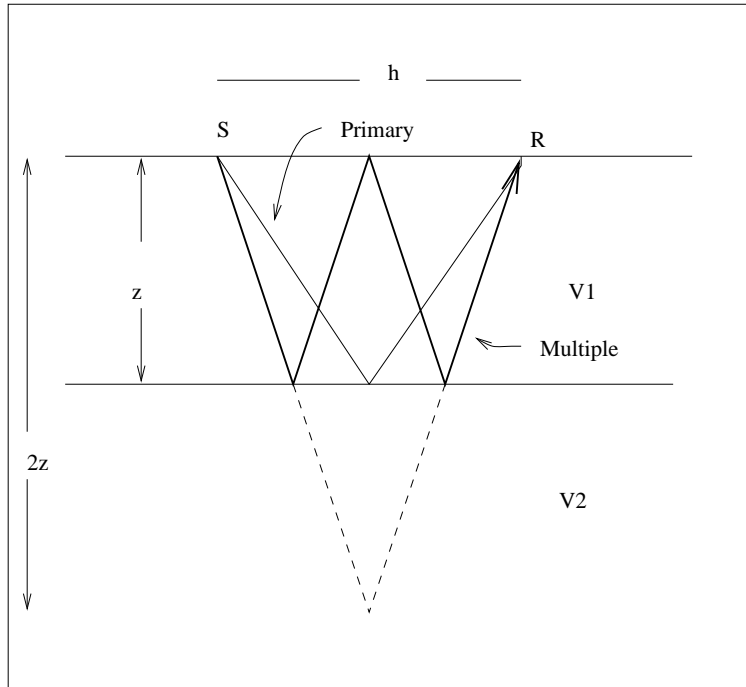


Figure 3.20: A primary reflection and its first order multiple.

$$T_p = \sqrt{(T_0)^2 + \left(\frac{h}{v/\cos(\phi)}\right)^2} \quad (3.83)$$

and

$$T_m = \sqrt{(2T_0)^2 + \left(\frac{h}{v/\cos(2\phi)}\right)^2} \quad (3.84)$$

We note that the first order multiple simulates a layer with velocity $v/\cos(2\phi)$ at intercept time $2T_0$.

3.6 Normal Moveout (NMO) correction

The traveltimes for a reflection in a CMP gather is given by

$$T = \sqrt{T_0^2 + \left(\frac{h}{v}\right)^2}, \quad (3.85)$$

where the variable h is the offset or source-receiver distance. The NMO correction is a correction that is used to remove the offset dependency in equation (3.85).

$$T = \sqrt{T_0^2 + \left(\frac{h}{v}\right)^2} \xrightarrow{NMO} T = T_0 \quad (3.86)$$

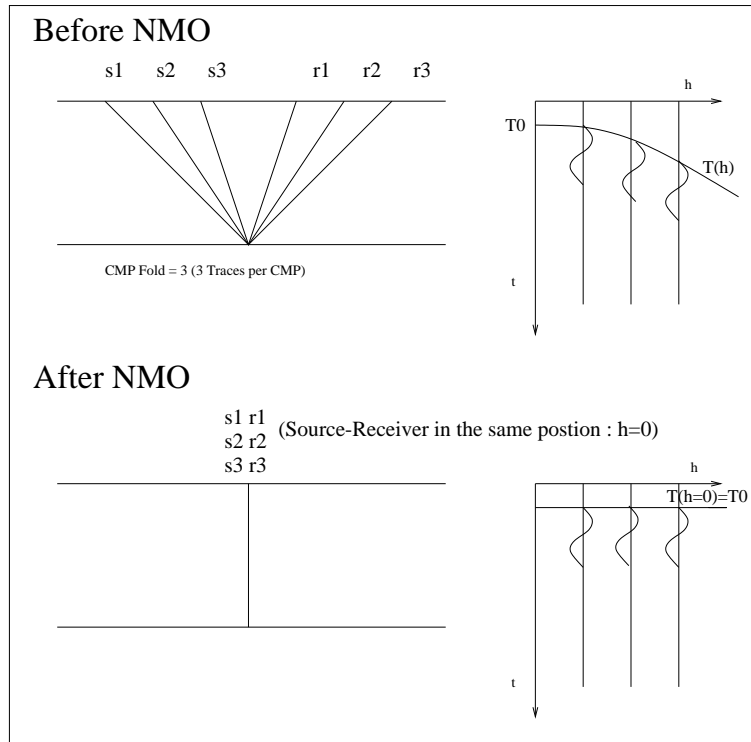


Figure 3.21: NMO correction attempts to simulate a seismic experiment where all the source-receiver pairs at a given midpoint position have offset $h = 0$.

Before NMO (Figure (3.21)) the travel-time for a primary reflection is given by a hyperbolic curve parametrized by the velocity of the layer. After NMO correction the offset dependency has been removed, this is equivalent to simulating a seismic experiment where each source-receiver pair shares the midpoint x_m and all traces have offset $h = 0$. After NMO correction all traces should look alike (this is not completely true because I am neglecting noise, amplitude variations with offset, and *multiples*). One can stack all the traces associated with a given midpoint position to obtain a **Stacked Trace**. Stacking is the process of summing together traces that belong to the same CMP gather. After applying the NMO correction, the process of stacking is equivalent to adding events that are aligned in time.

Short summary:

- **Data Before NMO:** $D(x_m, h, t)$. Traces with a fixed position x_m and variable offset corresponds to a CMP gather before NMO.
- **Data After NMO:** $D(x_m, h = 0, t)$. Traces with a fixed position x_m and variable offset corresponds to a CMP gather after NMO.
- **Data After NMO and Stacking:** $\text{Section}(x_m, t) = \sum_h D(x_m, h = 0, t)$

It is clear that after applying NMO and Stacking, we have removed one dimension from our data

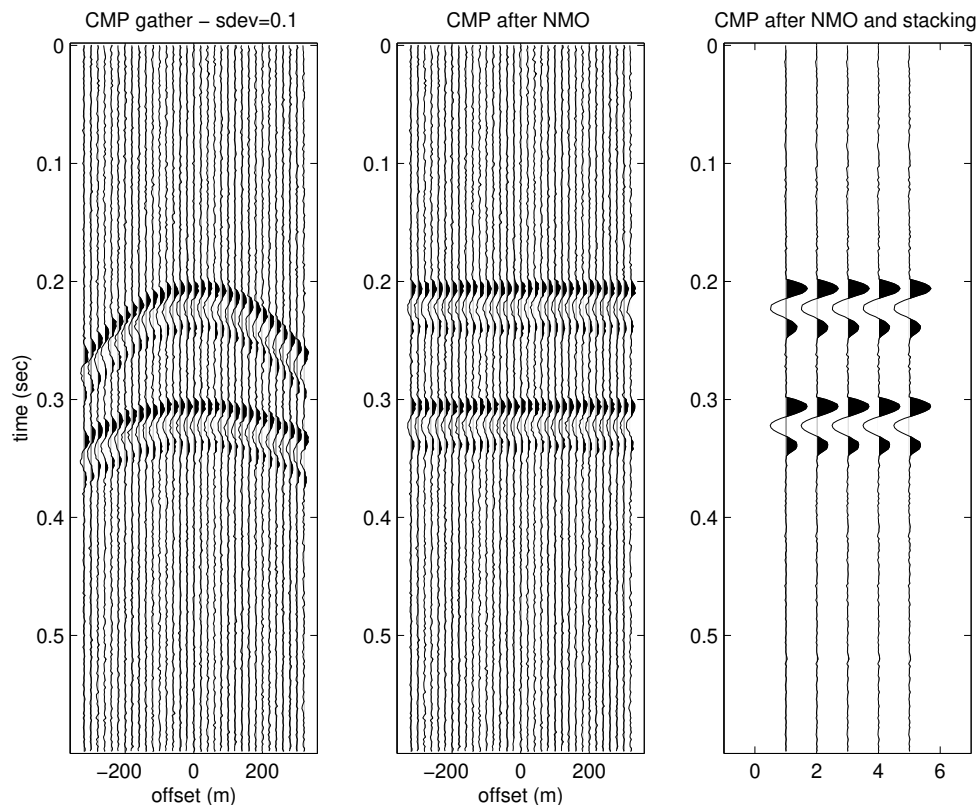


Figure 3.22: NMO and stacking. Left: CMP gather before NMO correction. Centre: CMP gather after NMO correction. Left: Stack CMP trace repeated 5 times.

volume. In other words,

$$D(x_m, h, t) \rightarrow \text{NMO+Stacking} \rightarrow \text{Section}(x_m, t).$$

A collection of **Stacked Traces** each one having a different midpoint position is what we call a **Seismic Section**. The Seismic Section represents an image in time of the earth's interior. Each trace in a seismic section corresponds to the trace one should have obtained after running an experiment where the midpoint position is variable whereas the source-receiver distance (offset) is kept constant and equal to zero ($h = 0$). Our discussion can be summarized as follows

- The NMO correction removes the dynamic term h^2/v^2 from the hyperbolic travelttime curve.
- NMO correction followed by stacking maps the data cube in (x_m, h, t) space into a 2D image in (x_m, t) space.
- NMO correction followed by stacking increases the SNR. This is shown by Figures 3.22, 3.23, and 3.24. The process is equivalent to sum seismic reflections that are now aligned in time.
- NMO correction followed by stacking also serves to attenuate multiple reflections. We will return to this point when we discuss the attenuation of multiples.

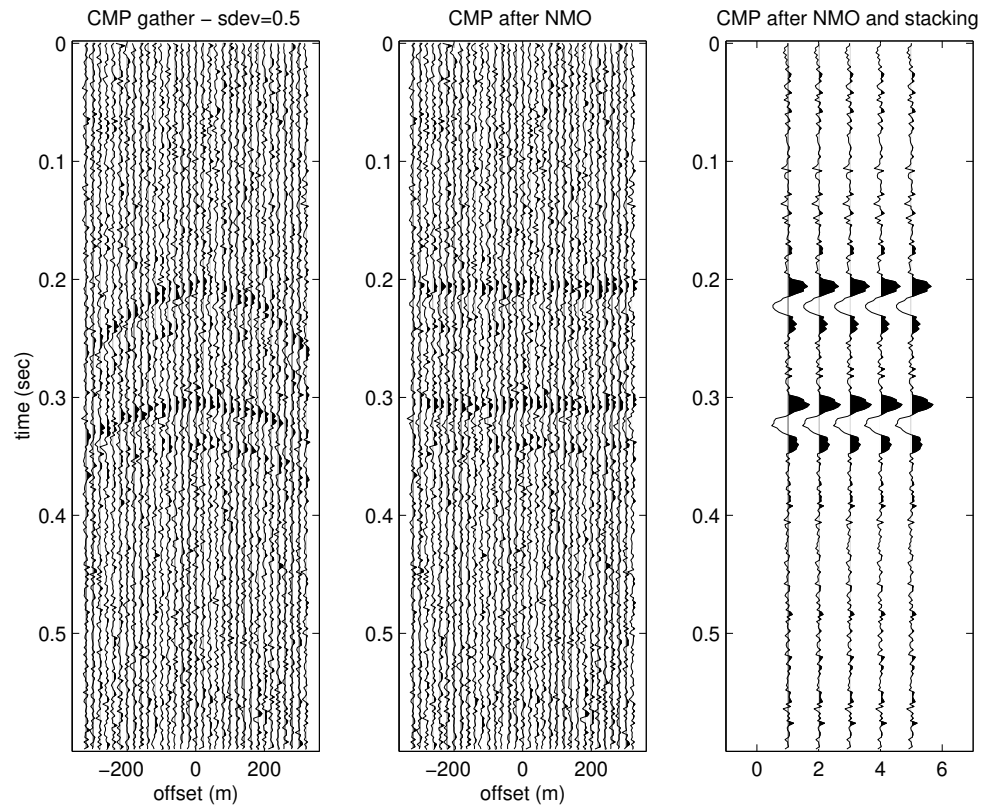


Figure 3.23: NMO and stacking. Left: CMP gather before NMO correction. Centre: CMP gather after NMO correction. Left: Stack CMP trace repeated 5 times. Notice the attenuation of random noise in the data.

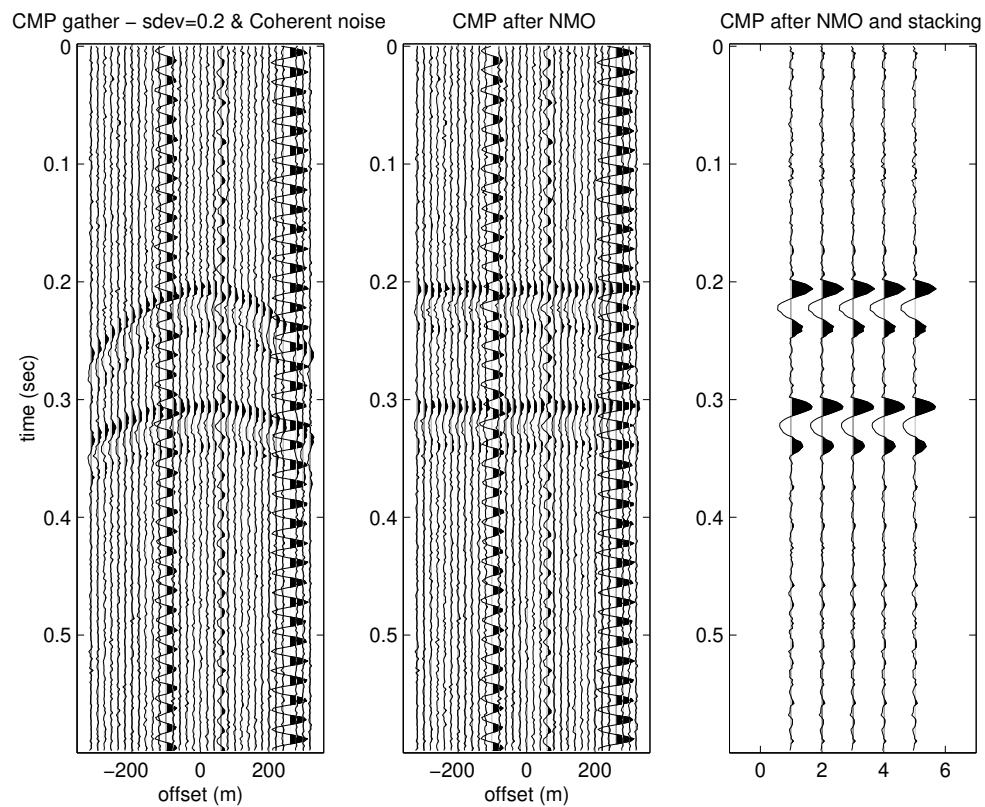


Figure 3.24: NMO and stacking. Left: CMP gather before NMO correction. Centre: CMP gather after NMO correction. Left: Stack CMP trace repeated 5 times. Notice the attenuation of the sinusoidal coherent noise.

Chapter 4

Reflection seismology: Normal Moveout Correction, Velocity Analysis and Stacking

In Chapter 3 we analyzed traveltime curves for refraction and reflection data. We have introduced Common Midpoint Gather (CMP) gathers and we briefly examined the NMO correction. In this chapter, we will explore these concepts again in more detail and discuss several procedures to estimate **Stack Sections**.

4.1 Stacking charts

First, I would like to mention a few words about the seismic acquisition. Conventional 2D seismic data are acquired by deploying a large number of receivers along a line and by having sources of energy activated at positions on the line. The source can be a chemical explosion (dynamite) or a mechanical vibratory unit also called a vibroseis. In general, only a group of receivers are active for a given source. In Figure (4.1) I portray a simple acquisition geometry that corresponds to $N_s = 20$ sources. See the vertical axis of the plot where I have indicated the source number or **field record number**. In this example, I have adopted an array of $NR = 24$ receivers per shot. The axis x indicates the position of the source or receiver for each field record. A seismogram also called a seismic trace is recorded by each source-receiver pair. The following spatial variables describe the experiment

- Distance between shots (sources): $\Delta s = 24 m$
 - Distance between receivers: $\Delta r = 25 m$
 - Near offset (The minimal distance source-receiver): $h_{min} = 100$
 - Distance between consecutive Common Mid Point (CMP) positions $\Delta x_m = \Delta s/2 = 12.5 m$
-

In our example the first shot point is located at $x_o = 1000\text{ m}$. We can express the source position as follows:

$$x_s(i) = x_o + (i - 1) \Delta s, i = 1, \dots, NS.$$

Similarly, the position of the receiver j associated to the source i is given by

$$x_r(i, j) = x_s(i) + h_{min} + (j - 1) \Delta r, j = 1, \dots, NR.$$

In Figure (4.1) we display the source-receiver position for each seismic trace. Rotated axis correspond to traces with the same midpoint position (CMP gather) and traces with the same offset (Common Offset gather). During acquisition, the recording unit stores seismic traces in field records. In other words, a binary file with a special format ¹ contains the seismic data. The file structure is as follows

```
Header & Trace for Shot 1 Receiver 1
Header & Trace for Shot 1 Receiver 2
Header & Trace for Shot 1 Receiver 3
.
.
.
Header & Trace for Shot 2 Receiver 1
Header & Trace for Shot 3 Receiver 2
Header & Trace for Shot 4 Receiver 3
.
.
.
```

The **Header** is a 240 bytes partition where the file stores all the relevant information needed to characterize the recorded **Trace** (e.g., source, receiver position, offset, CMP number, time sampling interval, etc.).

A procedure called **sorting** permits one to re-organize the seismic volume in CMP gathers. After **CMP sorting** the output will look like

```
Header & Trace for CMP 1 Offset 1
Header & Trace for CMP 1 Offset 2
Header & Trace for CMP 1 Offset 3
.
.
.
Header & Trace for CMP 2 Offset 1
Header & Trace for CMP 2 Offset 2
Header & Trace for CMP 2 Offset 3
.
```

¹SEG-Y file is a particular file format designed to store and distribute seismic data <https://seg.org/Publications/SEG-Technical-Standards>.

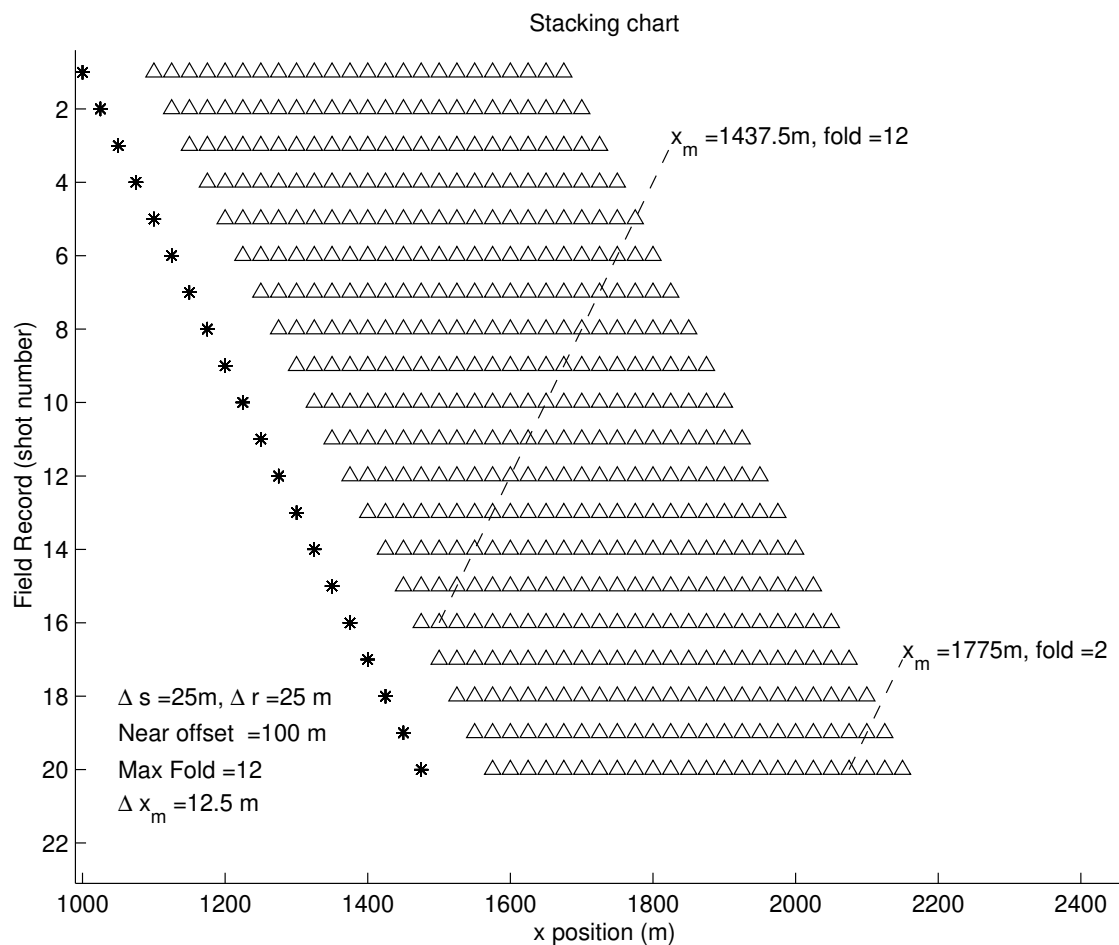


Figure 4.1: A stacking chart for a experiment that consists of 20 sources and 24 receivers. The receivers participating in the CMP gathers with midpoints $x_m = 1437.5m$ and $x_m = 1775.5m$ are also indicated. Note that the maximum fold is 12 (fold: number of traces per CMP).

where CMP 1 indicates the CMP number associated with the first midpoint x_m position.

4.2 Velocity analysis

We have already seen that in a CMP gather the moveout curve of a reflection can be approximated by a hyperbola

$$T = \sqrt{T_0^2 + h^2/v^2} \quad (4.1)$$

where h is the source-receiver distance (offset), v is the velocity of the reflection hyperbola. The

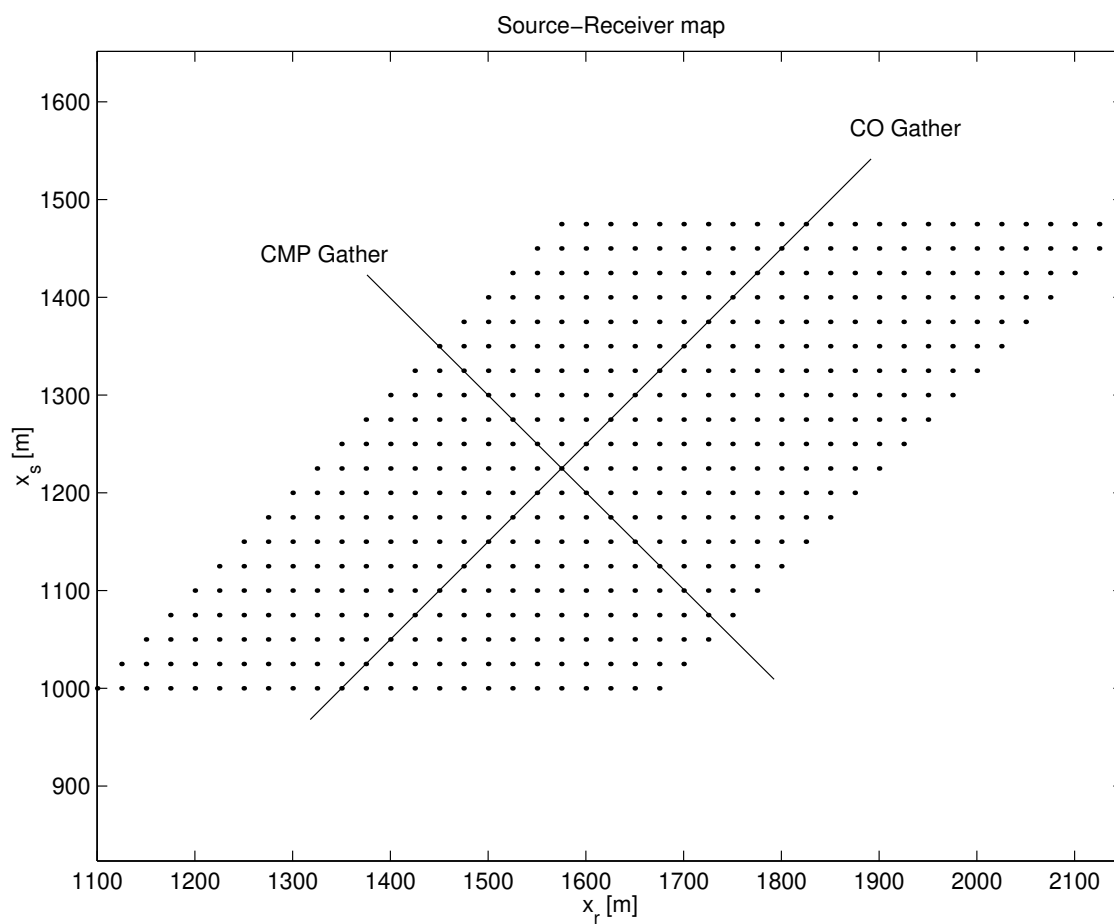


Figure 4.2: Source-receiver position for the experiment displayed in Figure (4.1). Each dot indicates a seismic trace. Rotated axes indicate the traces participating in a Common Offset (COF) gather and a Common Midpoint (CMP) gather, respectively.

term **Velocity Analysis** refers to a numerical algorithm that permits the retrieval of the pairs T_0, v that parametrize seismic reflections in a CMP gather.

The algorithm for Velocity Analysis operates in consecutive temporal windows by evaluating a coherence measure along a **tentative** moveout curve. The analysis is carried out for a set of tentative velocities; the velocity corresponding to the peak of the coherence, is interpreted as the velocity that best flattens the seismic event at which is the velocity you will use for NMO correction.

If $C(t_0, v)$ denotes the coherence at a window centered at $t = t_0$, an estimate of the velocity v is obtained at the peak value of $C(t_0, v)$. A standard coherence measure is the **semblance**. To derive the semblance; we first define the data window of length $2M + 1$ centred about a moveout curve with intercept time, t_i , and velocity, v_j

$$\mathbf{M}(t_i, v_j) = \begin{pmatrix} x_{t_i - M\Delta t, 1} & x_{t_i - M\Delta t, 2} & \dots & x_{t_i - M\Delta t, N} \\ \dots & \dots & \dots & \dots \\ x_{t_i + M\Delta t, 1} & x_{t_i + M\Delta t, 2} & \dots & x_{t_i + M\Delta t, N} \end{pmatrix}. \quad (4.2)$$

Where N indicates the number of traces and ΔT the time sampling interval of the seismogram. The following expression provides the semblance

$$S(t_i, v_j) = \frac{\sum_t (\sum_k x_{tk})^2}{\sum_k \sum_t x_{tk}^2}. \quad (4.3)$$

A pseudo-code for velocity analysis should look like

```
FOR all  $t_i$  and  $v_j$ 
  Construct the matrix  $\mathbf{M}(t_i, v_j)$ 
  Compute coherence measure ,i.e.,  $S(t_i, v_j)$ 
ENDDO
```

It is clear that when one of the tentative velocities matches the velocity of the reflection, the seismic event is entirely contained in the window, and therefore, the semblance will show a peak. A CMP gather and its semblance panel is portrayed in Figure (4.3). This CMP corresponds to a land survey in the Western Canadian Sedimentary Basin (WCSB). In this example, it is quite hard to identify multiple reflections.

4.2.1 Velocity Scans

We can also evaluate Velocity Scans by displaying the CMP gather after applying a **constant** velocity NMO correction ². By displaying consecutive NMO corrected scans we can visualize the

²Constant velocity NMO correction means that one velocity is used for all times

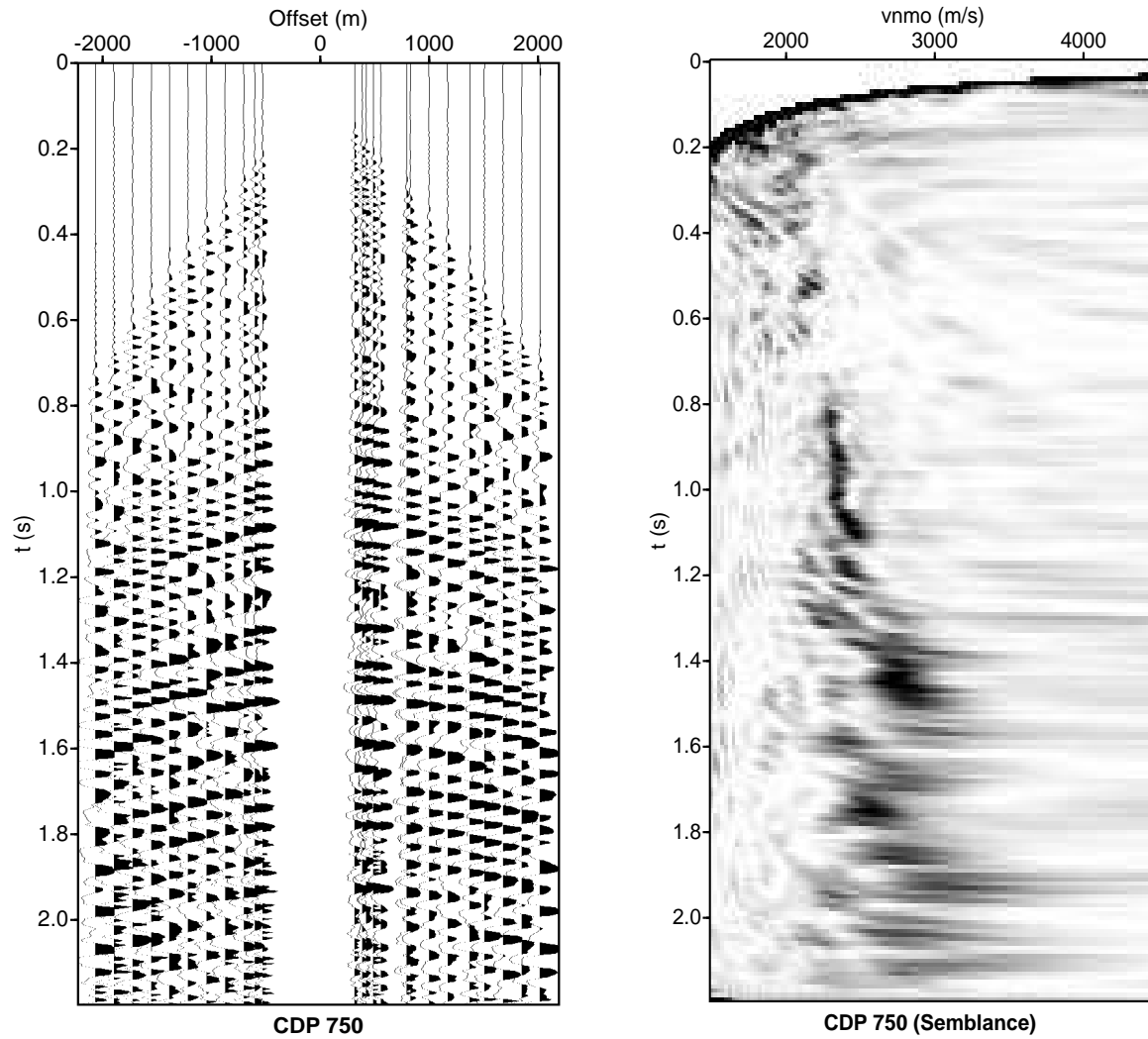


Figure 4.3: A CMP gather and its associated semblance panel.

velocity and the time at which an event becomes horizontal. After presenting successive scans, we can quickly select the T_0, v pairs corresponding to seismic reflections. An algorithm to compute velocity scans

```
FOR all  $v_j = v_{min} + \Delta v$   
    Apply constant NMO correction to the CMP gather with  $v = v_j$   
    Display Scan j  
ENDDO
```

In Figure (4.4) I portray the velocity scan for the CMP in Figure (4.3). The first panel was computed using a velocity $v = 1500m/sec$, the second $v = 1750m/sec$ and so on. You can try use Figures (4.3) and (4.4) to pick the NMO velocities.

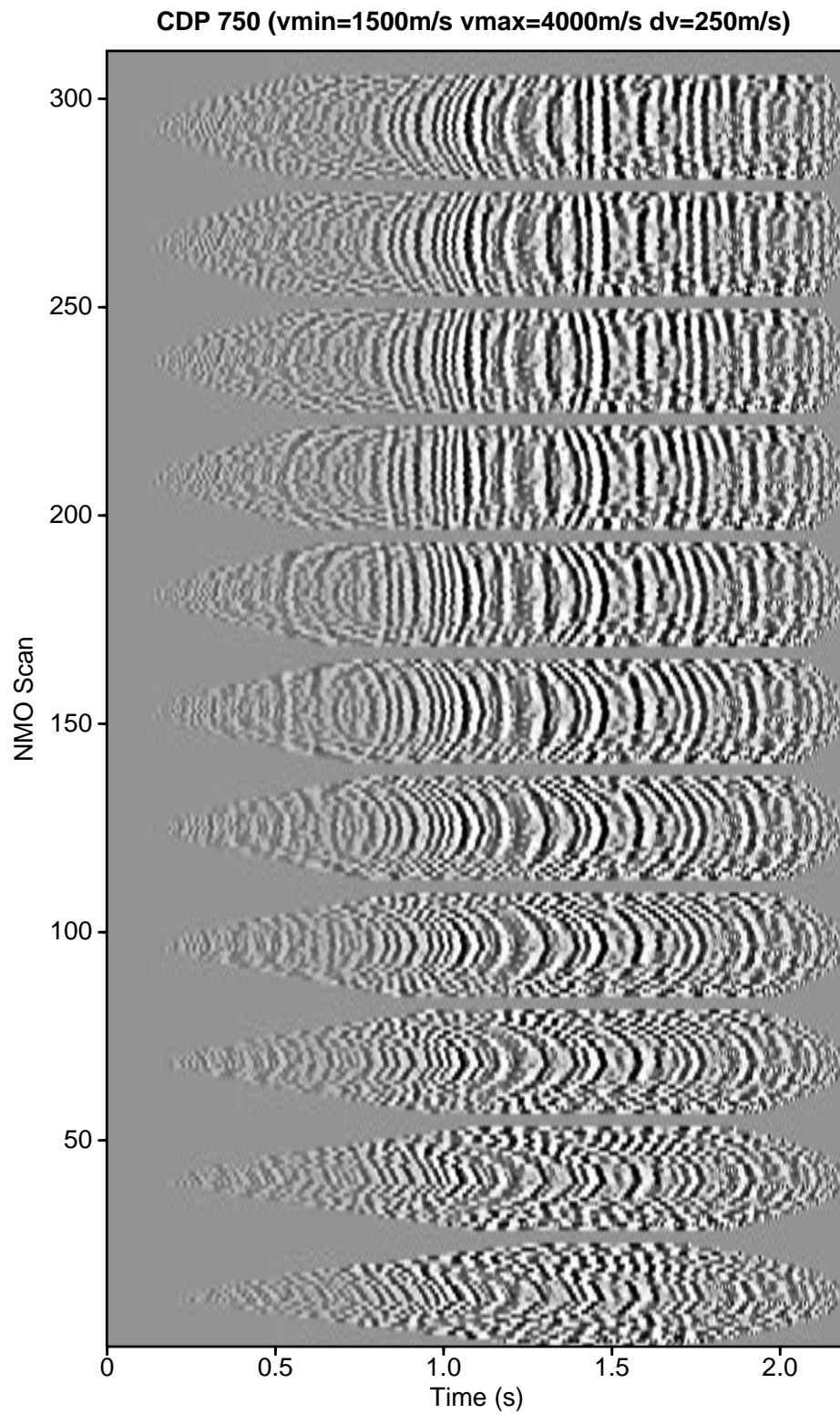


Figure 4.4: Velocity scan for the CMP portrayed in Figure (4.3), the minimal NMO velocity is 1500 m/s , the maximum velocity is 4000 m/s . We have adopted a velocity interval of 250 m/s .

4.2.2 Constant velocity stacks

Constant velocity stacks are obtained by NMO correcting a set of adjacent CMP gathers and stacking each CMP along offset. This procedure produces a small stacked section for each NMO velocity. We can use constant velocity stacks to retrieve the velocities that optimize the stack for the selected CMP gathers.

The flow chart looks like:

```

FOR cdp=1,N (pick N adjacent CMPs)
FOR all  $v_j = v_{min} + \Delta v$ 
    Apply constant NMO correction to the CMP gather with  $v = v_j$ 
    Stack the NMO corrected CMP along offset
ENDDO
    Display Constant Velocity Stack j
ENDDO

```

In Figure (4.5) I portray an ensemble of Constant Velocity Stacks computed using CMPs 640 to 660.

4.2.3 The seismic section

Velocity analysis, velocity scans and constant velocity stacks are processes to estimate NMO velocities at different CMP locations. In general, this is repeated for a set of CMP positions to yield an NMO velocity model. For instance, we estimate NMO velocities every 50 CMPs. The NMO velocities for the rest of the CMPs can be determined via interpolation.

Once we have picked the NMO velocities for different CMP positions, the remaining process entails the application of NMO corrections to all the CMP gathers and, finally, stacking. Each CMP will generate a stacked trace; the seismic section is composed of all these stacked traces plotted versus mid-point (or CMP or CDP number). Sometimes, all stacked traces versus CMP merely is called "the stack." It is important to stress that the stacked section, for a simple geological model, resembles the seismic section that one should have obtained after performing a zero-offset experiment. An experiment where source and receiver occupy the same field position.

These are the velocities that I picked³.

cdp=545,645,745,845

³The first line indicates the CDP number where we carried out velocity analysis.

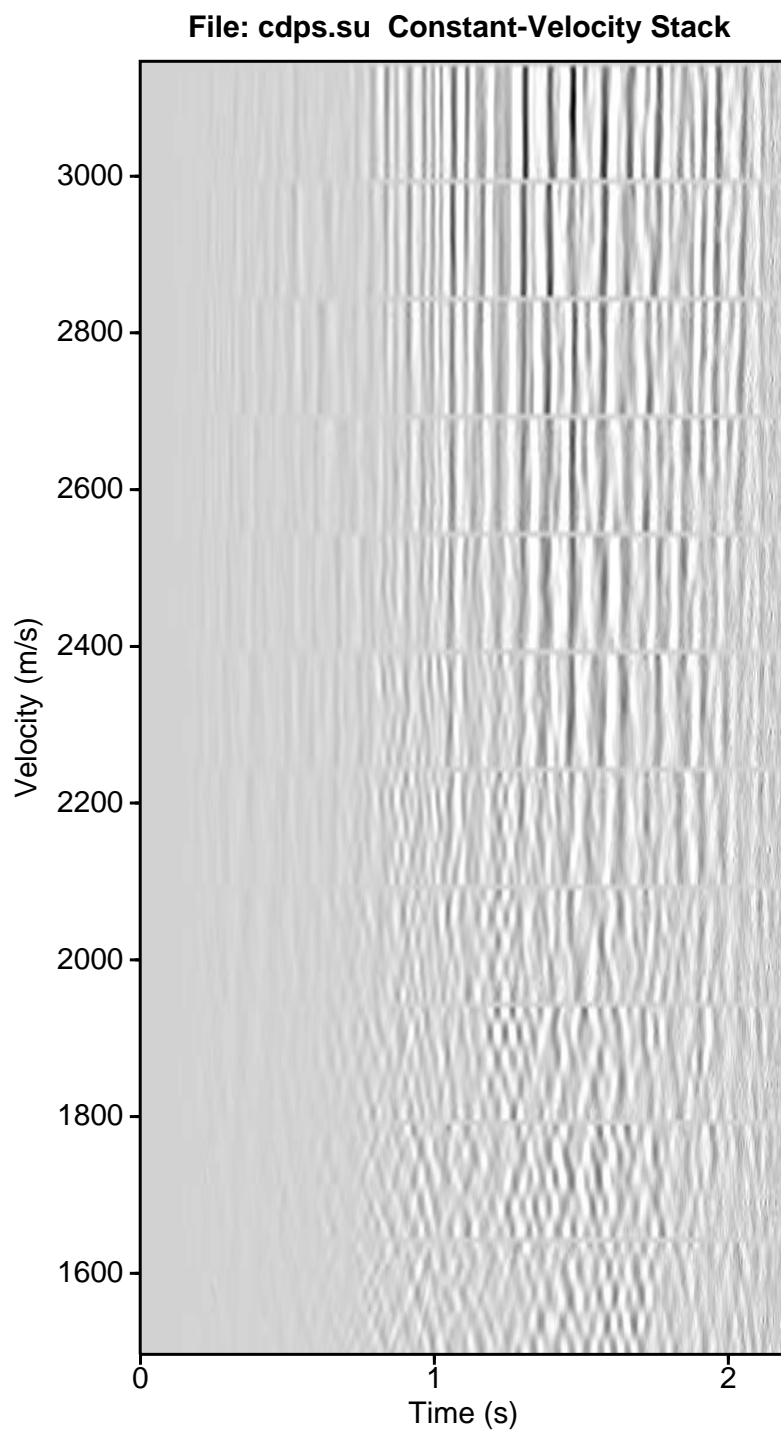


Figure 4.5: Constant velocity stacks for CMP 640 to 660.

tnmo=0.5954,0.8043,0.9087,0.9366,1.058,1.18,1.431,1.581,1.856,2.005
vnmo=2674,2964,3112,3135,3175,3249,3477,3517,3477,3449
tnmo=0.6058,0.8878,0.9958,1.152,1.737,1.852,1.988
vnmo=2691,3158,3232,3369,3608,3716,3722
tnmo=0.3934,0.9401,1.1,1.191,1.351,1.619,2.009
vnmo=2657,3243,3386,3426,3563,3534,3722
tnmo=0.5188,1.062,1.163,1.936,2.002,2.103
vnmo=2919,3375,3414,3563,3580,3631

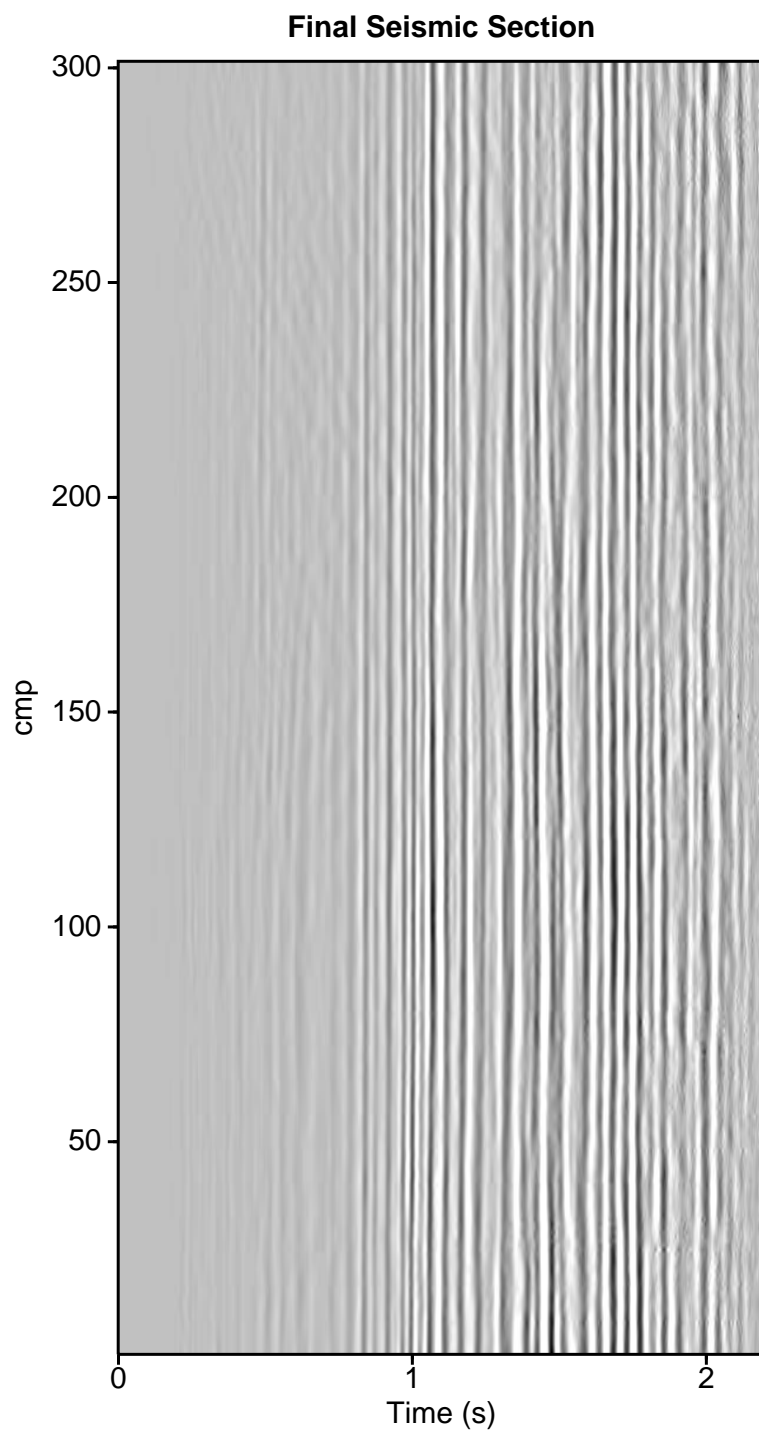


Figure 4.6: Final seismic section obtained after NMO correction and stacking all the CMP gathers

4.3 Staking and its the frequency response

We will analyze the frequency response of the stacking process when applied to a CMP gather after the NMO correction.

Consider the $t - h$ diagram for a primary reflection and a multiple reflection. We will assume that the intercept t_0 is the same for both reflections. The velocity of the primary reflection is denoted by v_p and the velocity of the multiple by v_m . The $t - h$ relations are

$$T_m^2 = T_0^2 + \frac{h^2}{v_m^2} \quad (4.4)$$

and

$$T_p^2 = T_0^2 + \frac{h^2}{v_p^2}. \quad (4.5)$$

We now assume that the NMO correction was applied, and that the primary reflection is correctly flattened. The residual moveout or time difference between the primary and the multiple is given by

$$M = T_m - T_p \quad (4.6)$$

The traveltim for the multiple can be written as follows

$$T_m^2 - T_0^2 = (T_m + T_0)(T_m - T_0) = \frac{h^2}{v_m^2}. \quad (4.7)$$

If we assume that $T_m \approx T_0$, we can write

$$2(T_0)(T_m - T_0) \approx \frac{h^2}{v_m^2} \quad (4.8)$$

From where it is easy to see that

$$(T_m - T_0) \approx \frac{1}{2T_0} \frac{h^2}{v_m^2} \quad (4.9)$$

A similar trick is used to obtain an expression for T_p ,

$$(T_p - T_0) \approx \frac{1}{2T_0} \frac{h^2}{v_p^2}. \quad (4.10)$$

Now that we have been able to eliminate the square roots, we can find the following expression for the residual moveout

$$M = \frac{h^2}{2T_0} \left(\frac{1}{v_m^2} - \frac{1}{v_p^2} \right). \quad (4.11)$$

This is the expression for a parabola in $h-t$. Consider the residual moveout at far offset ($h = h_{max}$), and the residual moveout at any generic offset h ,

$$M_{max} = \frac{h_{max}^2}{2T_0} \left(\frac{1}{v_m^2} - \frac{1}{v_p^2} \right). \quad (4.12)$$

we can write the residual moveout for the trace i with offset h_i as follows

$$M_i = M_{max} \frac{h_i^2}{h_{max}^2}. \quad (4.13)$$

When we design a seismic experiment we need to consider different field acquisition parameters. For instance, we need to define the minimum and maximum offset (near and far offset traces) and the fold (number of traces per CMP). We will examine the relationship between these variables and how one can select them to optimally attenuate multiples.

Let us assume that offset differences are constant:

$$h_4 - h_3 = h_3 - h_2 = h_2 - h_1$$

In this case, our fold is $N = 3$ because our CMP is composed of 3 seismograms. The fold $N = 3$ is only for illustrative purposes because the fold in modern acquisition system is 60 to 240 for 2D seismic data. We will need the following variables (see figure)

$$L = h_{max} - h_{min}$$

$$h_{min} = KL$$

where K is a constant to determine. One can express the increment in offset as follows

$$h_4 - h_3 = h_3 - h_2 = h_2 - h_1 = \frac{L}{N-1}.$$

The offset for the i -trace is given by

$$h_i = KL + (i-1) \frac{L}{N-1}, \quad h_{max} = KL + L = (K+1)L. \quad (4.14)$$

Now, we recall the expression for the residual moveout

$$M_i = M_{max} \frac{h_i^2}{h_{max}^2} = M_{max} \left(\frac{K(N-1) + (i-1)}{(K+1)(N-1)} \right)^2, \quad i = 1, 2, \dots, N \quad (4.15)$$

The residual moveout M_i is the time difference between the primary and the multiple at receiver i after NMO correction. When we stack the CMP gather after applying the NMO correction, the primary reflection stacks in phase and, therefore, its amplitude becomes larger than the amplitude

of multiple. Can we measure the magnitude of the multiple attenuation after stacking? To answer this question, first, we will consider that the primary and the multiple can be modelled using a complex exponential of frequency f and amplitude.

Primary after NMO (the delay between traces is 0 everywhere).

$$x_p(h_i) = Ae^{i2\pi f_0} = A \quad (4.16)$$

Multiple after NMO (the delay is now M_i).

$$x_m(h_i) = Ae^{i2\pi f M_i} = Ae^{i2\pi f M_{max} \left(\frac{K(N-1)+(i-1)}{(K+1)(N-1)} \right)^2}. \quad (4.17)$$

The frequency response of the stacking process can be evaluated via the following expression

$$R(f) = \frac{\text{Energy of the Multiple after NMO}}{\text{Energy of the Primary after NMO}} = \frac{E_m}{E_p} \quad (4.18)$$

where

$$E_p = \sum_{k=1}^N |x_p(h_i)|^2 = \sum_{k=1}^N A^2 = N A^2 \quad (4.19)$$

$$E_m = \sum_{k=1}^N |x_m(h_i)|^2. \quad (4.20)$$

The response function becomes

$$R(f) = \frac{E_m}{E_p} = \frac{1}{N} \sum_{k=1}^N |e^{i2\pi f M_{max} \left(\frac{K(N-1)+(i-1)}{(K+1)(N-1)} \right)^2}|^2 \quad (4.21)$$

In general, we need a priori knowledge of the velocities of the reflections and multiples to find an upper bound for M . In other words, we need to know the residual moveout at far offset. Once that we define h_{max} we compute M_{max} and the response function for given values of K and N . We iterate until we find a curve that rejects the energy of the multiple in the seismic band (e.g. 5 – 100Hz). Once we have K and N it is easy to compute the minimum offset and the distance between receivers in the field. We have shown that NMO followed by stacking acts as a filter. A particular type of filter that depends on the parameters used to acquire the data (K, N, h_{max}) .

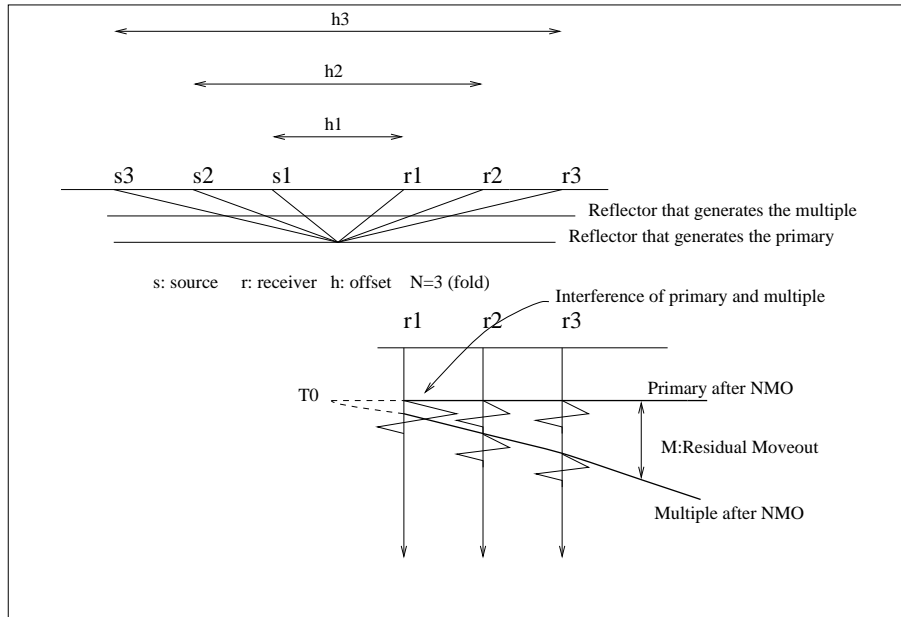


Figure 4.7: A primary event and a multiple after NMO correction. The velocity of the primary was used to perform the NMO correction. The residual moveout is designated by the variable M .

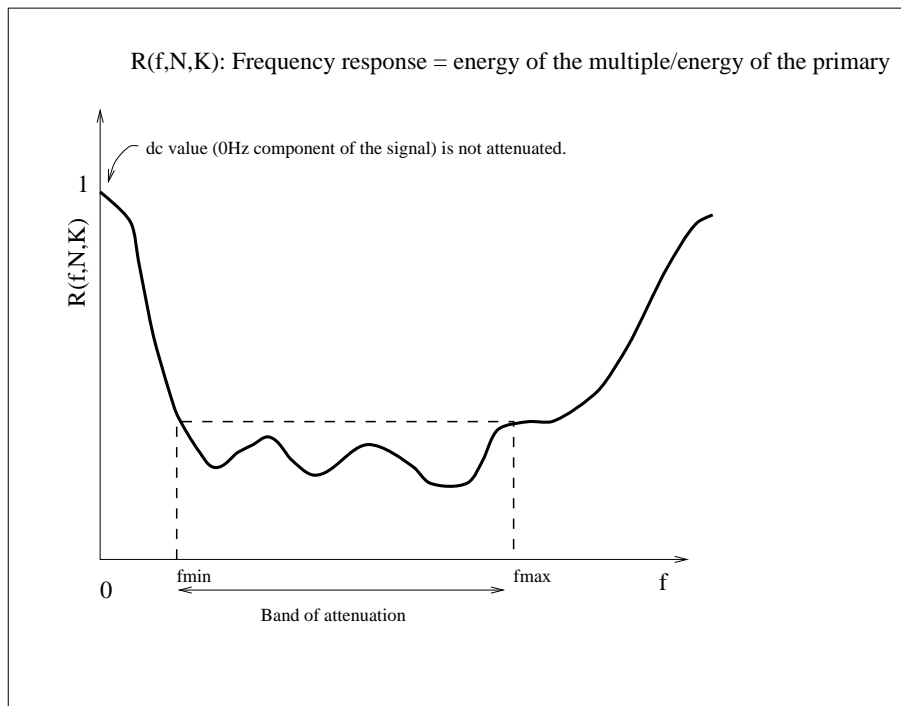


Figure 4.8: Response of the stack as function of frequency. The response curve measures the ratio of the energy of the multiple to the energy of the primary after NMO correction. Acquisition parameters are computed to obtain maximum attenuation in the seismic frequency band.

Chapter 5

Modeling Normal Incidence Seismograms

In this chapter, we will study the problem of computing reflection and transmission coefficients for a layered media when plane waves propagate in the earth with an angle of incidence $i = 0$ (Normal incidence).

5.1 Normal incidence

We assume an interface separating two media with P velocities v_1 and v_2 and densities ρ_1 and ρ_2 , respectively. Consider a plane wave impinging at an angle of propagation $i = 0$ (see Figure (5.1)). In this case, we have three waves

- Incident wave: \downarrow in medium 1
- Reflected wave: \uparrow in medium 1
- Transmitted wave: \downarrow in medium 2.

Let us assume that the amount of incident wave is equal to 1, the amount of reflected wave is given by r , and the amount of the transmitted wave is denoted by t . At the boundary the following condition should be satisfied (continuity of displacements)

$$1 + r = t$$

This equation has two unknowns, to compute the r and t we need one additional equation. We will consider conservation of energy. In the acoustic (vertical incidence case) conservation of energy leads to the following equation

$$I_1 \times 1^2 = I_1 \times r^2 + I_2 \times t^2 .$$

The quantities I_1 and I_2 are called **acoustic impedances**

$$I_1 = \rho_1 v_1, \quad I_2 = \rho_2 v_2$$

where ρ_1 and ρ_2 are the densities of the material above and below the interface and v_1 and v_2 the P-velocities, respectively. After combining the equations of continuity of displacement and conservation of energy we obtain the following expressions

$$r = \frac{I_1 - I_2}{I_2 + I_1} \quad \text{Reflection coefficient} \quad (5.1)$$

$$t = \frac{2I_1}{I_2 + I_1} \quad \text{Transmission coefficient} \quad (5.2)$$

The above analysis is valid for an incident plane wave propagating downwards. Let's consider the case of an incident wave propagating upwards (Figure (5.2)).

- Incident wave: \uparrow in medium 2
- Reflected wave: \downarrow in medium 2
- Transmitted wave: \uparrow in medium 1

In this case, the reflection and transmission coefficients are given by

$$r' = \frac{I_2 - I_1}{I_2 + I_1}, \quad (5.3)$$

and

$$t' = \frac{2I_2}{I_2 + I_1}. \quad (5.4)$$

From the above equations it is clear that

$$r' = -r \quad (5.5)$$

5.1.1 Impulse response

We now assume that we conduct a zero offset experiment in a stratified earth model composed of four layers plus a half-space of impedances given by I_1, I_2, I_3, I_4, I_5 . (Figure (5.3)). At $t = 0$ a delta-like source emits energy into the earth. Waves are transmitted and reflected from the layers. If we do not consider multiples, our seismogram will be composed of 4 arrivals (4 reflections).

To simplify the problem, I will show how to compute the amplitude of the wave recorded at the surface of the earth generated (reflected) at the interface number 4. First, we have to

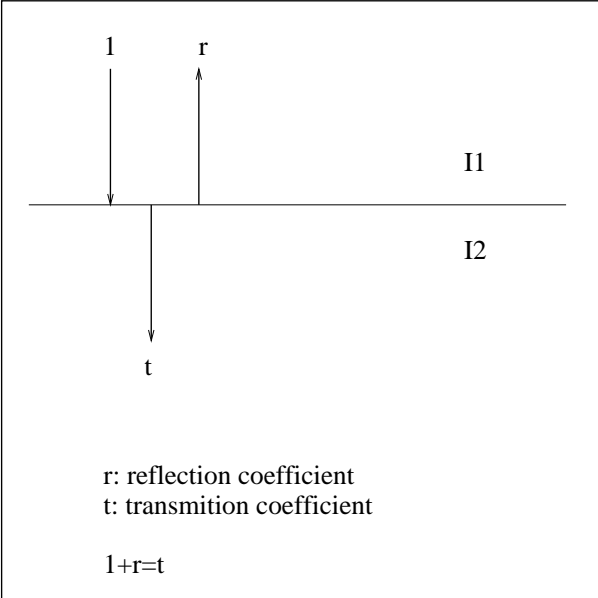


Figure 5.1: P-wave normal incidence. The incident wave is propagating downwards.

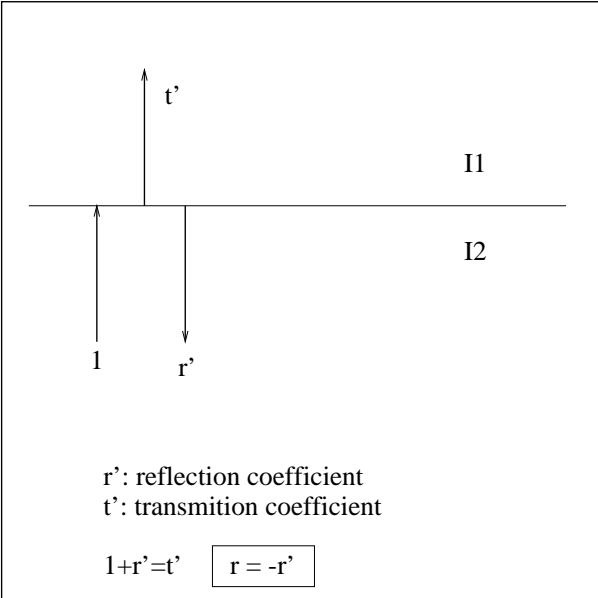


Figure 5.2: P-wave normal incidence. The incident wave is propagating upwards.

compute the amount of amplitude transmitted to each one of the layers until reaching layer 4. In Figure (5.3) the transmission coefficients t are replaced by the equivalent expression $(1 + r)$. The amplitude of the wave reaching layer 4 is given by the following expression:

$$1 \times t_1 \times t_2 \times t_3 = (1 + r_1)(1 + r_2)(1 + r_3),$$

when the wave is reflected at interface 4 the total amplitude at that point (last expression) needs to be multiplied by the reflection coefficient of interface 4, in other words

$$1 \times t_1 \times t_2 \times t_3 \times r_4 = (1 + r_1)(1 + r_2)(1 + r_3)r_4$$

The wave (reflected wave) is now propagating upwards, therefore

$$1 + r' = 1 - r.$$

The final amplitude after propagating the wave to the surface of the Earth (this is what the receiver is measuring!) is given by

$$\underbrace{(1 + r_1)(1 + r_2)(1 + r_3)}_{\text{Transmission } \downarrow} \times \underbrace{r_4}_{\text{Reflection}} \times \underbrace{(1 - r_1)(1 - r_2)(1 - r_3)}_{\text{Transmission } \uparrow}.$$

The final expression for the amplitude of the wave reflected by the interface number 4 can be written down as follows

$$(1 - r_1^2)(1 - r_2^2)(1 - r_3^2)r_4.$$

It is clear that reflections occur at all the layers

Amplitude of the reflection generated at interface number 1

$$A_1 = r_1$$

Amplitude of the reflection generated at interface number 2

$$A_2 = (1 - r_1^2)r_2$$

Amplitude of the reflection generated at interface number 3

$$A_3 = (1 - r_1^2)(1 - r_2^2)r_3$$

Amplitude of the reflection generated at interface number 4

$$A_4 = (1 - r_1^2)(1 - r_2^2)(1 - r_3^2)r_4$$

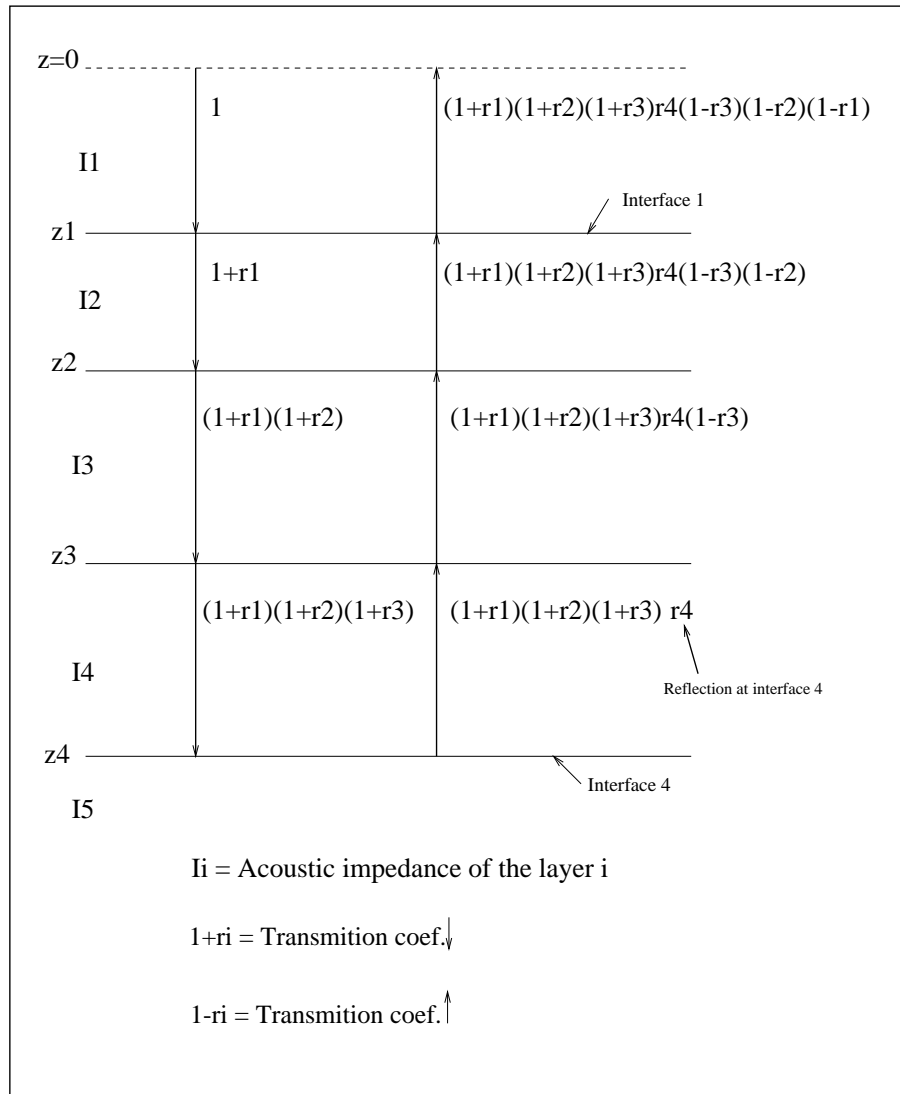


Figure 5.3: Amplitude of a wave plane wave propagating in a layered medium. Analysis of the wave reflected in the interface 4.

We can write a general expression for the amplitude of a reflection generated at the k interface

$$A_1 = r_1$$

$$A_k = \prod_{i=1}^{k-1} (1 - r_i^2) r_k, \quad k = 2, 3, 4, \dots$$

How do we interpret these results?. If we assume that the earth is excited with a delta function, and neglecting the presence of multiples, our zero-offset seismogram will be a collection of delta functions (spikes) at arrival times given by the two-way travel time formula. The strength of each arrival will be proportional to the amplitude of A_k .

However, in real exploration seismology, it is nor feasible to design a source that resembles a delta function. The source signature is called the wavelet or source wavelet. The wavelet is a finite length time function that we will denote as $w(t)$. In this case, the seismogram is represented by a superposition of wavelets arriving at different times and amplitudes proportional to A_k .

In our model consisting of 4 interfaces (Figure (5.3)) we will have 4 arrivals of amplitude A_1, A_2, A_3 and A_4 . The seismogram can be expressed as follows

$$s(t) = A_1 w(t - \tau_1) + A_2 w(t - \tau_2) + A_3 w(t - \tau_3) + A_4 w(t - \tau_4) \quad (5.6)$$

where $\tau_i, i = 1, 4$ are the arrival times of each reflection ¹ In GEOPH-426 we will see that the last equation can be expressed as a convolution sum. This is a pivotal concept in linear system theory.

5.1.2 Example

Let's put some numbers to the configuration in Figure (5.3).

Layer	z(m)	v (km/s)	ρ (g/cm ³)	
1	200	1.5	1.0	Water
2	500	2.0	2.4	limestone
3	630	3.0	2.4	sandstone
4	700	2.1	2.3	limestone
Half-space	1300	4.3	2.1	Hard deeper layer

Table 5.1:

Figure (5.4) portrays the acoustic impedance ($I = v \times \rho$), the reflectivity series and the synthetic seismogram obtained by convolving a synthetic source function with the reflectivity series. In this example, we have not considered transmission effects and multiple reflections.

¹Notice that $w(t - \tau)$ is $w(t)$ after being delayed τ seconds.

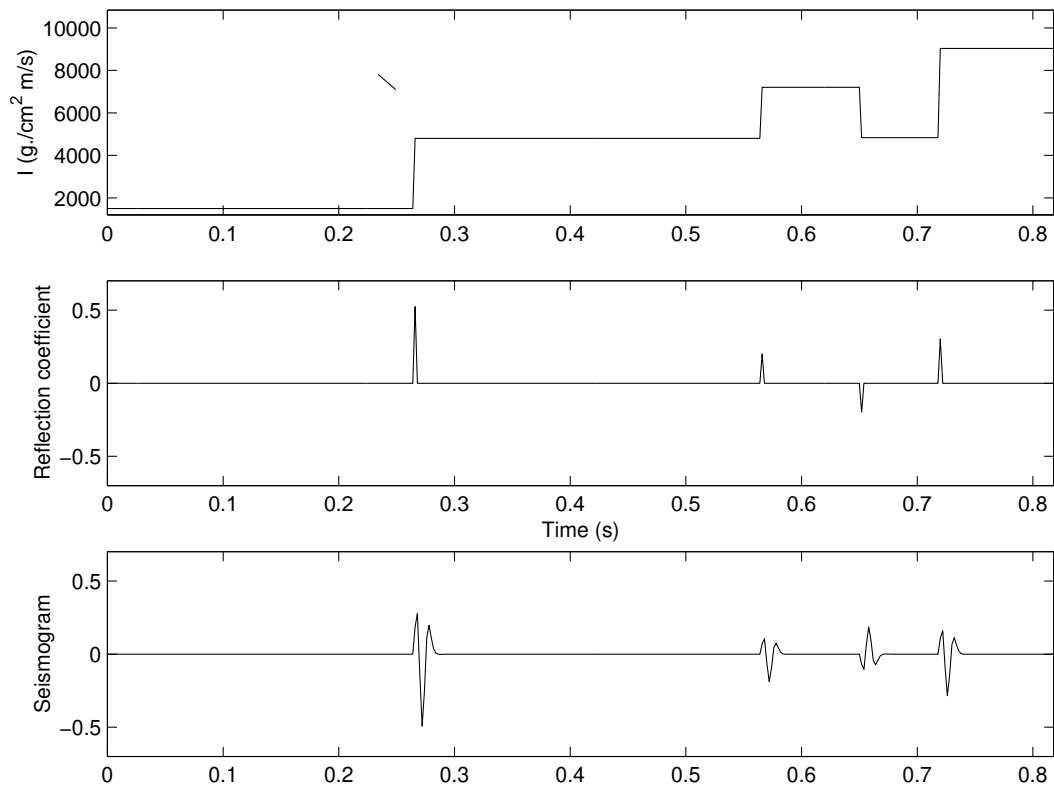


Figure 5.4: Acoustic impedance versus two-way travel time for the example in Table (5.1) (top). The reflectivity sequence (centre). The synthetic seismogram (bottom).

Chapter 6

Deconvolution

6.1 Deconvolution in the frequency domain

The classical model to represent a seismic trace states

$$s(t) = \int w(\tau - t) r(\tau) d\tau \quad (6.1)$$

where

- $s(t)$: seismic trace
- $w(t)$: source wavelet
- $r(t)$: reflectivity

the variable t indicates two-way traveltime (TWT). The reflectivity encodes information about the subsurface. Equation 6.1 is called a convolution integral. In simple words, the seismic trace is equal to the convolution of the reflectivity and the source wavelet. The process of recovering $r(t)$ from $s(t)$ is called *deconvolution*.

In seismic deconvolution, we are trying to recover $r(t)$, but in general, this is not possible. The best one can do is to estimate a good approximation to $r(t)$ that we will denote $\hat{r}(t)$. We will assume that the wavelet was correctly estimated or measured from the data. The latter is usually not true; in general, all we can determine is an approximation to the wavelet.

The deconvolution process can be carried out in the time domain or the frequency domain. We will deal with deconvolution in the frequency domain. The Fourier transform of a signal $x(t)$ is given by

$$X(\omega) = \int_{-\infty}^{\infty} x(t) e^{-i\omega t} dt. \quad (6.2)$$

We will indicate that $X(\omega)$ and $x(t)$ are related via the Fourier Transform via the following compact notation

$$x(t) \quad \leftrightarrow \quad X(\omega)$$

The Fourier convolution theorem states that convolution in the time domain is equivalent to multiplication in the frequency domain. Therefore, the convolution integral that expresses the seismic trace in equation (6.1) transforms into the multiplication of two complex functions

$$s(t) = r(t) * w(t) \quad \leftrightarrow \quad S(\omega) = R(\omega) \cdot W(\omega)$$

where

•

$$s(t) \quad \leftrightarrow \quad S(\omega)$$

•

$$w(t) \quad \leftrightarrow \quad W(\omega)$$

•

$$R(t) \quad \leftrightarrow \quad R(\omega).$$

It is clear that convolution is now the simple multiplication of two functions in the frequency domain. Therefore, the Fourier transform of the reflectivity series can be estimated via spectral division

$$S(\omega) = R(\omega) \cdot W(\omega) \quad \rightarrow \quad R(\omega) = \frac{S(\omega)}{W(\omega)}. \quad (6.3)$$

The problem with the above spectral division is that the amplitude the spectrum of the wavelet can be zero (or very small) at high frequencies, and therefore the deconvolution process could amplify the noise that is present in the data. In general, the spectral division is regularized¹ as follows

$$\hat{R}(\omega) = \frac{S(\omega) \cdot W^*(\omega)}{|W(\omega)|^2 + \mu} \quad (6.4)$$

where μ is a small positive number used to guarantee the stability of the division. In the previous expression, $|W(\omega)|^2 = W(\omega) \cdot W^*(\omega)$ is the squared amplitude spectrum of the wavelet and $W^*(\omega)$ is the conjugate of $W(\omega)$.

We must notice that $\hat{R}(\omega)$ is an estimate of the reflectivity in the frequency domain. To compute the reflectivity in the time domain, we adopt the Inverse Fourier transform

$$\hat{r}(t) = \frac{1}{2\pi} \int_{-\infty}^{\infty} \hat{R}(\omega) e^{i\omega t} d\omega. \quad (6.5)$$

The algorithm to deconvolve the data will be numerically implemented using the "Discrete Fourier Transform" (DFT). The discrete Fourier transform is used to compute the Fourier transform of discrete time series.

¹Regularization methods are methods used to obtain a stable solution of an inverse problem.

6.2 Example

In Figures 6.1 and 6.2, I provide deconvolution examples of clean and noisy data. In Figure 6.1 the solution is stable for different values of the parameter μ . However, it is clear that the resolution of the deconvolution process decreases with increases trade-off parameter μ . In Figure 6.2 we have added noise to the data. In this case, the solution is unstable for small values of the trade-off parameter μ . Increasing μ leads to a stable solution with decreased resolution. In general, stability to noise requires that one accepts decreasing the resolution of the deconvolution process. The instability of the solution arises from the denominator in equation 6.4, the denominator becomes small at low and high frequencies, and therefore the noise in the data is divided by a small number and consequently, is amplified.

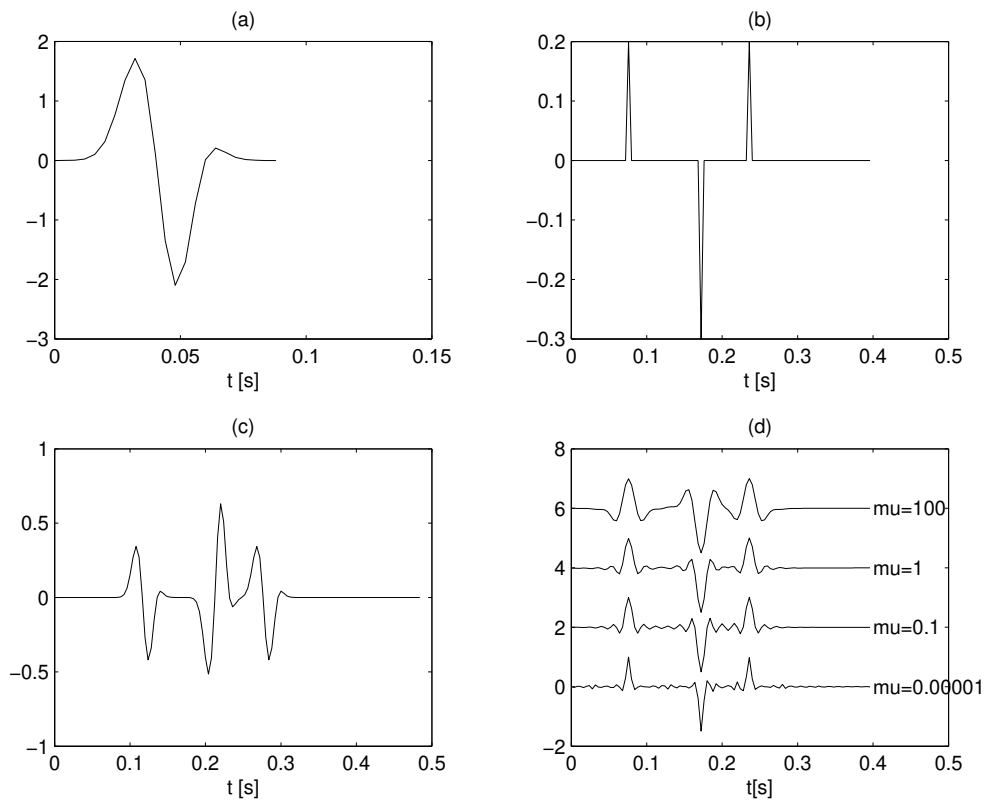


Figure 6.1: (a) Wavelet. (b) Reflectivity. (c) Noise-free seismogram. (d) Deconvolution with different values of μ (pre-whitening parameter).

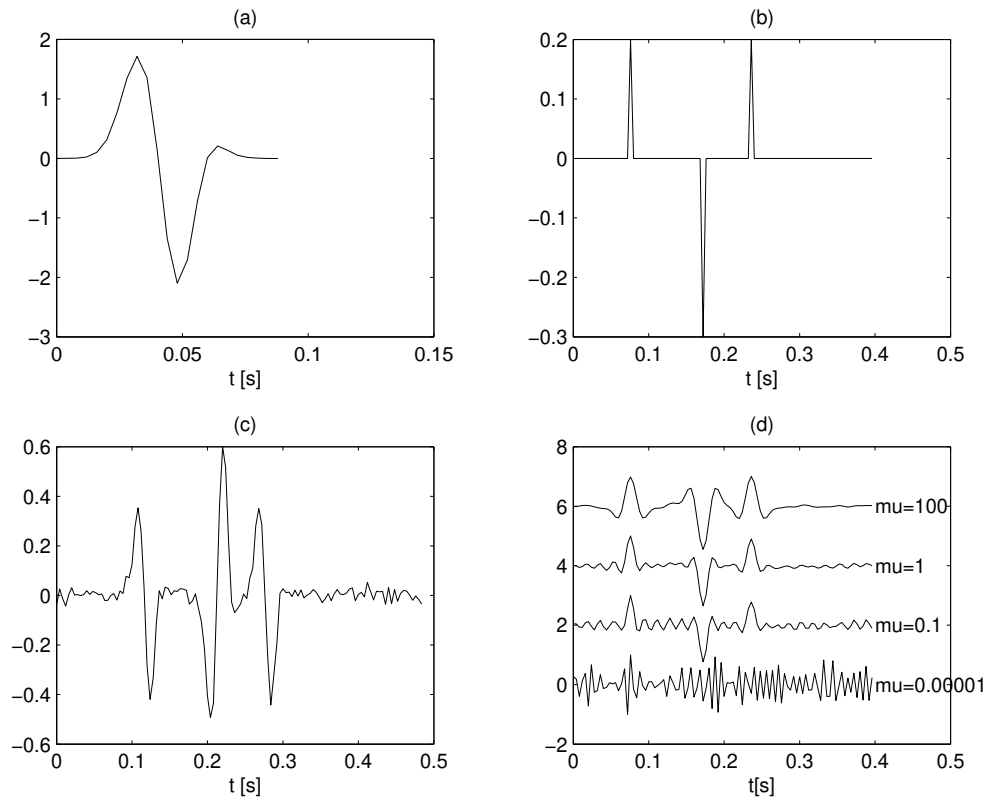


Figure 6.2: (a) Wavelet. (b) Reflectivity. (c) Seismogram contaminated with white noise (additive). (d) Deconvolution with different values of μ (pre-whitening parameter).

Chapter 7

The tomographic problem and introduction to linear inverse theory

So far we have been dealing with seismic reflection seismology and with the problem of constructing a seismic section. We still need to see how to convert a time section into a depth section. But, first I would like to spend a couple of lectures discussing inverse problems in seismology. I will start with the tomographic problem.

7.1 Inverse Theory

Inverse theory provides a mathematical framework to solve ill-posed problems. These are mathematical problems where the solution does not exist, or the solution is unstable.

In this section, we will briefly study the tomographic inverse problem. Bear in mind that other geophysical problems can be approached using the inverse problem formalism, i.e., inversion of gravity and magnetic anomalies, free oscillation of the earth, determination of density distribution of Earth, etc.

We can talk for hours about inversion but in simple terms imagine we have some data d , that is related to an earth model m via an operator \mathcal{F} ,

$$\mathcal{F} m = d,$$

in inversion, we look for a stable solution to the last problem. In other words, given the observed data d , one desires to estimate the subsurface mode m that caused the observations. We also consider data d perturbed by errors ¹. For instance, if we assume that the was perturbed an amount δd , the objective of the inverse theory is to find an inverse mapping operator such that

¹noise, systematic errors, etc

$$m_{sol} = \mathcal{F}^{-1} d$$

$$m_{sol} + \delta m_{sol} = \mathcal{F}^{-1} (d + \delta m)$$

where δm_{sol} is small. In other words, the inverse operator should not amplify noise or errors contaminating the data. We often prefer solutions m_{sol} to exhibit certain features. For instance, if we are inverting for velocity, we might desire the solution to be positive. We could also desire to estimate smooth solutions or sparse solutions.

7.2 Tomography

The goal in the tomographic inversion is to determine a velocity field from a multi-source multi-receiver experiment. Figure (7.1) provides an example of a tomographic experiment. The geological model is illuminated with seismic rays. The geological structure is approximated by a mathematical model composed of $n_x \times n_z$ cells. The velocity within each cell is constant. A perturbation travelling from the source i to the receiver j will take time t to reach the receiver. Let us denote the time to go from the source i to the receiver j , t_{s_i, r_j} . The travel time will depend on the velocity structure of the medium. The goal here is to determine the velocity of the geological formation from travel-times observed using the tomography experiment.

If we assume that velocity variations within the model are small, we can use the **straight ray approximation**. In this case, the travel times are given by

$$T_{s_i, r_j} = \sum_i^{ncells} l(k)_{i,j} s_k$$

where s_k is the slowness in the cell k and $l(k)_{i,j}$ are the segments on which the ray travels in each cell (Figure (7.1)). If we consider more than one ray, we can write the tomographic problem in matrix form

$$\mathbf{A}\mathbf{s} = \mathbf{t} \tag{7.1}$$

where \mathbf{t} is a vector containing the travel-times and \mathbf{s} is the vector containing the slowness of each cell. The matrix \mathbf{A} is called the tomographic matrix. The experiment defines this matrix. In other words, to obtain \mathbf{A} we need to know the position of the receivers and the size of the tomographic grid. In general, the travel-times are contaminated with noise (i.e., picking errors). In this case, we can write

$$\mathbf{A}\mathbf{s} + \mathbf{n} = \mathbf{t}_{obs} \tag{7.2}$$

Where \mathbf{t}_{obs} are noisy travel-times (this is what you can observe). In general we can assume that the errors are Gaussian and uncorrelated. In this case, the optimum solution for the tomographic

problem is given by the standard least-squares inverse. Here I'm assuming that we have more data than unknowns which is not always true. The least squares solution is given by

$$\mathbf{s} = (\mathbf{A}^T \mathbf{A})^{-1} \mathbf{A}^T \mathbf{t}_{obs} \quad (7.3)$$

The story does not finish here. The matrix $\mathbf{A}^T \mathbf{A}$ is an ill-conditioned matrix (some of its rows are linearly or quasi-linearly dependent). This is why we need to *regularize the problem*, or in other words, we need to make the problem well-posed (stable).

A simple trick is to add a perturbation to the main diagonal of the matrix $\mathbf{A}^T \mathbf{A}$. If \mathbf{I} is the identity matrix, and μ is a small scalar ($\mu > 0$) called the regularization parameter. The solution is now given by

$$\mathbf{s} = (\mathbf{A}^T \mathbf{A} + \mathbf{I}\mu)^{-1} \mathbf{A}^T \mathbf{t}_{obs} \quad (7.4)$$

The parameter μ called the regularization parameter is often also named the trade-off parameter or the damping parameter. In filter theory this parameter is often called the pre-whitening parameter (this is something coming from the deconvolution jargon.).

The effect of the least-squares inversion is seen in Figures (7.4b) and (7.4c). You can see that the technique has not been able to recover the true model (7.3b). This is because this is an inverse problem, and therefore, the solution is non-unique. In fact, in Figure (7.4b) we show the solution of the same problem, but now using smoothing constraints on the vertical and horizontal derivatives of the slowness field. Both solutions are honouring the data (they reproduce the observations) and therefore they are both valid solutions. Which one should you pick? It all depends on *prior* information, or in other words, on external information (i.e., velocities extracted from bore-hole data, geological information, etc.)

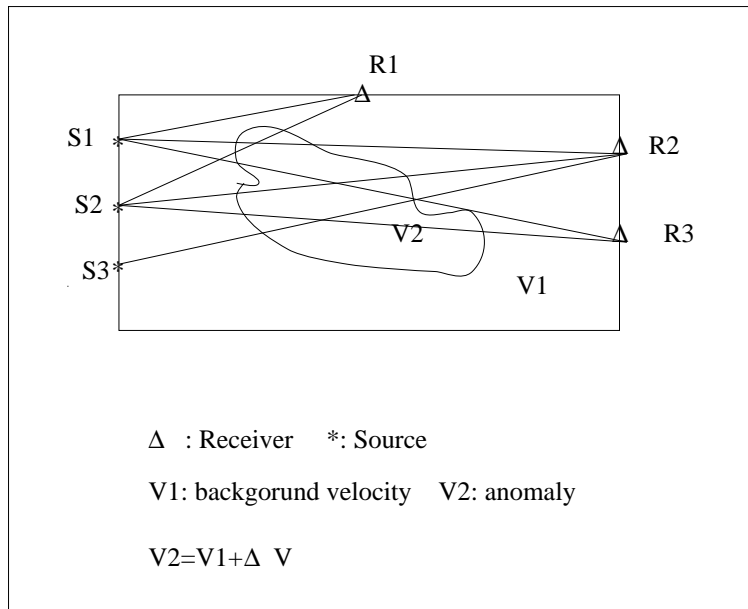


Figure 7.1: Tomographic experiment.

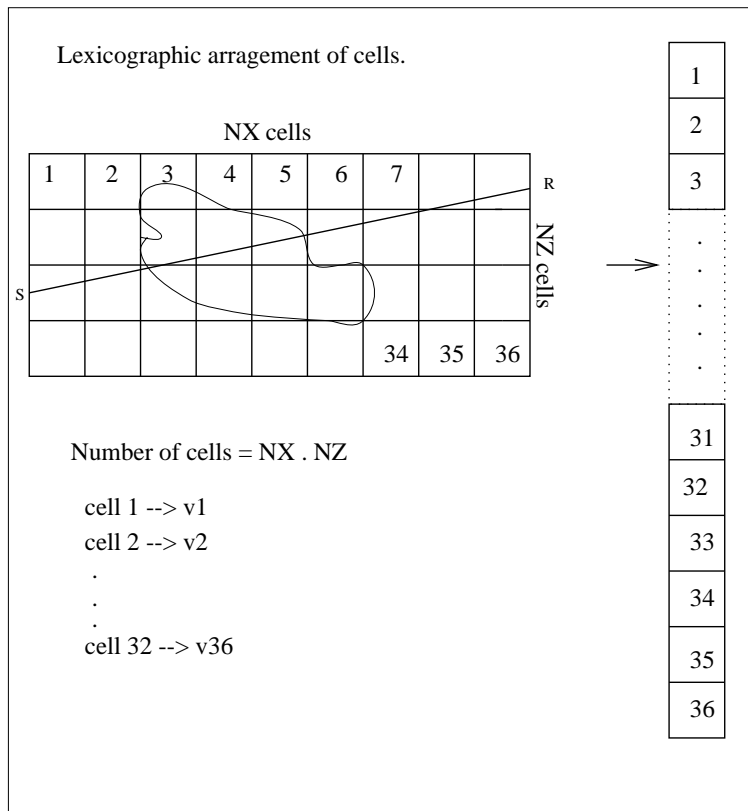


Figure 7.2: Tomographic experiment. Lexicographic arrangement of cells.

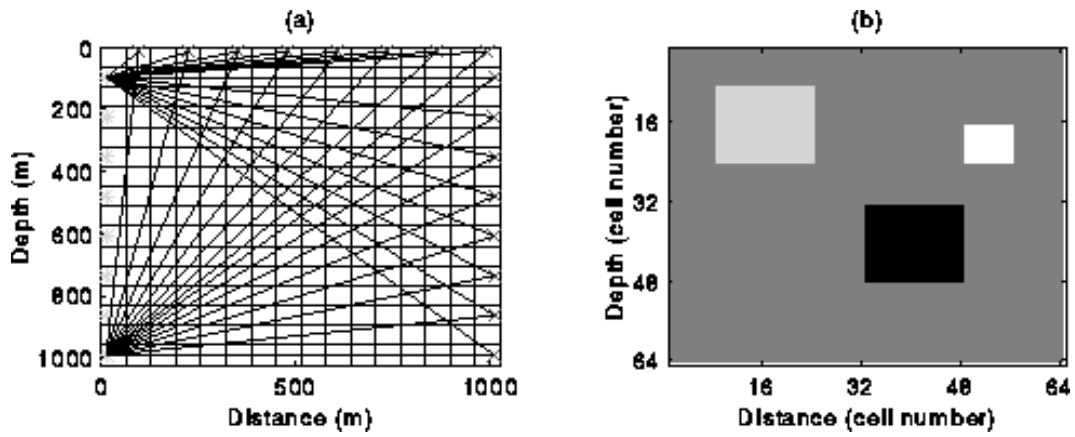


Figure 7.3: Tomographic experiment. a). Distribution of rays. b) Model that we would like to retrieve from travel-time observations (From Li and Ulrych, SEG 1997)

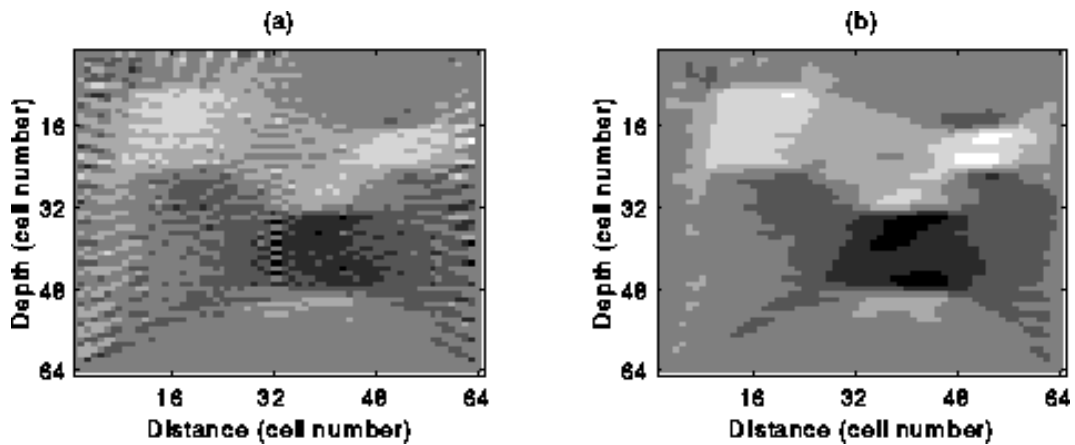


Figure 7.4: Tomographic experiment. a) least-squares solution with damping. b) In this case the norm of the vertical and horizontal derivatives of the model were minimized.

Chapter 8

Migration

In this chapter I will provide an overview of the pivotal process called migration. The migration process is used to locate seismic reflectors in the right position, it is also a mean to increase lateral resolution.

We will first introduce the concept of exploding reflectors and deal with the **post-stack migration** case. The seismic section computed after NMO correction and stacking is artificially simulating a zero-offset experiment (source and receiver are in the same location). I will use the term **post-stack migration** and migration of zero-offset data as equivalent concepts.

8.1 Exploding reflectors

This is a powerful analogy that can be used to simplify various wave propagation problems. Figure (8.1) shows a "field experiment" where the data have been acquired via repeated zero-offset experiments. In fact, this is obtained after processing CMP gathers.¹

In Figure (8.1) we show a fictitious experiment where the sources are located on top of the reflector. This is the exploding reflector case. Both experiments are equivalent in the sense that they will produce the same wavefield. If the travel time in the first experiment is divided by two, the two wave-fields obtained by these two experiments are equal. We can instead assume that the velocity of the medium in the real experiment is half its true value ($v = v/2$).

The exploding reflector analogy permits us to migrate post-stack data ($D(x_m, h = 0, t)$). The exploding reflector analogy assumes that the real experiment can be replaced by a fictitious one where only up-going waves generated by the hypothetical explosion of the reflector are considered.

We can now define migration as the operation that maps the data recorded at the surface of the Earth ($z = 0$) into an image of the subsurface. If the wavefield recorded at $z = 0$ is denoted by $p(t, x, z = 0)$ the migration process is used to compute the image as follows:

¹We have already studied that CMP gathers after NMO and stack simulate a zero offset experiment

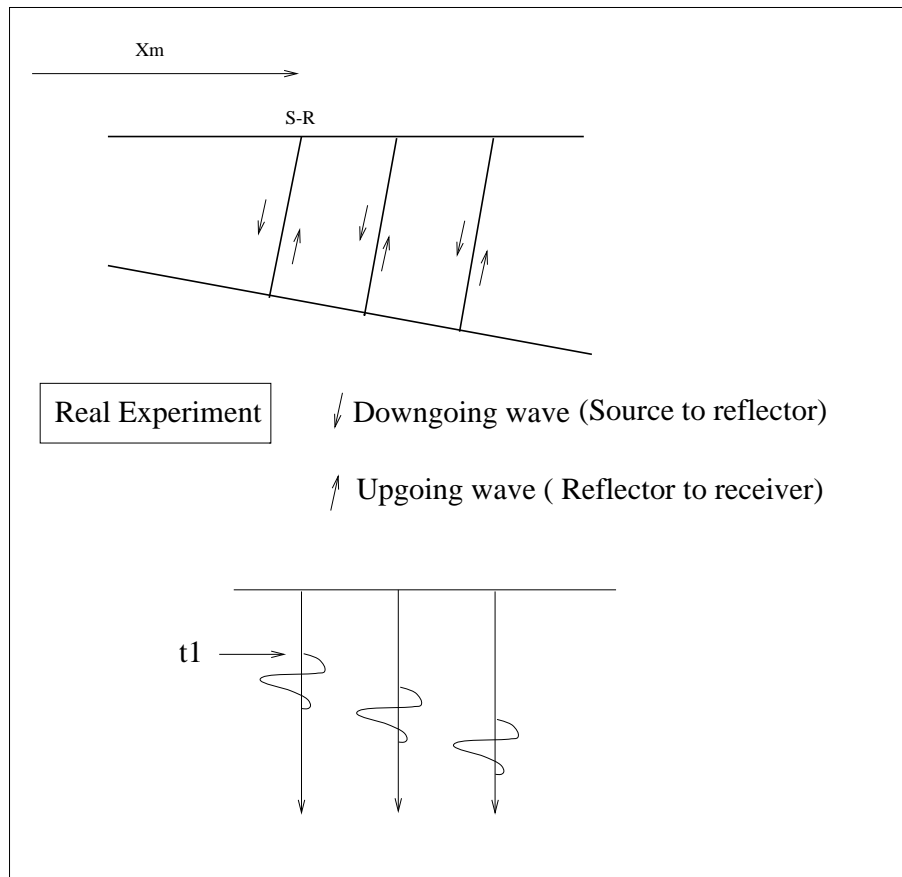


Figure 8.1: A zero offset experiment.

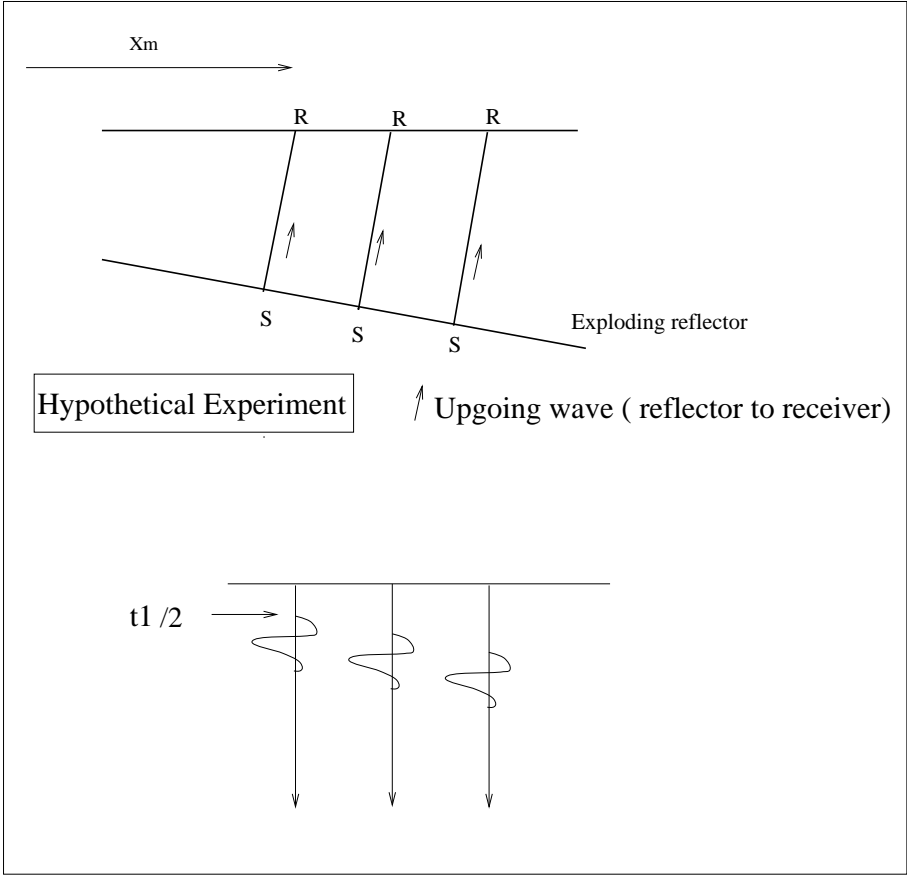


Figure 8.2: The exploding reflector analogy.

$$I(x, z) = p(t = 0, x, z)$$

Where $I(x, z)$ is an estimate of the reflector strength (the reflectivity of the layer). The exploding reflector analogy implies that the reflector explodes at $t = 0$. Therefore, the wavefield at $t = 0$ is nothing else than the image of our fictitious sources located on the reflector. The core of the migration process is an algorithm that permits to propagate our wavefield recorded at $z = 0$ (data) into the subsurface.

In general, one can say that a migration algorithm is composed of two components:

1. A procedure to extrapolate wavefields in depth.
2. An imaging condition.

The imaging condition is described above: reflectors explode at $t = 0$. Next, we will describe a simple procedure to extrapolate wavefields in depth.

8.1.1 The wave equation in (k_x, ω) : introduction to one-way propagators

We will start our analysis by considering the acoustic wave equation in a 2D earth:

$$p_{xx} + p_{zz} = \frac{1}{v^2} p_{tt}, \quad ^2 \quad (8.1)$$

The wavefield $p(t, x, z)$ can be transformed into the Fourier space as follows:

$$P(\omega, x, z) = \frac{1}{2\pi} \int p(t, x, z) e^{-i\omega t} dt \quad (8.2)$$

So far we have only applied the Fourier transform to the temporal variable t . The wave equation in the (ω, x, z) domain is given by ³ .

$$P_{xx} + P_{zz} = -\frac{\omega^2}{v^2} P, \quad P = P(\omega, x, z). \quad (8.3)$$

Now we apply again the Fourier transform but with respect to the spatial variable x .

$$P(\omega, k_x, z) = \frac{1}{2\pi} \int P(\omega, x, z) e^{-ik_x x} dx \quad (8.4)$$

² $p_{xx} = \frac{\partial^2 p}{\partial x^2}$

³I have used the following property: $\frac{d^n f(x)}{dx^n} \rightarrow (i\omega)^n F(\omega)$

The wave equation in (ω, k_x, z) is given by

$$-k_x^2 P + P_{zz} = -\frac{\omega^2}{v^2} P, \quad P = P(\omega, k_x, z). \quad (8.5)$$

We can rearrange the above equation as follows:

$$P_{zz} = -\left(\frac{\omega^2}{v^2} - k_x^2\right)P \quad (8.6)$$

The dispersion equation of the scalar wave equation is given by

$$k_x^2 + k_z^2 = \frac{\omega^2}{v^2} \quad (8.7)$$

where k_z is the vertical wavenumber. In equation (8.6) we can recognize the vertical wavenumber $k_z^2 = \frac{\omega^2}{v^2} - k_x^2$.

$$P_{zz} + k_z^2 P = 0, \quad P = P(\omega, k_x, z). \quad (8.8)$$

The solution to the last equation is a simple exponential of the form

$$P(\omega, k_x, z) = A e^{i\pm k_z(\omega, k_x)z} \quad (8.9)$$

The wavefield recorded at the surface is denoted by $p(t, x, z = 0)$ (the seismic data). In the (ω, k_x, z) domain, the wavefield is given by $P(\omega, k_x, z = 0)$. The constant A can be evaluated by considering the wavefield at $z = 0$ (the data).

$$P(\omega, k_x, z) = P(\omega, k_x, z = 0) e^{i\pm k_z(\omega, k_x)z} \quad (8.10)$$

We have found the expression for the downward continuation operator. This is an operator that extrapolates the wavefield at the surface into a depth z below the surface. The exploding reflector idea uses up-going waves. This is why we will choose the minus sign in the extrapolator,

$$P(\omega, k_x, z) = P(\omega, k_x, z = 0) e^{-ik_z(\omega, k_x)z} \quad (8.11)$$

$$k_z = -\sqrt{\left(\frac{\omega^2}{v^2} - k_x^2\right)}. \quad (8.12)$$

The story doesn't end here. It is clear that if we know the velocity v we can extrapolate our wavefield recorded at $z = 0$ down into the earth, in other words, we can compute $P(\omega, k_x, z) \forall z$ the

imaging condition is obtained by transforming back to time and space using the inverse Fourier transforms,

$$P(\omega, k_x, z) \rightarrow \mathcal{F}_t^{-1} \rightarrow P(t, k_x, z) \rightarrow \mathcal{F}_x^{-1} \rightarrow p(t, x, z). \quad ^4$$

Finally we apply the imaging condition:

$$I(x, z) = p(0, x, z)$$

Wavefield extrapolation can be also done in the t, x, z space. Note that wavefield extrapolation in (ω, k_x) is equivalent to a convolution in the (ω, x) domain.

We have described a technique to migrate seismic data in the case where the velocity is laterally invariant, $v(z)$. This technique is called **Gazdag migration**.

The following MATLAB implementation permits to run constant velocity Gazdag migration; simple modifications would allow us to migrate data in $v(x, z)$ media.

8.1.2 Gazdag Migration: Examples

I have generated a syncline model using SeismicUnix. I have computed the associated zero offset section and finally, I have migrated it using different velocities. In Figure (8.4) we portray the zero offset section corresponding to the syncline model. In this example we are using a constant velocity medium ($V = 1km/sec$).

First, we migrate the zero-offset section using the correct velocity. The result is portrayed in Figure (8.5). It is clear, that the migration process has removed diffraction patterns produced by multiple arrivals of energy from the flanks of the syncline. In Figures (8.6) and (8.7) we have used the wrong velocity to migrate the data.

⁴ \mathcal{F}_t^{-1} is the inverse Fourier transform over t

```

function [dout] = down_constant_v(din,v,dx,dt);
% Migration using the phase shift method
% v is constant.
% din: input data
% v: velocity (MKS)
% dx: distance between receivers
% dt: sampling interval
% dout: migrated data
%
D = fft2(din) ;          2D fft of the data
nx = min(size(D));
nt = max(size(D));
% Compute wavenumbers, symmetries are imposed
knyq = pi/dx; dkx = 2*pi/(nx*dx); kx = [0:dkx:dkx*(nx/2) -(dkx*(nx/2-1):-dkx:dkx)];
wnyq = pi/dt; dw = 2*pi/(nt*dt); w = [0:dw:dw*(nt/2) -(dw*(nt/2-1):-dw:dw)];
i = sqrt(-1);
for l=1:nt
    for j=1:nx
        kzkz = w(l)*w(l)-v*v*kx(j)*kx(j);    % Predicted squared vertical wavenumber
        if kzkz > 0
            C(l,j) = exp( i*sign(w(l))*dt*sqrt(kzkz));
        else
            C(l,j) = 0;
        end
    end
end
for l=1:nt
    D = D.*C;          % Downward continuation
    IMAGE(l,:) = ones(1,nt)*D;    % imaging condition
end
image = real(ifft(IMAGE,[],2));
dout = image;

```

Figure 8.3: Gazdag migration algorithm for constant velocity

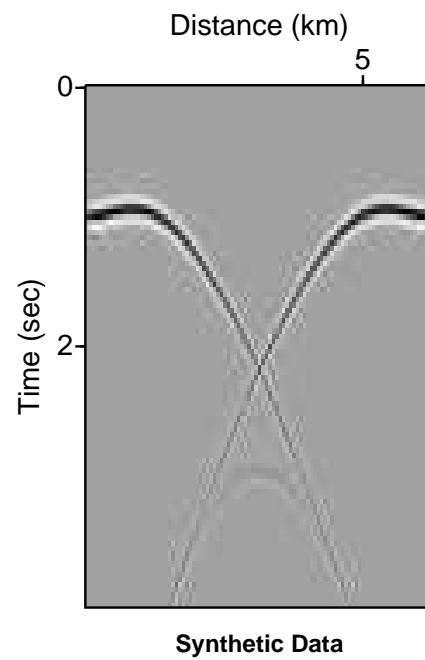


Figure 8.4: Zero-offset synthetic data used to test Gazdag migration.

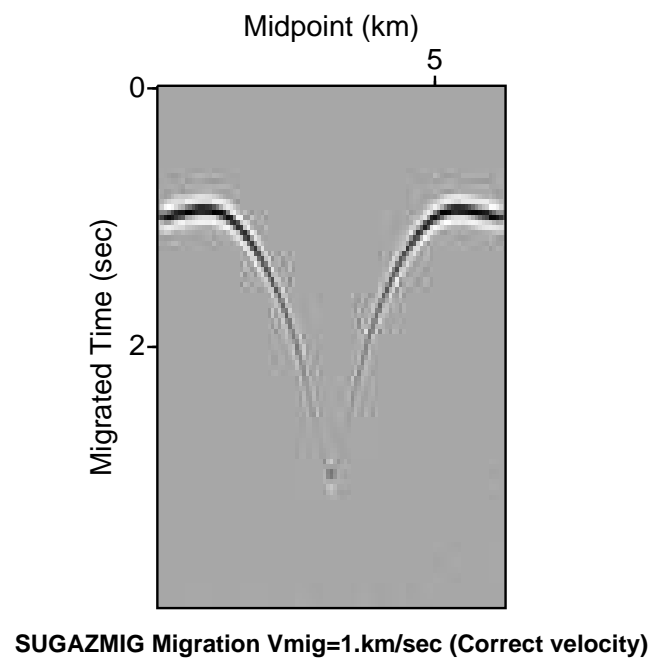


Figure 8.5: Gazdag migration using the correct velocity.

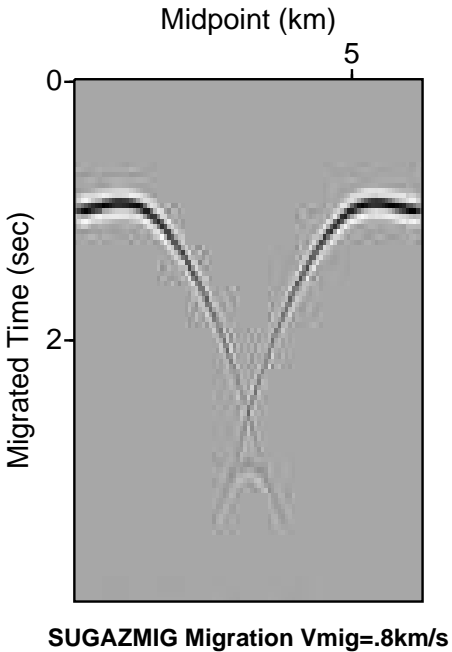


Figure 8.6: Gazdag migration using the wrong velocity.

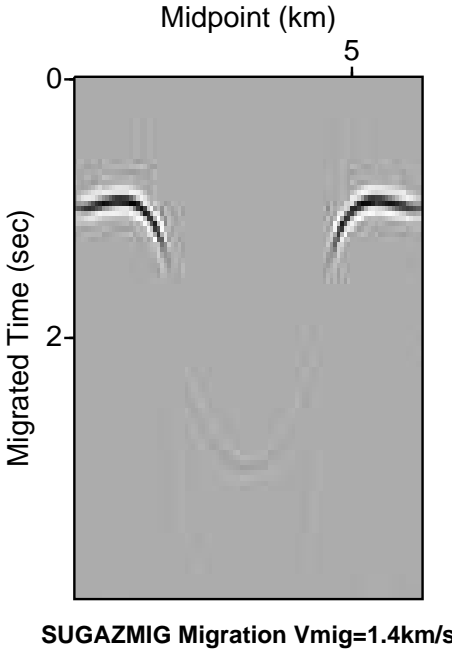


Figure 8.7: Gazdag migration using the wrong velocity.

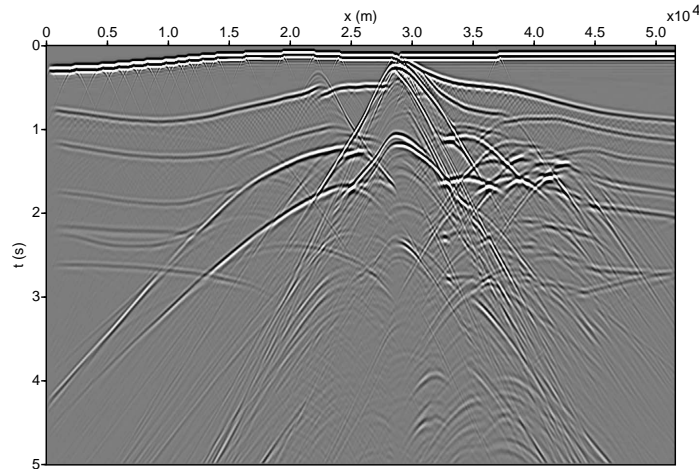


Figure 8.8: Zero offset synthetic data obtained from the SEG-EAEG sub-salt model

8.1.3 Phase shift Migration plus interpolation (PSPI)

We will study a modification to Gazdag migration that is capable of dealing with the problem of migrating data in $v(x, z)$.

The algorithm outlined in the previous section was valid for $v(z)$. In this case, the algorithm is often called Gazdag migration or phase-shift migration in $v(z)$.

In PSPI the wavefield is downward continued using several velocities. The algorithm is equivalent to running Gazdag migration for a set of reference velocities and then interpolating to compute the the local wavefield by interpolating the wavefield obtained by propagating the data using reference velocities.

In Figure (8.8) I portrayed the zero offset data associated to the SEG-EAGE subsalt model. This model is often used to study the performance of imaging algorithms. In Figure (8.9) the data has been migrated using Gazdag $v(z)$ algorithm, in other words the velocities of geological structure were assumed to be laterally invariant. The result is portrayed in Figure(8.9). The correct velocities where used to run the PSMPI algorithm, in this case 10 reference velocities per depth step were adopted. The result is displayed in Figure (8.10). In general migration velocities are also called **macro velocities** or the **macro model**. These velocities are usually a smooth representation of the real velocities of the subsurface. Techniques to estimate migration velocities are often referred as migration velocity analysis.

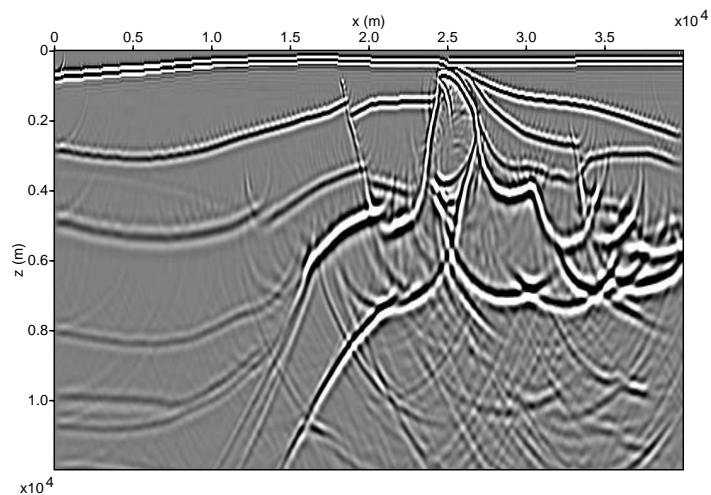


Figure 8.9: Gazdag $v(z)$ migration. Note that the incorrect assumption of laterally invariant velocity leads to an image dominated by artifacts.

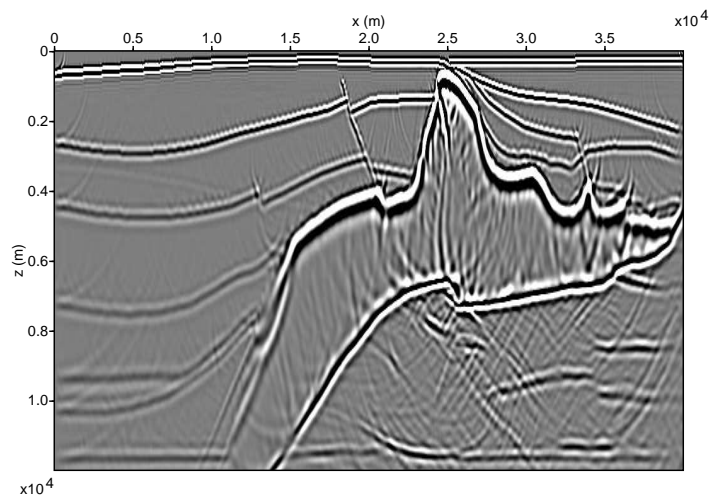


Figure 8.10: PSMPI using 10 reference velocities per depth step. In this example the salt body is properly migrated.

8.2 Summation along hyperbolic paths

We can describe the migration process in very simple terms by first understanding how to model seismic data in constant velocity media.

Modeling: MODEL of the subsurface \longrightarrow DATA

Imaging: DATA \longrightarrow MODEL of the subsurface

When one uses the exploding reflector analogy, it is possible to imagine that a reflector is composed of a continuous distribution of sources. To understand this concept, we will simulate a seismic reflection by placing sources on a reflector and compute the total response as the superposition of individual sources. The position of the source i in Figure (8.11) is denoted by x_i, z_i and the position of the receiver is given by x_m (this is also the midpoint position for our zero-offset experiment).

The travelttime for the ray going from the source i – th to the receiver is

$$T_i = \frac{1}{v} \sqrt{z_i^2 + (x_m - x_i)^2} \quad (8.13)$$

If each source is represented by a time function $s(t)$ (a wavelet), and if we assume that all the sources explode at the same time ($t = 0$), the seismogram at the receiver x_r is modeled as the superposition of individual sources delayed in time according to the following equation

$$data(x_m, t) = \sum_i s\left(t - \frac{1}{v} \sqrt{z_i^2 + (x_m - x_i)^2}\right). \quad (8.14)$$

This is a simple but very important equation that enables us to model seismic data (only primary reflections)⁵. It is clear that the reflector in Figure 8.11 needs an infinite number of sources very close to each other to be properly modeled.

In Figure 8.12 we present a model that consists of 10 sources distributed in $x - z$. Now, you can imagine that this sources are small pieces a of broken reflector. The data generated by this model are a superposition of hyperbolas. In the same figure I have also shown the migrated data, in this case the data has been migrated with an algorithm that undo the process outline in equation (8.14). I will come back to this point in a minute.

In Figure 8.13, I have used 20 sources to model the reflector, the data generated from this model and the migrated image are shown in the same figure.

In Figure 8.14, I have used 200 sources to model the reflector, the data generated from this model and the migrated image are shown in the same figure. In this case each piece of reflector

⁵To simplify the problem, I didn't include amplitude terms, but bear in mind that there is an amplitude variation.

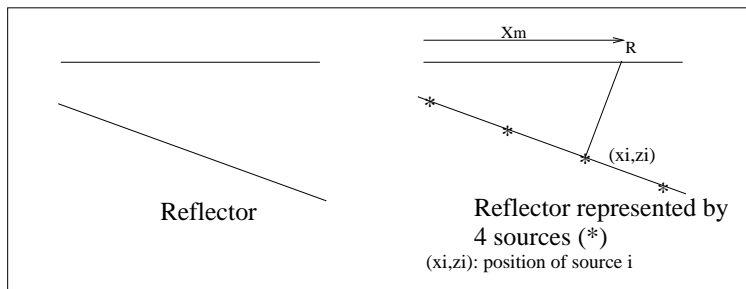


Figure 8.11: Reflectors are represented by a superposition of sources.

in $x - z$ is an active source. It is clear, that the exploding reflector model leads to a very simple integral formulation for modeling data (equation (8.14)). Now we have to find the equation to undo the modeling process (The migration algorithm).

Equation (8.14) is a forward operator (creates data from a subsurface model). The following equation does the reverse process (creates a subsurface model from data)

$$image(x, z) = \sum_{x_m} d(x_m, \frac{1}{v} \sqrt{z^2 + (x_m - x)^2}). \quad (8.15)$$

The last equation that can be formally derived corresponds to a *poor man* Kirchoff migration algorithm. Equation (8.15) permits to construct an image by summation along hyperbolas in the $t - x_m$ plane.

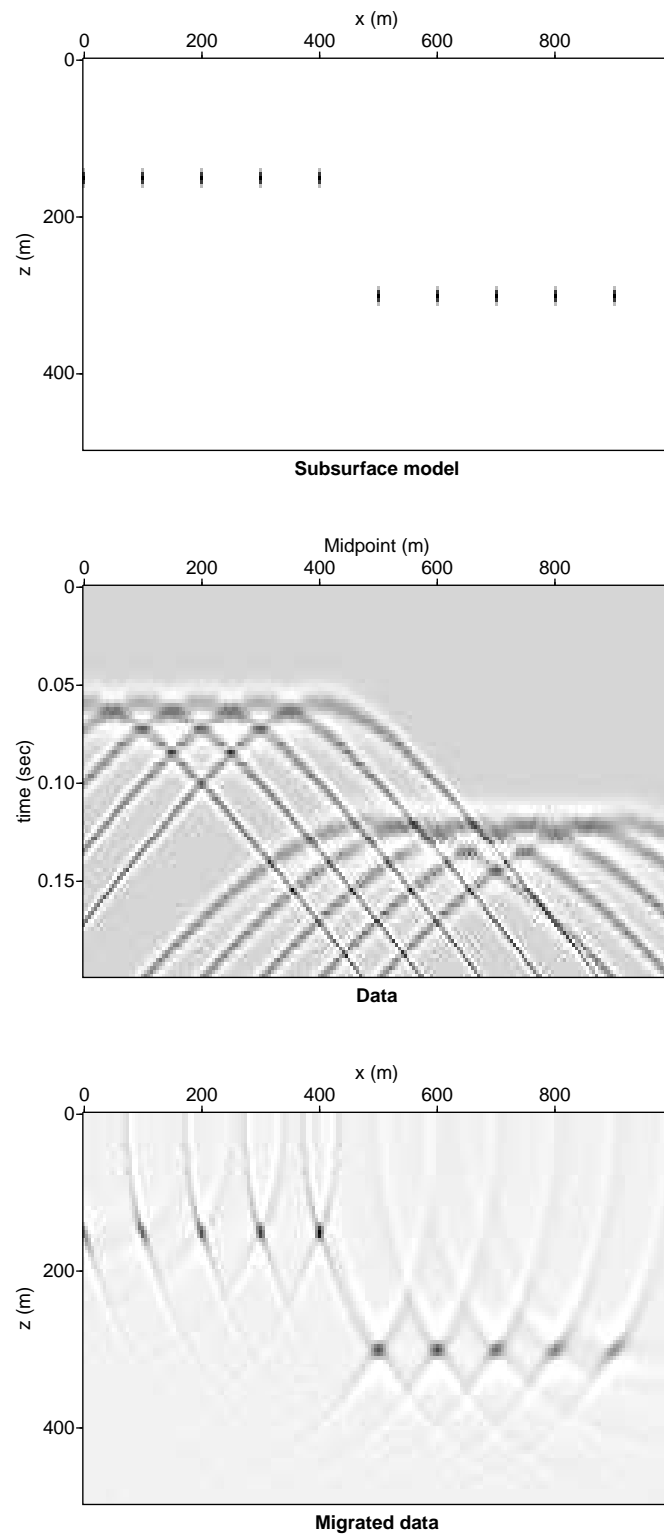


Figure 8.12: Hyperbola summation for 10 sources

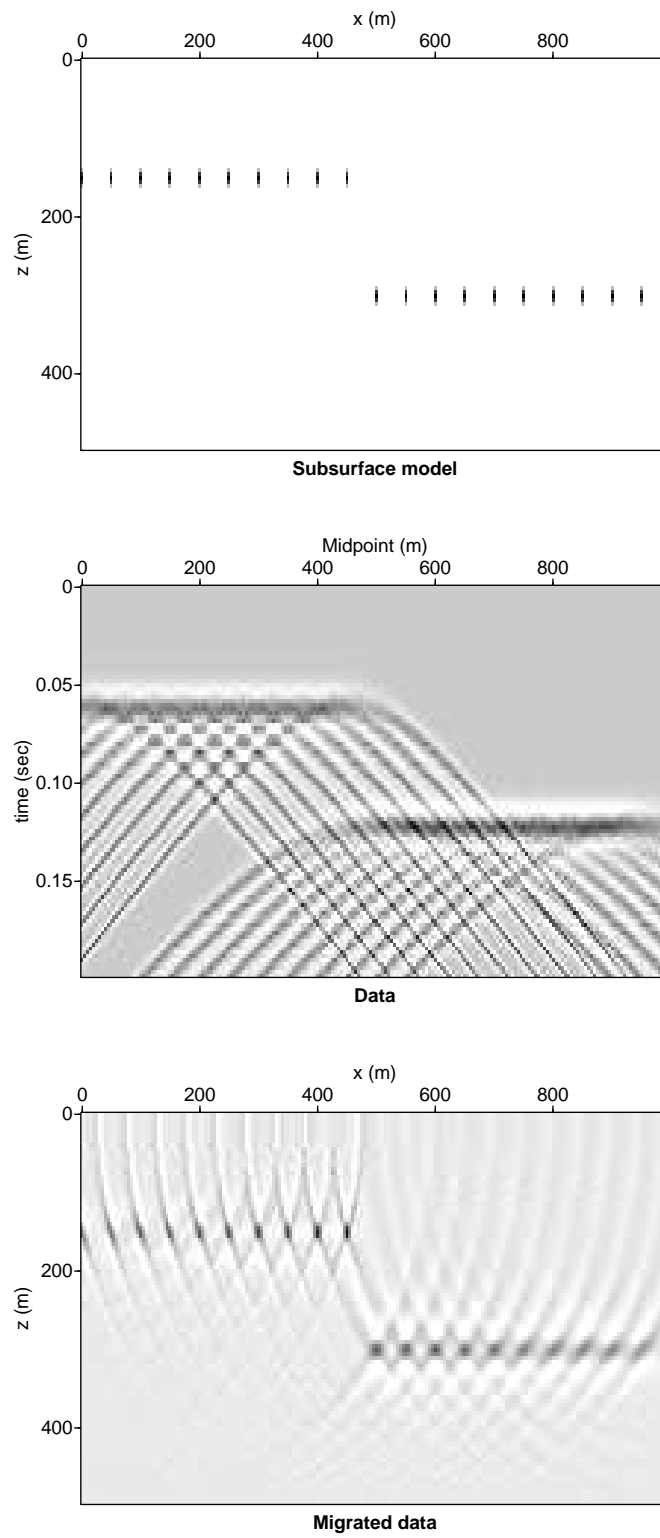


Figure 8.13: Hyperbola summation for 20 sources

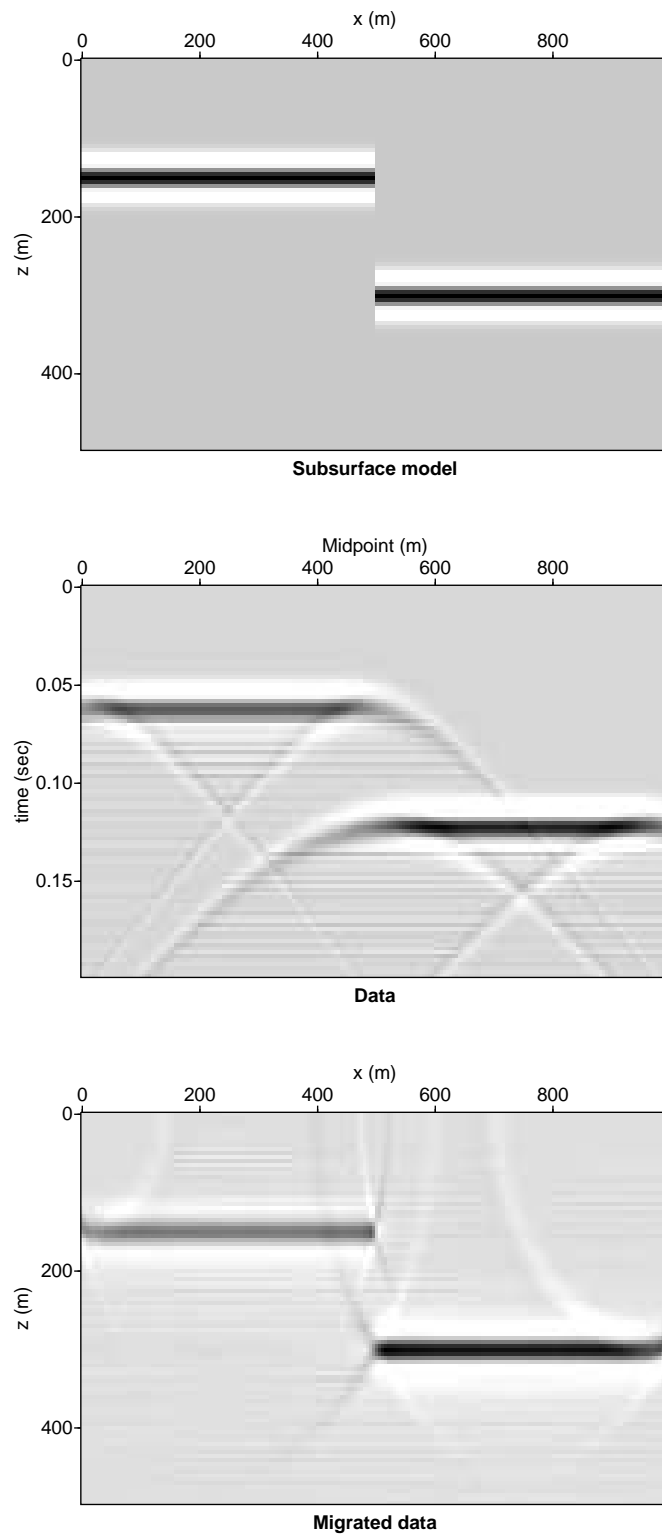


Figure 8.14: Hyperbola summation for 200 sources

8.2.1 Subroutine F77 to do and undo wavefields

This is a prototype of a migration code in Fortran77. You have two options given by the variable `adj`, `adj=0` means modeling, `adj=1` means undo the modeling (do the migration).

In this case, we have zero-offset data and a constant velocity medium.

```

subroutine hyperbola_sum(adj,vhalf,dt,dx,dz,nt,nx,nz,m,d)

c Zero offset example
c This code can be optimized.
c Input: m if adj=0 (Modeling)      Output: d
c Input: d if adj=1 (Migration)    Output: m

real      m(500,200),d(500,200)
integer   adj

if(adj.eq.0) then
  do ix=1,nx
    do it=1,nt
      d(it,ix)=0.
    enddo
  enddo
endif
if(adj.ne.0) then
  do ix=1,nx
    do iz=1,nz
      m(iz,ix)=0.
    enddo
  enddo
endif
do ir=1,nx          ! loop on receivers
  xr=(ir-1)*dx
do ix=1,nx          ! loop on lateral position
  x=(ix-1)*dx
do iz=1,nz          ! loop on depth
  z=(iz-1)*dz
  t=(sqrt(z*z+(xr-x)**2))/vhalf
  it=1.5+t/dt
  if(it.le.nt) then
    if(adj.eq.0) d(it,ir)=d(it,ir)+m(iz,ix)
    if(adj.ne.0) m(iz,ix)=m(iz,ix)+d(it,ir)
  endif
enddo
enddo
enddo
return

```

end